



MONASH University

Closed form path integral based approximate solutions of stochastic differential equations

Author:

Antonios MEIMARIS
B.Sc., M.Res.

*A thesis submitted for the degree of Doctor of Philosophy
at Monash University in 2020*

Department of Econometrics and Business Statistics

Copyright Notices

Notice 1

Under the Copyright Act 1968, this thesis must be used only under the normal conditions of scholarly fair dealing. In particular no results or conclusions should be extracted from it, nor should it be copied or closely paraphrased in whole or in part without the written consent of the author. Proper written acknowledgement should be made for any assistance obtained from this thesis.

Notice 2

I certify that I have made all reasonable efforts to secure copyright permissions for third-party content included in this thesis and have not knowingly added copy-right content to my work without the owner's permission.

Contents

Abstract	i
Publications during enrolment	ii
Declaration of Authorship	iii
Acknowledgements	v
1 Introduction	1
2 Preliminaries	5
2.1 Itô Stochastic Differential Equations	5
2.2 Connection between Stochastic Differential and Fokker-Planck equations	6
2.3 The Path Integral Method	7
3 Approximate solutions for a case of Itô SDEs	10
3.1 Published Material	10
3.2 Discussion	28
4 Approximate solutions for nonlinear Itô SDEs	29
4.1 Published Material	29
4.2 Quantitative Finance Applications	45
4.3 Summary	49
5 Approximate solutions for a case of coupled Itô SDEs	50
5.1 Published Material	51
5.2 The "labyrinth" model	70
6 Summary and Conclusions	73
6.1 Future Directions and Projected Impact	74
Bibliography	76

MONASH UNIVERSITY

Abstract

Monash Business School

Department of Econometrics and Business Statistics

Doctor of Philosophy

Closed form path integral based approximate solutions of stochastic differential equations

by Antonios MEIMARIS

As stochastic models are commonly used in a wide range of scientific disciplines for modelling the complex dynamics of diverse systems, the task of determining solutions efficiently, in a distributional sense, becomes increasingly challenging and impactful in modern applications. A significant advantage of this modelling treatment relates to the ability of the estimation of probability distributions of potential solutions by allowing for disturbances or random variations over time. Although, numerical Monte Carlo simulation methodologies have been among the most versatile tools for solving stochastic differential equations of general form, in many cases simulations can be computationally prohibitive, and thus, the need for developing alternative efficient approximate solution techniques arises.

This thesis aims to produce an innovative method to approximate the solutions of stochastic differential equations in order to use stochastic models with confidence. A very important element used as the basis of the approximations is the recently developed Wiener Path Integral technique, which sets the framework for determining the probability density function of various models. Although, implementing the Wiener Path Integral technique is impractical in most modelling cases, different approaches exist for expanding its usage by adapting the exact solution methodology to an approximation. One such approximation relates to the "most probable path" approach, where the problem of solving a functional integral is reduced to a boundary value problem. To speed up the process, i.e., tracking probability distribution functions efficiently, a new path integral framework is utilized that avoids the computational cost of determining explicitly the "most probable path", deriving closed-form approximate solutions with essentially zero computational cost.

The developed technique is advantageous since it yields a priori error estimates of the aforementioned approximations, once again with essentially zero computational cost, which is then used for an error correction process. Based on the Fokker-Planck equation, an error minimization scheme is established for further augmenting the precision of the approximate solutions with the addition of "degrees of freedom". Letting the approximations become more complex, comes at a minimal cost of computational power, but allows more control over the achieved accuracy of the derived basic approximate solution.

The multi-disciplinary impact of the derived approximations is illustrated by the results presented in the main chapters of the thesis. Specifically, initially by focusing on a special case of stochastic differential equations, results are presented in a civil and biochemical engineering framework. Subsequently, a more general form of stochastic differential equations is considered, which illustrates the applicability of the developed method in options pricing and smart materials. Finally, a multi-dimensional variant is provided next, and the results are validated in applications ranging from labyrinth models commonly used in chemical reactions to non-linear mechanical oscillators and non-linear predator-prey models.

Publications during enrolment

List of research outputs used in the thesis.

1. Antonios Meimaris, Ioannis Kougoumtzoglou and Athanasios Pantelous, "Approximate analytical solutions for a class of nonlinear stochastic differential equations", European Journal of Applied Mathematics 30(5), (2018): 928-944.
2. Antonios Meimaris, Ioannis Kougoumtzoglou, Athanasios Pantelous and Antonina Pirrotta, "An approximate technique for determining in closed form the response transition probability density function of diverse nonlinear/hysteretic oscillators", Nonlinear Dynamics 97(4), (2019): 2627-2641.
3. Antonios Meimaris, Ioannis Kougoumtzoglou and Athanasios Pantelous, "Closed-form approximate solutions for a class of coupled nonlinear stochastic differential equations", Applied Mathematics and Computation 364, (2020): 124669: 1-18.

The following papers were published during the candidature, but are not part of the thesis.

1. Antonios Meimaris, Ioannis Kougoumtzoglou and Athanasios Pantelous, "A closed form approximation and error quantification for the response transition probability density function of a class of stochastic differential equations", Probabilistic Engineering Mechanics 54 (2018): 87-94.
2. Konstantinos Liaskos, Athanasios Pantelous, Ioannis Kougoumtzoglou and Antonios Meimaris, "Implicit analytic solutions for the linear stochastic partial differential beam equation with fractional derivative terms", Systems & Control Letters 121, (2018): 38-49.
3. Konstantinos Liaskos, Athanasios Pantelous, Ioannis Kougoumtzoglou, Antonios Meimaris and Antonina Pirrotta, "Implicit analytic solutions for a nonlinear fractional partial differential beam equation", Communications in Nonlinear Science and Numerical Simulation 83, (2020): 105219: 1-19.

Declaration of Authorship

Declaration for thesis based or partially based on conjointly published or unpublished work

I hereby declare that this thesis contains no material which has been accepted for the award of any other degree or diploma at any university or equivalent institution and that, to the best of my knowledge and belief, this thesis contains no material previously published or written by another person, except where due reference is made in the text of the thesis.

This thesis includes three original papers published in peer reviewed journals. The core theme of the thesis is a novel way of approximating, in an efficient manner, the solution, in a distributional sense, of nonlinear Itô Stochastic Differential Equations. The ideas, development and writing up of all the papers in the thesis were the principal responsibility of myself, the student, working within the Department of Econometrics and Business Statistics under the supervision of Athanasios Pantelous.

The inclusion of co-authors reflects the fact that the work came from active collaboration between researchers and acknowledges input into team-based research.

In the case of Chapters 3-5 my contribution to the work involved the following:

Publication Title & Status:

Approximate analytical solutions for a class of nonlinear stochastic differential equations

(Status: Published, Thesis Chapter 3)

Nature and % of student contribution

Developed the ideas. Implemented the relevant code. Produced the results. Contributed to the write-up (first draft). 70%

Nature and % of co-author's contribution

- 1) Ioannis Kougoumtzoglou, Contributed to discussions. Contributed to the write-up. 10%
- 2) Athanasios Pantelous, Contributed to discussions. Contributed to the write-up. 20%

Publication Title & Status:

An approximate technique for determining in closed form the response transition probability density function of diverse nonlinear/hysteretic oscillators

(Status: Published, Thesis Chapter 4)

Nature and % of student contribution

Developed the ideas. Implemented the relevant code. Produced the results. Contributed to the write-up (first draft). 60%

Nature and % of co-author's contribution

- 1) Ioannis Kougoumtzoglou, Contributed to discussions. Contributed to the write-up. 10%
- 2) Athanasios Pantelous, Contributed to discussions. Contributed to the write-up. 20%
- 3) Antonina Pirrotta, Contributed to discussions. 10%

Publication Title & Status:

Closed-form approximate solutions for a class of coupled nonlinear stochastic differential equations
(Status: Published, Thesis Chapter 5)

Nature and % of student contribution

Developed the ideas. Implemented the relevant code. Produced the results. Contributed to the write-up (first draft). 70%

Nature and % of co-author's contribution

- 1) Ioannis Kougoumtzoglou, Contributed to discussions. Contributed to the write-up. 10%
 - 2) Athanasios Pantelous, Contributed to discussions. Contributed to the write-up. 20%
-

I have not renumbered sections of submitted or published papers in order to generate a consistent presentation within the thesis.

Student signature: Antonios Meimaris

Date: June 8, 2020

The undersigned hereby certify that the above declaration correctly reflects the nature and extent of the student's and co-authors' contributions to this work. In instances where I am not the responsible author I have consulted with the responsible author to agree on the respective contributions of the authors.

Main Supervisor signature: Athanasios Pantelous

Date: June 8, 2020

Acknowledgements

Firstly, I would like to thank my supervisors, who have provided me with wisdom throughout this journey. In particular, I would like to thank Professor Athanasios Pantelous, for recommending this research theme to me, as well as for his patience and support.

I am also very grateful to Professor Ioannis Kougoumtzoglou, not only for his support during my research visits at Columbia University, but also for his guidance and helpful feedback, strengthening the scientific relevance of my papers.

In addition, I would like to thank Professor Antonina Pirrotta, for her supporting role and extremely valuable comments leading to the acceptance of my papers.

As always, much love goes to my family. Naturally, I would like to thank my parents, who have wholeheartedly supported me in all my endeavours throughout my life.

Finally, I would like to thank my beloved Eleonora, for her continuous love and support, in this as in all things.

Thank you all.

Chapter 1

Introduction

The objective of this thesis is to develop a novel methodology around the subject of approximating the solutions of Itô Stochastic Differential Equations in a distributional sense. The bulk of the study is based on the mathematical theory around Wiener path integrals and specifically the idea of the "Most Probable Path". Although, the mathematical study of path integrals for Itô Stochastic Differential Equations provide a way for determining the exact solution in analytical terms (e.g. see Chaichian and Demichev, 2001), in practise this analytical solution is of little use. Thus, using the idea of the "Most Probable Path" approximation, which is extensively used in stochastic engineering dynamics for determining response and reliability statistics of complex systems (e.g. see Kougioumtzoglou et al., 2015), and studying it through a more mathematical lens, serves as a starting point of this thesis.

This thesis not only details the derivation of closed-form formulas for approximating efficiently the solutions of Itô Stochastic Differential Equations in a distributional sense, but presents their numerical implementation in various applications as well. As a natural choice for verifying the reliability of this new method, the applications begin within the classical discipline of engineering where the "Most Probable Path" approach has been used extensively. However, the applications presented in the following chapters relate to an even broader scientific audience, e.g., models from biochemistry are studied and even the more complex systems of predator-prey population models are analysed. In addition, the developed method is put to the test in quantitative finance applications (option pricing), which pose a great challenge for approximative techniques, where both efficiency and accuracy is of the essence, especially in our age.

Indeed, the idea of trading commodities can be found to have its roots as far as the ancient times at the cradle of all human civilization (e.g. see Bernstein, 2008, Blake and Knapp, 2005 and references therein for more information). This concept evolved throughout the years, from mercantilism (e.g. see Braudel, 1982), the dominant economic theory and practice of Europe during the 16th until the 18th century, resulting into methods which have developed a complicated system that involves billions of simultaneous transactions in the world. Today every transaction is computerized; this revolution started in the 1980s (e.g. Michie, 1999) when electronic trading, or eTrading, already a part of the environment of the major stock exchange, was adapted to the foreign exchange market. This has led to a novel view and understanding of a wide variety of derivatives, specifically one of particular interest; options.

The implementation of options in daily life is not a modern idea. On the contrary, options are ancient financial tools, used for speculative purposes or for hedging major market transactions against unexpected changes in the market environment. These changes can produce large fluctuations in the price of assets, and options are intended to prevent the destruction of large amounts of capital. Historically, it was not uncommon for ancient civilizations, such as the Greeks (e.g. *Politics, Book 1*), to trade options even for speculative purposes, against outgoing cargo from their local sea ports or using the manufacturing facilities of the era (e.g. olive-presses). In more recent times, option pricing techniques have their roots in early

work by C. Castelli (e.g. see Castelli, 1877). The earliest known analytical calculations for options were offered by Louis Bachelier in Bachelier, 1900. Present day options are contracts between two parties where each party has the right, but not the obligation, to buy (Call option) or sell (Put option) a number of assets by a certain date for a certain price. In addition, variety of various forms of options exist, like American options, which might exercised at any time up to the expiration date, European options, which might be exercised only on the expiration date itself and Exotic or Path dependent options (e.g. Bermuda options¹), which have values which depend on the history of an asset price not just its value on exercise. Examples of the latter are the Barrier options, which can either come into existence or become worthless if the underlying asset reaches some prescribed value before expiring, Asian options, where the price depends on some form of average and others (e.g. see Fabozzi, 2002). For all the options listed above, this right has a value which must be purchased at a given price. This price usually depends on the value of the asset, or assets, in question, hence the name of derivative security by pricing and risk management of such financial instruments is a major focus of financial market research.

Scientists, from a wide range of disciplines, such as economists and mathematicians, are known to develop models in order to make predictions about parameters or trends in financial markets (e.g. see Allison and Abbott, 2000). However, in recent years, engineers and physicists are becoming more involved in the analysis of economic systems and are bringing new concepts and tools to some long standing problems in financial markets research (e.g. see Piotrowski and Śladkowski, 2002; Otto, 2000). Indeed, this is not unexpected; during the last decades *Stochastic Calculus* and the usage of stochasticity in a variety of models have been flourishing in modern applications. Specifically, for a wide range of scientific disciplines, this modeling treatment facilitates the estimation of probability distributions of potential solutions by allowing for disturbances or random variations over time, capturing the complex dynamics of diverse problems. Indicatively, in the physical-mechanical spectrum (e.g. see Grigoriu, 2002) as well as in the chemical and biological fields (predator-prey models) which have clear connections with finance & economics, (e.g. see Addison, Bhatt, and Owen, 2016; Asada, 2012; Bolton and Scharfstein, 1990; Louzoun and Solomon, 2001; Sprott, 2004) nonlinear stochastic models are commonly studied. Several problems that arise in these domains tend to be high in complexity and thus, solutions with standard *Probabilistic Methods* or *Classical Analysis* are scarce.

One of the promising techniques relates to the concept of the path integral, which can be viewed as an efficient alternative to standard procedures used in computational finance, such as Monte Carlo simulations (MCS), binomial or trinomial lattice algorithms and partial differential equation solvers (e.g. Eydeland, 1994). The path integral method, which traces back to the original work of Wiener and Kac in stochastic calculus (Wiener, 1921; Kac, 1966) and of Feynman in quantum mechanics (Feynman, 1948), is widely employed today in chemistry and physics, and very recently also in finance (e.g. see Bonnet, Allison, and Abbott, 2004; Bormetti et al., 2006; Capriotti, 2006; Decamps, De Schepper, and Goovaerts, 2006; Ingber, 2000; Linetsky, 1998; Montagna et al., 2003; Montagna, Nicrosini, and Moreni, 2002), because it gives the possibility of applying powerful analytical and numerical techniques (e.g. Schulman, 1981).

In quantum, i.e. probabilistic, physics, one talks about probabilities of different paths a stochastic process in a dynamical environment can take. In a nutshell, one defines a measure on the set of all possible paths from an initial state x_i to a final state x_f of the stochastic dynamical system under consideration, and expectation values (averages) of various quantities dependent on paths are given by path integrals over all possible paths from x_i to x_f (path integrals are also called sums over histories, as well as functional integrals, because

¹Note that the terms "American" and "Bermuda" do not refer to the place of the option or the exchange.

the integration is performed over a set of continuous functions of time (paths)). A certain action functional, a time integral of the Lagrangian function defining the dynamical system, is evaluated to a real number on each path, and the exponential of the negative of this number gives a weight of the path in the path integral. According to Feynman, a path integral is defined as a limit of the sequence of finite-dimensional multiple integrals, in a much the same way as an integral, in the Riemann sense, is defined as a limit of a sequence of finite sums. The path integral representation of averages can also be obtained directly as the Feynman-Kac solution to the partial differential equation describing the time evolution of the stochastic dynamical system (diffusion (Kolmogorov) equation in the theory of stochastic processes).

However, it should be noted that analytical evaluation of the path integral is a highly difficult task in the general case even for the simple case of analyzing a single stochastic differential equation (SDE). To address this challenge, research efforts in the literature have focused on applying an extremum condition (e.g. see Ewing, 1969) and accounting, essentially, for the contribution of only one path in the path integral, the so-called most probable path. Of course, it is possible to include additional terms in the related expansion and account for fluctuations around the most probable path (e.g. see Wio, 2013), at the expense, however, of computational efficiency. Note that the path integral technique should not be confused with a purely numerical solution scheme based on a discrete version of the Chapman-Kolmogorov equation, which is usually cited in the literature as numerical path integration (e.g. see Wehner and Wolfer, 1983; Naess and Johnsen, 1993; Chen, Jakobsen, and Naess, 2015).

In this context, the aim of this thesis is to provide an innovative method to approximate the solutions of stochastic differential equations, in particular with applications to derivative pricing. However, to achieve this goal, simpler applications are studied first, e.g. engineering systems, providing the basis for dealing with more complex financial and ecological systems. This is a great opportunity to follow and apply in practice dialectical reasoning and the theory of forms of motion, or phase transitions, (e.g. see Engels, 1976; Ed. Frolov, 1984; Oliveira, 2014) where transitions progress from mechanical, physical, chemical, biological and conclude to the socio-economical spectrum and complex ecological systems. Thus, the main objectives of the thesis are:

1. To derive closed-form approximations for SDEs based on a path integral formalism
2. To evaluate the associated error of the aforementioned approximations based on a novel error definition
3. To use the derived closed-form approximations as a benchmark for other approximations with enhanced accuracy
4. To expand the applicability to systems of coupled SDEs
5. To reveal the range of applications of the derived approximations

This thesis is organized as follows: in Chapter 2 the mathematical foundations and formulation of the Itô Stochastic Differential Equations is reviewed, with an emphasis on the connection between Stochastic Differential and Fokker-Planck equations. The basic elements of the Wiener Path Integral Method are introduced, focusing on the parts that are relevant later on. The following chapters present published work; specifically, three published papers constitute the basis of this thesis. In Chapter 3, the first main chapter of the thesis will expand on the ideas presented in Meimaris, Kougioumtzoglou, and Pantelous, 2018a, i.e. dealing with the special case of SDEs, where the diffusion coefficient is constant and the drift coefficient is a nonlinear function of the stochastic process, providing an improvement

of the precision of the proposed approximation, giving fruit to applications in engineering and biochemistry. This method is revised and enhanced in Chapter 4, where only the restriction of time-homogeneity on the drift and diffusion coefficients of the SDE is assumed. This more general form of SDE provides a wide variety of applications, ranging from smart materials to derivative pricing models such as the *Cox-Ingersoll-Ross* (CIR) and the *constant elasticity of variance* (CEV) models. In this section the developed technique is implemented for pricing a Bermuda call option under a drift-less CEV process. In Chapter 5 the generalization of the previous results for systems of SDEs is discussed and an approximation for the case where the drift coefficient is a nonlinear vector of the stochastic process and the diffusion coefficient is constant is developed. This kind of modeling is then used to study chemical (labyrinth models) and complex ecological (predator-prey) applications. Finally, Chapter 6 contains a summary and concluding remarks.

Chapter 2

Preliminaries

In general, analyzing a problem, or a subject, from a different perspective usually leads to fruitful insights (e.g. see Polya, 1971). An elementary example of this idea can be seen below in the following

Example. Let Z be a standard normal random variable, i.e. $Z \sim \mathcal{N}(0, 1)$, then for $k \in \mathbb{N}$ what is $\mathbb{E}(Z^k)$?

This question can be answered using traditional probabilistic techniques. However, it can also be solved by incorporating time for a stochastic process.

Let $B = (B_t)_{t \geq 0}$ be a standard *Brownian motion* on a complete filtered probability space $(\Omega, \mathcal{F}, \mathcal{F}_{t \geq 0}, \mathbb{P})$. Then, $B_t \stackrel{d}{=} \sqrt{t}Z$ and $(B_t)^k = t^{\frac{k}{2}}Z^k$. Thus,

$$\mathbb{E}(Bt^k) = t^{\frac{k}{2}} \mathbb{E}(Z^k). \quad (2.1)$$

If $a_k(t) = \mathbb{E}(Bt^k)$, then it is known that $a_0(t) = 1$, $a_1(t) = 0$ and it can be proven that $a_k(t) = \frac{1}{2}k(k-1) \int_0^t a_{k-2}(s)ds$ and this yields

$$\begin{aligned} a_{2k+1}(t) &= 0, \\ a_{2k}(t) &= \frac{(2k)!}{k!2^k} t^k. \end{aligned} \quad (2.2)$$

As a result, from Eqs. (2.1) and (2.2), it is concluded that $E(Z^{2k}) = \frac{(2k)!}{k!2^k} = (2k-1)!!$, else it is equal to 0.

In the above example, we see the potential of implementing time in order to find the solution to a stationary problem. Based on the aforementioned perspective, a similar idea is implemented when the connection between the *Itô Stochastic Differential Equations* (SDEs) and the corresponding *Fokker-Planck* (F-P) equation is presented, i.e., looking at both sides of the coin, and transforming a probabilistic problem into a deterministic one.

This chapter is divided into sections, covering a variety of topics needed to address the most probable *Wiener path integral* (WPI) method, however, for this purpose, the familiarity of the reader with *random variables* and their formal, axiomatic definition as was introduced in Kolmogorov, 1950 is considered. Specifically, this section is organized as follows. Section 2.1 covers the basic concepts of the theory of *Itô Stochastic Differential Equations* (SDEs) and a special case of Itô's lemma is also presented. In Section 2.2 a connection between Itô SDEs and the *Fokker-Planck* (F-P) equation is displayed, concluding with Section 2.3 which presents the path integral technique, which is of vital importance for the results presented in the following Chapters.

2.1 Itô Stochastic Differential Equations

In probability and statistics, a stochastic, or random, process is a family of random variables, frequently representing the dynamic evolution of a process or system over time. Rather than

defining a process which can only evolve in a predetermined or deterministic way, such as the *Ordinary Differential Equation* (ODE) of the Malthusian growth model (see Malthus, 1798), in a stochastic process there is a fair amount of uncertainty; even when allowing for the initial condition(s) to be known, there is a considerable amount of paths in which the process may unfold. Prime examples include the world's population or the price of a specific stock after a period of time. For the purpose of this study, a special kind of stochastic processes is of interest, those that can be described by Itô SDEs, which are described below.

Itô SDEs are a class of differential equations in which at least one of the terms is a stochastic process, producing a solution which is also a stochastic process (e.g. see Øksendal, 1985). SDEs are used to model various phenomena such as unstable stock prices or physical systems subject to noise. Typically, SDEs contain a variable which represents a disturbance which is implemented with a Brownian motion. However, it should be mentioned that other types of random behaviour are possible (exotic excitations), which usually incorporate more information than a Brownian motion or a *Wiener process*.

A typical (one) dimensional Itô SDE is of the form

$$dX_t = \mu(X_t, t) dt + \sigma(X_t, t) dB_t, \quad (2.3)$$

where B_t denotes a Wiener process (Standard Brownian motion) and μ (*drift coefficient*), σ (*diffusion coefficient*) are real functions. Eq. (2.3) should be interpreted as in the following (integral) sense

$$X_{t+s} - X_t = \int_t^{t+s} \mu(X_u, u) du + \int_t^{t+s} \sigma(X_u, u) dB_u, \quad (2.4)$$

where dB_u represents the stochastic noise component involved in the above expression and is treated as a stochastic Itô integral with respect to the Brownian motion.

As seen in Øksendal, 1985, solving SDEs is not an easy task. In addition, systems of SDEs are even harder to solve, however, their solutions are needed for a wide range of applications as outlined in Chapter 1. Nevertheless, specific transformations (e.g. see Schilling and Partzsch, 2012) or Itô's lemma can be used to find special solutions, if they exist, as presented in the following

Example 1. Assuming that the SDE of Eq. (2.3) with the initial condition $X_0 = x_0 \in \mathbb{R}$ has a solution of the form $X_t = f(B_t, t)$, then one way of finding f is the following. Based on Ito's lemma, $Y_t := f(B_t, t)$ satisfies the equation

$$dY_t = \left\{ \frac{\partial f}{\partial t}(B_t, t) + \frac{1}{2} \frac{\partial^2 f}{\partial x^2}(B_t, t) \right\} dt + \frac{\partial f}{\partial x}(B_t, t) dB_t, \quad (2.5)$$

which coincides with Eq. (2.3), if the following system is satisfied

$$\begin{aligned} \frac{\partial f}{\partial t}(x, t) + \frac{1}{2} \frac{\partial^2 f}{\partial x^2}(x, t) &= \mu(f(x, t), t), \\ \frac{\partial f}{\partial x}(x, t) &= \sigma(f(x, t), t), \end{aligned} \quad (2.6)$$

which for some special cases of μ, σ can be solved or shown that such form of solution, i.e. $X_t = f(B_t, t)$, does not exist.

2.2 Connection between Stochastic Differential and Fokker-Planck equations

As presented in Wio, 2013, if for the functions μ, σ a solution for Eq. (2.3) exists in a distributional sense, i.e. X_t has a transition probability density function (PDF), denoted by p^* ,

then this exact transition PDF p^* is given as the solution of the associated *Fokker-Planck* (F-P) equation (e.g. see Van Kampen, 2007), i.e.

$$\frac{\partial}{\partial t} p^*(x, t) = -\frac{\partial}{\partial x} (\mu(x, t) p^*(x, t)) + \frac{1}{2} \frac{\partial^2}{\partial x^2} (\sigma(x, t)^2 p^*(x, t)), \quad (2.7)$$

with the initial condition $X_0 = x_0 \in \mathbb{R}$ translating to $p^*(x, 0) = \mathbb{1}_{x_0}$, i.e. the indicator or characteristic function of point x_0 .

The relation, described by Eq. (2.7) between SDEs and F-P equations, proves useful when trying to check if a particular PDF \tilde{p} is a solution to an SDE. For instance, denoting the F-P operator as

$$\mathcal{L}_{FP}[p(x, t)] = \frac{\partial}{\partial t} p(x, t) + \frac{\partial}{\partial x} (\mu(x) p(x, t)) - \frac{1}{2} \frac{\partial^2}{\partial x^2} (\sigma(x)^2 p(x, t)), \quad (2.8)$$

and considering that $\mathcal{L}_{FP}[p^*] = 0$, checking if $\mathcal{L}_{FP}[\tilde{p}] = 0$ is satisfied, provides the distributional solution to the original SDE.

A common theme, which is observed in both Example 1 and the method described by Eq. (2.8), is the transformation of the stochastic problem, i.e. Eq. (2.3), into an equivalent deterministic one. However, the complexity remains the same, since either applying a naive Euler-Maruyama *Monte Carlo simulation* (MCS) scheme to Eq. (2.3) or finding a solution to Eq. (2.7) numerically is computationally prohibitive¹ especially when dealing with the N -dimensional counterparts of the above. That is the reason why one needs to find new techniques of solving these equations and one such technique is the *Wiener Path Integral* (WPI), presented below.

2.3 The Path Integral Method

In general, by considering an initial point in state space x_i at time t_i and a final point x_f at time t_f , where $t_f > t_i$, for a stochastic process X_t the transition PDF $p(x_f, t_f | x_i, t_i)$ can be expressed as a functional integral over the space of all possible paths $C\{x_i, t_i; x_f, t_f\}$ (see Fig. 2.1 below) in the form (e.g. see Chaichian and Demichev, 2001)

$$p(x_f, t_f | x_i, t_i) = \int_{\{x_i, t_i\}}^{\{x_f, t_f\}} \Phi \exp \left(- \int_{t_i}^{t_f} L(x, \dot{x}) dt \right) [dx(t)], \quad (2.9)$$

where a dot over a variable denotes differentiation with respect to time (t), Φ is a normalization constant and $L(x, \dot{x})$ is the Lagrangian function corresponding to the dynamical system under consideration²; see Di Matteo et al., 2014; Kougoumtzoglou et al., 2015 and references therein for more details.

It can be readily seen that the analytical solution of the WPI of Eq. (2.9) is at least a rather daunting, if not impossible, procedure; thus, an approximate solution technique is required. To this aim, it is noted that the largest contribution to the WPI comes from the trajectory for which the integral in the exponential of Eq. (2.9) becomes as small as possible. Variational calculus rules (e.g. see Ewing, 1969) dictate that this trajectory with fixed end points satisfies the extremality condition

$$\delta \int_{t_i}^{t_f} L(x_c, \dot{x}_c) dt = 0, \quad (2.10)$$

¹That is not the case, however, when trying to find stationary solutions, i.e. as $t \rightarrow \infty$.

²It is worth mentioning that there is some indeterminacy about the exact form of the L function for the general form of Eq. (2.3) as seen in the works of Dekker and Graham (e.g. see Dekker, 1978; Graham, 1977).

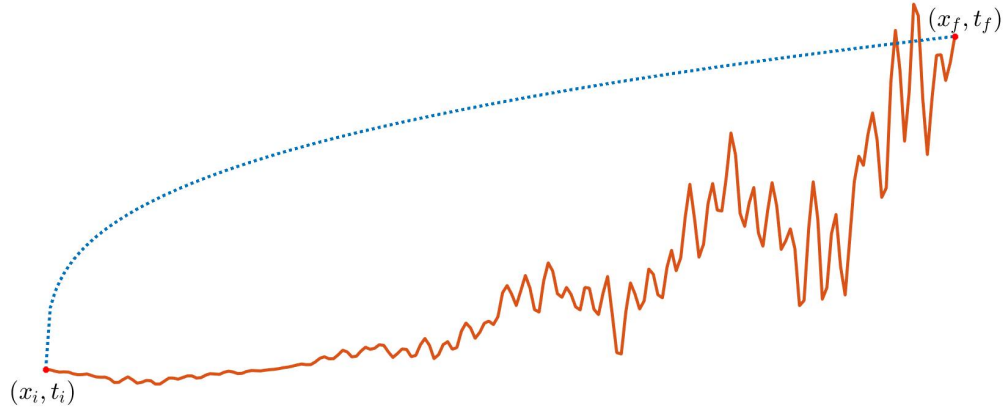


FIGURE 2.1: A sample visualization of the space of all possible paths, i.e,
 $C \left\{ x_i, t_i; x_f, t_f \right\}$.

where x_c denotes the “most probable path” to be determined by the functional optimization problem

$$\text{Min}(\text{Max}) \quad J[x_c(t)] = \int_{t_i}^{t_f} L(x_c, \dot{x}_c) dt, \quad (2.11)$$

together with the boundary conditions $x_c(t_i) = x_i$ and $x_c(t_f) = x_f$ (see Fig. 2.2 below).

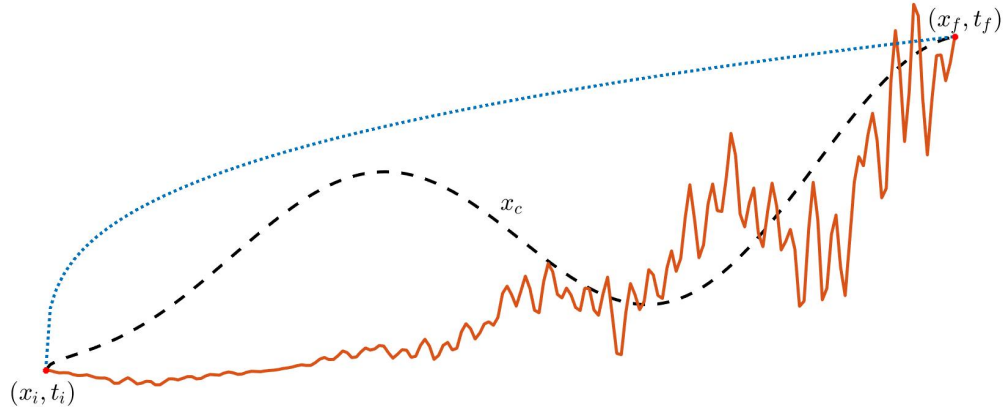


FIGURE 2.2: A sample visualization of the “most probable path”, x_c , in accordance with Fig. 2.1.

Depending on the complexity of the problem, $x_c(t)$ can be determined either by deriving and solving the Euler-Lagrange (E-L) equations associated with Eq. (2.10), i.e.

$$\frac{\partial L}{\partial x_c} - \frac{\partial}{\partial t} \frac{\partial L}{\partial \dot{x}_c} = 0, \quad (2.12)$$

in conjunction with the boundary conditions $x_c(t_i) = x_i$, $x_c(t_f) = x_f$, or, alternatively, by treating directly the deterministic *boundary value problem* (BVP) of Eq. (2.11). Once $x_c(t)$ is determined, the joint transition PDF can be approximated by

$$p(x_f, t_f | x_i, t_i) \approx \Phi \exp \left(- \int_{t_i}^{t_f} L(x_c, \dot{x}_c) dt \right). \quad (2.13)$$

Comparing Eqs. (2.9) and (2.13), it is seen that only the largest contribution to the WPI of Eq. (2.9) is considered in the approximation of Eq. (2.13); this comes from the most probable path $x_c(t)$ for which the integral in Eq. (2.11) becomes as small as possible. It is noted that the approximation of Eq. (2.13) has demonstrated satisfactory accuracy when compared to pertinent brute-force MCS data for the considered engineering dynamical systems (e.g. Di Matteo et al., 2014; Kougioumtzoglou et al., 2015). Nevertheless, clearly, there is a need for quantifying the degree of accuracy of the approximation of Eq. (2.13) in a rigorous manner and/or deriving other approximate methods based on the above framework.

Remark. This approach closely resembles the basic concept of approximating a definite integral from Classical Analysis when using the trapezoid or midpoint rule, i.e. approximating the exact solution with only one point. A basis for this approach originates from the mean value theorem, which states that for a smooth real function f on the interval $[a, b]$, there exists some $c \in (a, b)$ such that

$$f'(c) = \frac{f(b) - f(a)}{b - a}. \quad (2.14)$$

Consequently, Eq. (2.14) is equivalent to

$$f(b) - f(a) = f'(c)(b - a), \quad (2.15)$$

or in integral form

$$\int_a^b f'(t) dt = f'(c)(b - a), \quad (2.16)$$

similar to the way that Eq. (2.9) transformed to Eq. (2.13).

Chapter 3

Approximate solutions for a case of Itô SDEs

This chapter deals with the special case of Eq. (2.3), where the diffusion coefficient is constant and the drift coefficient is a nonlinear function that depends only on the space variable, i.e.

$$dX_t = \mu(X_t) dt + \sigma dB_t. \quad (3.1)$$

Altough the form of Eq. (3.1) seems restrictive, even without applying any transformations to SDEs of more general form to achieve reductions to the case of Eq. (3.1), applications can be found in engineering dynamics (e.g. see Meimaris, Kougioumtzoglou, and Pantelous, 2018a).

As demonstrated in Meimaris, Kougioumtzoglou, and Pantelous, 2018a, a basic closed form approximation for the PDF of processes evolving under Eq. (3.1) is derived, based on the most probable WPI method. In the publication presented in Section 3.1 we extend this approximation by enhancing its accuracy through an optimization scheme.

A discussion regarding the importance of the results achieved in Meimaris, Kougioumtzoglou, and Pantelous, 2018b for the subsequent chapters is given in Section 3.2.

3.1 Published Material

Approximate analytical solutions for a class of nonlinear stochastic differential equations

Meimaris Antonios, Kougioumtzoglou Ioannis and Pantelous Athanasios

Published in the European Journal of Applied Mathematics, Cambridge University Press (2018)

DOI: 10.1017/S0956792518000530

Reproduced with permission.

Begins overleaf.

Approximate analytical solutions for a class of nonlinear stochastic differential equations

A. T. MEIMARIS¹, I. A. KOUGIOUMTZOGLOU² and A. A. PANTELOUS¹

¹*Department of Econometrics and Business Statistics, Monash Business School,
Monash University, 20 Chancellors Walk, Wellington Road, Clayton, Victoria 3800, Australia
emails: Antonios.Meimaris@monash.edu, Athanasiос.Pantelous@monash.edu*

²*Department of Civil Engineering and Engineering Mechanics,
The Fu Foundation School of Engineering and Applied Science, Columbia University,
500 West 120th Street, New York, NY 10027, USA
email: ikougioum@columbia.edu*

(Received 13 January 2018; revised 27 July 2018; accepted 31 July 2018)

An approximate analytical solution is derived for a certain class of stochastic differential equations with constant diffusion, but nonlinear drift coefficients. Specifically, a closed form expression is derived for the response process transition probability density function (PDF) based on the concept of the Wiener path integral and on a Cauchy–Schwarz inequality treatment. This is done in conjunction with formulating and solving an error minimisation problem by relying on the associated Fokker–Planck equation operator. The developed technique, which requires minimal computational cost for the determination of the response process PDF, exhibits satisfactory accuracy and is capable of capturing the salient features of the PDF as demonstrated by comparisons with pertinent Monte Carlo simulation data. In addition to the mathematical merit of the approximate analytical solution, the derived PDF can be used also as a benchmark for assessing the accuracy of alternative, more computationally demanding, numerical solution techniques. Several examples are provided for assessing the reliability of the proposed approximation.

Key words: Stochastic Differential Equations, Stochastic Dynamics, Path Integral, Error quantification, Cauchy–Schwarz inequality

2010 Mathematics Subject Classification: 34K50, 60H10, 60H35, 81P20, 97K60

1 Introduction

Stochastic differential equations (SDEs) have been widely used over the past decades for modelling the complex dynamics of diverse systems in a wide range of scientific disciplines. Numerical Monte Carlo simulation (MCS) methodologies such as the Euler–Maruyama and the Milstein schemes have been among the most versatile tools for solving SDEs of general form [6]. Nevertheless, in many cases they can be computationally prohibitive, and thus, there is a need for developing alternative efficient approximate analytical solution techniques. Indicative alternative approaches include stochastic averaging [20], Markov approximations and related Fokker–Planck equations, probability density evolution schemes [13], as well as numerical versions of the Chapman–Kolmogorov equation [16, 25].

One of the promising semi-analytical techniques relates to the concept of path integral, developed independently by Wiener [26] and Feynman [4]. The rationale relates to expressing the stochastic process transition probability density function (PDF) as a functional integral over the space of all possible paths [1]; see also [23] for a large deviation theory perspective on the topic. Kougioumtzoglou and co-workers extended and applied recently the technique to engineering dynamics problems, where the structural/mechanical system under consideration is typically modelled as a set of coupled nonlinear SDEs [2, 12, 10, 11]. Although the aforementioned Wiener path integral (WPI) technique has exhibited satisfactory accuracy in determining the response PDF, its numerical implementation is associated, in general, with non-negligible computational cost [12]. In this regard, the authors derived recently an approximate analytical solution PDF for a certain class of SDEs with constant diffusion, but nonlinear drift coefficients, by relying on the WPI and on a Cauchy–Schwarz inequality treatment of the problem [14].

In this paper, the accuracy exhibited by the derived approximation of [14] is enhanced by introducing a more general form for the response process PDF. This enhancement aims at ‘tightening’ the Cauchy–Schwarz inequality as well as increasing the overall accuracy of the basic approximation in [14]. To this aim, an optimisation problem is formulated and solved by relying on an error definition based on the Fokker–Planck equation operator. Several numerical examples are included to demonstrate the accuracy of the derived approximate PDF. Comparisons with pertinent MCS data are included as well.

2 Preliminaries

Let $(\Omega, \mathcal{F}, \mathcal{F}_{t \geq 0}, \mathbb{P})$ be a complete filtered probability space on which a scalar standard Brownian motion $(B_t, t \geq 0)$ is defined; and \mathcal{F}_t is the augmentation of $\sigma\{B_s | 0 \leq s \leq t\}$ by all the \mathbb{P} -null sets of \mathcal{F} .

2.1 WPI overview

In general, for a stochastic process X_t , the transition PDF $p(x_f, t_f | x_i, t_i)$ from a point in state space x_i at time t_i to a point x_f at time t_f , where $t_f > t_i$, can be expressed as a functional integral over the space of all possible paths $C\{x_i, t_i; x_f, t_f\}$ in the form (e.g. see [1])

$$p(x_f, t_f | x_i, t_i) = \int_{\{x_i, t_i\}}^{\{x_f, t_f\}} W[x(t)] [dx(t)]. \quad (2.1)$$

In (2.1), $W[x(t)]$ represents the probability density functional, which can be explicitly determined only for relatively simple cases of stochastic processes. For instance, denoting the expectation operator as \mathbf{E} , the probability density functional for the white noise process $v(t)$, i.e. $\mathbf{E}(v(t)) = 0$ and $\mathbf{E}(v(t_1)v(t_2)) = 2\pi S_0 \delta(t_1 - t_2)$, is given by [22]:

$$W[v(t)] = \Phi \exp \left[- \int_{t_i}^{t_f} \frac{1}{2} \frac{v(t)^2}{2\pi S_0} dt \right], \quad (2.2)$$

where Φ is a normalisation coefficient. A detailed derivation and discussion of (2.2) can be found in standard path integral-related books such as [1]. In the ensuing analysis, the SDE

$$dX_t = \mu(X_t) dt + \sigma dB_t \quad (2.3)$$

Analytical solutions for nonlinear stochastic differential equations

3

is considered, where $\sigma^2 = 2\pi S_0$ and dB_t represents the formal time derivative of a white noise process of unit intensity. In this regard, combining (2.1)–(2.3) yields the transition PDF of the response process X_t (e.g. see [2, 12, 10, 11, 8])

$$p(x_f, t_f | x_i, t_i) = \int_{\{x_i, t_i\}}^{\{x_f, t_f\}} \Phi \exp \left(- \int_{t_i}^{t_f} L(x, \dot{x}) dt \right) [dx(t)], \quad (2.4)$$

where $L(x, \dot{x})$ represents the Lagrangian function associated with the process X_t and is given by

$$L(x, \dot{x}) = \frac{1}{2\sigma^2} (\dot{x} - \mu(x))^2. \quad (2.5)$$

Next, it is readily seen that evaluating analytically, the WPI of (2.4) is at least a rather challenging, if not impossible, task; thus, an approximate solution technique is required. To this aim, it is noted that the largest contribution to the WPI comes from the trajectory for which the integral in the exponential of (2.4) becomes as small as possible. According to calculus of variations [3], this trajectory with fixed end points satisfies the extremality condition

$$\delta \int_{t_i}^{t_f} L(x_c, \dot{x}_c) dt = 0, \quad (2.6)$$

where x_c denotes the ‘most probable path’ to be determined by solving the functional optimisation problem

$$\text{Min}(\text{Max}) \quad J[x_c(t)] = \int_{t_i}^{t_f} L(x_c, \dot{x}_c) dt, \quad (2.7)$$

or alternatively, by solving the Euler–Lagrange (E–L) equation associated with (2.6) (e.g. see [2, 12]), i.e.

$$\frac{\partial L}{\partial x_c} - \frac{\partial}{\partial t} \frac{\partial L}{\partial \dot{x}_c} = 0, \quad (2.8)$$

in conjunction with the boundary conditions $x_c(t_i) = x_i$, $x_c(t_f) = x_f$. Once $x_c(t)$ is determined, the response transition PDF can be approximated by

$$p(x_f, t_f | x_i, t_i) \approx \Phi \exp \left(- \int_{t_i}^{t_f} L(x_c, \dot{x}_c) dt \right). \quad (2.9)$$

Comparing (2.4) and (2.9), it is seen that only the largest contribution to the WPI of (2.4) is considered in the approximation of (2.9); this comes from the most probable path $x_c(t)$ for which the integral in (2.7) becomes as small as possible. From a computational point of view, the numerical solution of a boundary value problem (BVP) of the form of (2.7) yields a single point of the response PDF via (2.9). Therefore, following a brute force discretisation of the response PDF domain into N points requires the solution of N BVPs of (2.7). This translates into considerable computational cost, and thus, there is merit in developing more efficient solution methodologies. This is also the scope of the present paper; see also [12] for a detailed presentation.

2.2 Cauchy–Schwarz inequality

Applications of the Cauchy–Schwarz inequality have been fruitful across many areas of mathematics and applied sciences, ranging from analysis and geometry to combinatorics, probability

theory and statistics [7, 15]. For completeness, the integral form of the Cauchy–Schwarz inequality is included below, whereas a detailed presentation of the topic can be found in [21].

Lemma 2.1 *Let f and g be real functions that are continuous on the closed interval $[a, b]$. Then*

$$\left(\int_a^b f(t)g(t)dt \right)^2 \leq \int_a^b f(t)^2 dt \int_a^b g(t)^2 dt. \quad (2.10)$$

Clearly, setting $g = 1$ yields the special case

$$\int_a^b f(t)^2 dt \geq \frac{1}{b-a} \left(\int_a^b f(t)dt \right)^2. \quad (2.11)$$

3 Main results

3.1 Approximate solution PDF for a class of SDEs with constant diffusion and nonlinear drift coefficients

In this section, relying on the WPI-based approximation of (2.9) and on the Cauchy–Schwarz inequality of (2.11) in conjunction with an optimisation scheme, approximate non-stationary response PDFs are derived for the SDE of (2.3) at a minimal computational effort. The herein developed technique can be construed as a generalisation and enhancement from an accuracy perspective of the results presented in [14].

Considering (2.5) and (2.8), for fixed t_i, t_f yields

$$\ddot{x}_c = \mu(x_c) \frac{\partial \mu(x_c)}{\partial x_c}, \quad (3.1)$$

which, equivalently, can be transformed into

$$\dot{x}_c^2 = \mu(x_c)^2 + b, \quad (3.2)$$

where b is a constant. Following the derivation in [14], by substituting (3.2) into (2.5) and integrating yields

$$\int_{t_i}^{t_f} L(x_c, \dot{x}_c) dt = \frac{1}{2} \left(\frac{2 \int_{t_i}^{t_f} \dot{x}_c^2 dt - b(t_f - t_i) - 2M(x_f) + 2M(x_i)}{2\pi S_0} \right), \quad (3.3)$$

where $M(\cdot)$ denotes an antiderivative of $\mu(\cdot)$.

Next, utilising the Cauchy–Schwarz inequality (2.11), the quantity $2 \int_{t_i}^{t_f} \dot{x}_c^2 dt$ in (3.3) is bounded by

$$2 \int_{t_i}^{t_f} \dot{x}_c^2 dt \geq \int_{t_i}^{t_f} \dot{x}_c^2 dt \geq \frac{(x_f - x_i)^2}{t_f - t_i}, \quad (3.4)$$

whereas combining (3.3) and (3.4) yields

$$\int_{t_i}^{t_f} L(x_c, \dot{x}_c) dt \geq \frac{1}{2\sigma^2} \left(\frac{(x_f - x_i)^2}{t_f - t_i} - b(t_f - t_i) - 2M(x_f) + 2M(x_i) \right). \quad (3.5)$$

Analytical solutions for nonlinear stochastic differential equations

Thus, considering (2.9) and (3.5), an approximation for the response transition PDF of (2.3) was derived in [14] in the form

$$\hat{p}(x_f, t_f | x_i, t_i) = F(t_f | x_i, t_i) \exp(-G(x_f, t_f | x_i, t_i)), \quad (3.6)$$

where

$$G(x_f, t_f | x_i, t_i) = \frac{(x_f - x_i)^2 + (-2M(x_f) + 2M(x_i))(t_f - t_i)}{2(t_f - t_i)\sigma^2}. \quad (3.7)$$

Note that the constant, for given t_i and t_f , term $\exp\left(\frac{-b(t_f - t_i)}{2\sigma^2}\right)$ has been merged with the constant F in (3.6) to be determined as

$$F(t_f | x_i, t_i) = \left(\int_{\mathcal{D}(M)} \exp(-G(y, t_f | x_i, t_i)) dy \right)^{-1}, \quad (3.8)$$

where $\mathcal{D}(M)$ denotes the domain of M .

It can be readily seen that $\hat{p} : \mathcal{D}(M) \times (t_i, +\infty) \times \{x_i\} \times \{t_i\} \rightarrow \mathbb{R}_+$ in (3.6) can be directly used as an analytical approximation of the response process PDF without resorting to the numerical solution of the E–L equation (2.8) and, thus, requires essentially zero computational effort for its determination. However, as demonstrated in [14], although the approximation of (3.6) is capable, in general, of capturing the salient features of the solution PDF, in many cases the degree of accuracy exhibited can be inadequate. In this regard, a more general form is proposed herein for the solution PDF, i.e.

$$\hat{p}_{(k,n)}(x_f, t_f | x_i, t_i) = F_{(k,n)}(t_f | x_i, t_i) \exp(-G_{(k,n)}(x_f, t_f | x_i, t_i)), \quad (3.9)$$

where

$$G_{(k,n)}(x_f, t_f | x_i, t_i) = \frac{k(x_f - x_i)^2 + n(-2M(x_f) + 2M(x_i))(t_f - t_i)}{2(t_f - t_i)\sigma^2}, \quad (3.10)$$

and the constant F in (3.9) to be determined as

$$F_{(k,n)}(t_f | x_i, t_i) = \left(\int_{\mathcal{D}(M)} \exp(-G_{(k,n)}(y, t_f | x_i, t_i)) dy \right)^{-1}. \quad (3.11)$$

Note that the general solution form in (3.9) has two additional ‘degrees of freedom’, i.e. the parameters k and n to be determined based on an appropriate optimisation scheme as detailed in the following section. The rationale behind this choice relates to utilising available knowledge and integrating it in an optimisation scheme for enhancing the overall accuracy of (3.9). In particular, the parameter k relates to optimising and ‘tightening’ the Cauchy–Schwarz inequality of (3.4), whereas the parameter n refers to the overall accuracy of the WPI approximation of (2.9). In comparison to (3.6), it is anticipated that the approximation of (3.9) will exhibit higher accuracy, at the expense of course of some added modest computational cost related to the optimisation algorithm.

3.2 Error minimisation and optimisation scheme

To determine the parameters k and n in (3.9), for a given norm ($\|\cdot\|_q$), the error quantity $\|\hat{p}_{(k,n)} - p^*\|_q$ is sought to be minimised, where p^* denotes the exact solution PDF. Nevertheless, since p^* is unknown, an alternative error minimisation scheme is adopted in the ensuing analysis based on the Fokker–Planck equation operator (see also [14] and references therein). Specifically, the exact transition PDF p^* for the SDE of (2.3) is given as the solution of the associated Fokker–Planck equation [24], i.e.

$$\frac{\partial p^*(x,t)}{\partial t} = -\frac{\partial (\mu(x)p^*(x,t))}{\partial x} + \frac{\sigma^2}{2} \frac{\partial^2 p^*(x,t)}{\partial x^2}. \quad (3.12)$$

Next, denoting the Fokker–Planck operator as

$$\mathcal{L}_{FP}[p(x,t)] = \frac{\partial p(x,t)}{\partial t} + \frac{\partial (\mu(x)p(x,t))}{\partial x} - \frac{\sigma^2}{2} \frac{\partial^2 p(x,t)}{\partial x^2}, \quad (3.13)$$

and considering that $\mathcal{L}_{FP}[p^*] = 0$, the error is defined as

$$err_q = \|\mathcal{L}_{FP}[\hat{p}_{(k,n)} - p^*]\|_q = \|\mathcal{L}_{FP}[\hat{p}_{(k,n)}] - \mathcal{L}_{FP}[p^*]\|_q = \|\mathcal{L}_{FP}[\hat{p}_{(k,n)}]\|_q. \quad (3.14)$$

Due to the analytical expression of $\hat{p}_{(k,n)}$, the error quantity $err_q = \|\mathcal{L}_{FP}[\hat{p}_{(k,n)}]\|_q$ can be explicitly determined as a function of k and n , see also [14]. In this regard, for a chosen q norm and final time t_f , the values of k, n are numerically evaluated by solving the optimisation problem

$$\hat{z}_q = (\hat{k}, \hat{n})_q = \arg \min_{k, n \in \mathbb{R}} err = \arg \min_{k, n \in \mathbb{R}} \|\mathcal{L}_{FP}[\hat{p}_{(k,n)}(\cdot, t_f)]\|_q, \quad (3.15)$$

and, thus, the approximate response PDF of (3.9) is determined.

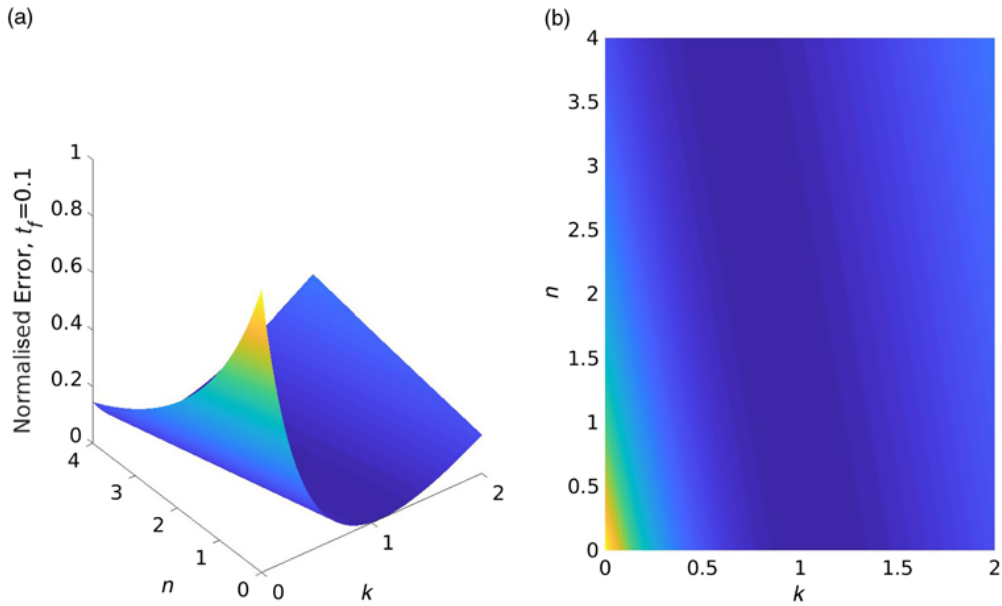
4 Examples

In the ensuing numerical examples, a standard interior point method [5, 17] using Matlab’s *fmincon* built-in function is employed to solve the unconstrained optimisation problem of (3.15), in conjunction with the $\|\cdot\|_2$ norm. To this aim, the basic approximation of (3.6) with $(k, n) = (1, 1)$ serves as a natural choice for the initial starting point of the algorithm. Of course, in the current setting, the global minimum can be readily and directly identified by the three-dimensional plot of the corresponding objective function of (3.14) at minimal computational cost. However, the proposed numerical optimisation scheme has the additional merit that it can still be applied even in cases of potentially more sophisticated than (3.9) PDF approximations, where more than two parameters would need to be determined.

In all the numerical examples, the algorithm converged in less than approximately 50 iterations, which translates into a matter of few seconds from a computational cost perspective. The accuracy of the approximate PDF of (3.9) is demonstrated by comparisons to the PDF estimated based on pertinent MCS data (100,000 realisations) produced by numerically integrating the original equation (2.3).

Analytical solutions for nonlinear stochastic differential equations

7

FIGURE 1. Example 4.1 objective function of (3.15) for $t_f = 0.1$.**4.1 Duffing kind nonlinearity: Hardening system**

Consider the SDE of (2.3) with the hardening Duffing kind (e.g. [18]) nonlinear drift coefficient of the form

$$\mu(x) = -x - \lambda x^3. \quad (4.1)$$

In (4.1), λ is a parameter controlling the nonlinearity magnitude, whereas in the following, zero initial conditions are assumed, i.e. $X_0 = 0$, and the value $\sigma^2 = 2\pi S_0 = 1$. Taking into account that $M(x) = -\frac{x^2}{2} - \frac{\lambda}{4}x^4$, the PDF $\hat{p}_{(k,n)}$ of (3.9) takes the form

$$\hat{p}_{(k,n)}(x_f, t_f | 0, 0) = F(t_f | 0, 0) \exp \left(-\frac{kx_f^2 + n \left(x_f^2 + \frac{\lambda}{2}x_f^4 \right) t_f}{2t_f} \right). \quad (4.2)$$

Next, utilising the parameter values $\lambda = 1$, $\sigma^2 = 2\pi S_0 = 1$, and applying the numerical optimisation scheme of (3.15) based on the $\|\cdot\|_2$ norm, yields the values for k and n . Specifically, in Figures 1 and 2, the objective functions of (3.14) are plotted for time instants $t_f = 0.1$ and $t_f = 1$, respectively, while in Table 1, the computed values of k and n are shown. In Figure 3, the approximate PDF $\hat{p}_{(k,n)}$ of (4.2) as well as the basic approximation \hat{p} of (3.6) are plotted and compared with MCS-based estimated PDFs. It is seen that the herein proposed solution PDF approximation is in very good agreement with MCS data and yields enhanced performance as compared to the basic approximate PDF of (3.6).

4.2 Duffing kind nonlinearity: Bimodal response PDF

Consider next the SDE of (2.3) with the Duffing kind nonlinear drift coefficient of the form

$$\mu(x) = x - \lambda x^3. \quad (4.3)$$

Table 1. Computed (k, n) values for various final time instants t_f and starting point $(1, 1)$ for example 4.2

	$t_f = 0.1$	$t_f = 1$
k	0.8957	0.3218
n	1.5981	1.8080

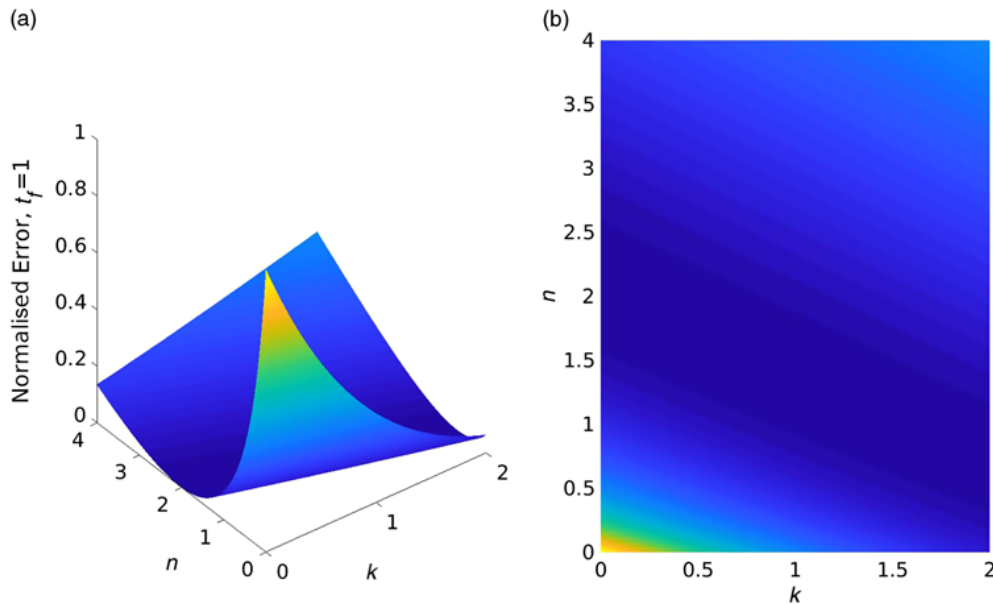


FIGURE 2. Example 4.1 objective function of (3.15) for $t_f = 1$.

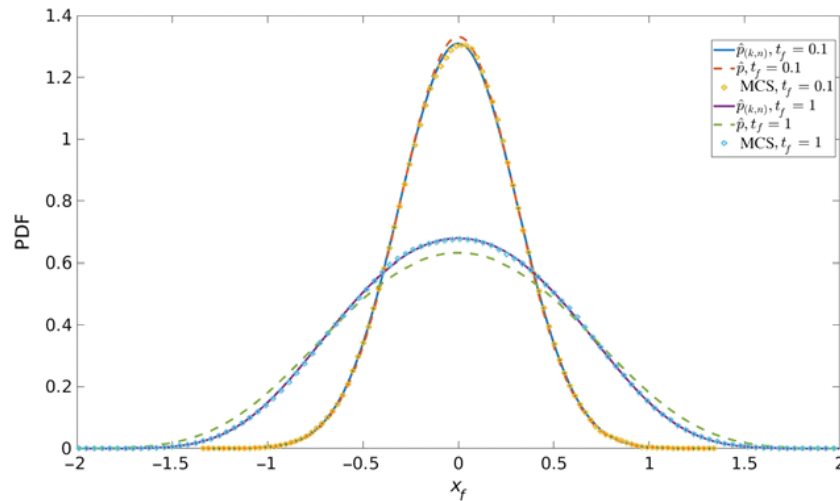


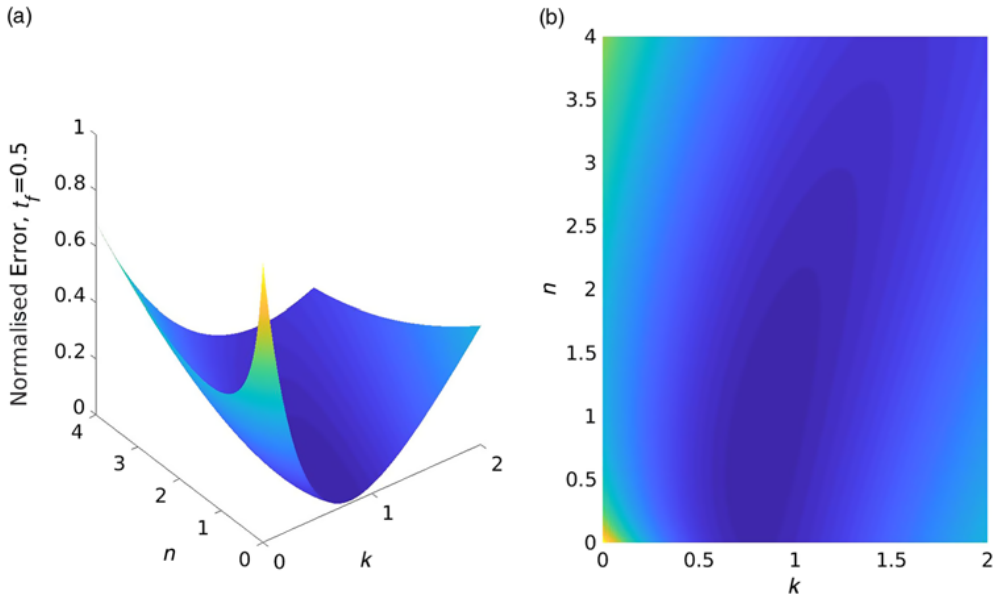
FIGURE 3. Approximate response PDFs $\hat{p}_{(k,n)}$ and \hat{p} for a first-order hardening Duffing kind nonlinear SDE and comparisons with the MCS-based (100,000 realisations) PDF estimates.

Analytical solutions for nonlinear stochastic differential equations

9

Table 2. Computed (k, n) values for various final time instants t_f and starting point $(1, 1)$ for example 4.2

	$t_f = 0.5$	$t_f = 5$
k	0.8253	1.2224
n	0.7373	1.4920

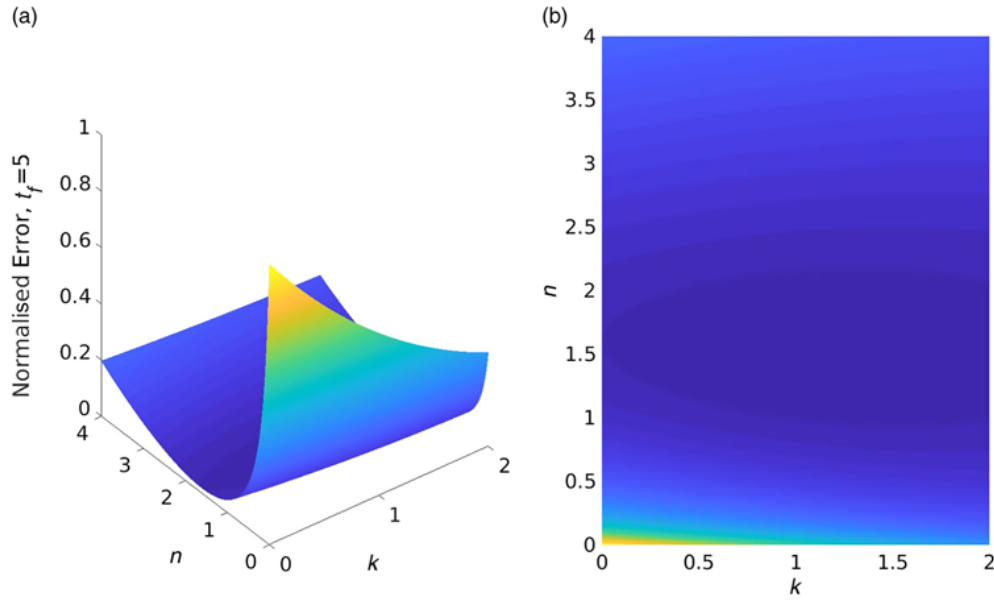
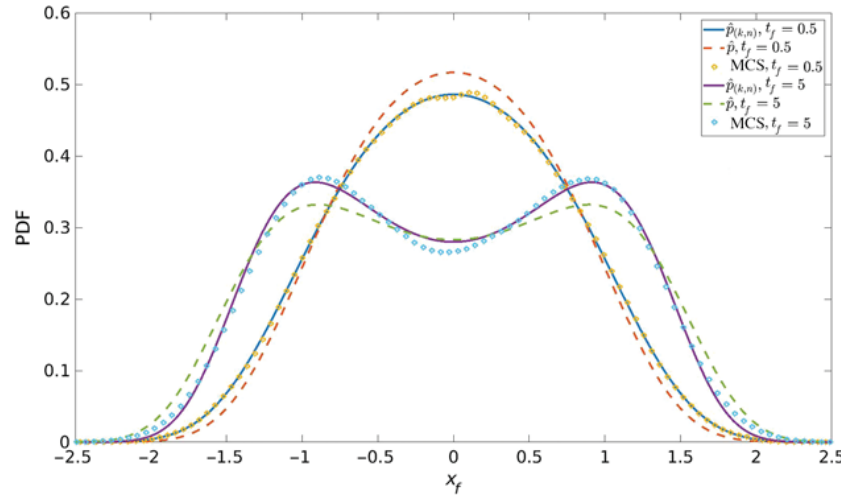
FIGURE 4. Example 4.2 objective function of (3.15) for $t_f = 0.5$.

Note that in comparison to (4.1), the nonlinearity form of (4.3) yields a bimodal response PDF for relatively large time instants t_f [18]. Thus, it can be argued that this bimodal PDF is more challenging to be estimated than the unimodal PDF corresponding to (4.1). Similarly as in (4.1), for zero initial conditions, (3.9) takes the form

$$\hat{p}_{(k,n)}(x_f, t_f | 0, 0) = F(t_f | 0, 0) \exp \left(-\frac{kx_f^2 + n \left(-x_f^2 + \frac{\lambda}{2} x_f^4 \right) t_f}{2t_f} \right), \quad (4.4)$$

while for the parameter values $\lambda = 1$, $\sigma^2 = 2\pi S_0 = 1$, the objective functions of (3.14) are plotted for time instants $t_f = 0.5$ and $t_f = 5$ in Figures 4 and 5, respectively. In Table 2, the values of k and n , as determined by the numerical optimisation scheme, are shown, whereas in Figure 6 the approximate PDF $\hat{p}_{(k,n)}$ of (4.4) as well as the basic approximation \hat{p} of (3.6) are plotted and compared with MCS-based estimated PDFs. It is readily seen that even in the relatively challenging case of the bimodal PDF, the herein proposed enhanced approximation is in very good agreement with MCS data and manages to capture the salient features of the PDF.

10

A. T. Meimaris et al.FIGURE 5. Example 4.2 objective function of (3.15) for $t_f = 5$.FIGURE 6. Approximate response PDFs $\hat{p}_{(k,n)}$ and \hat{p} for a first-order bimodal Duffing kind nonlinear SDE and comparisons with the MCS-based (100,000 realisations) PDF estimates.

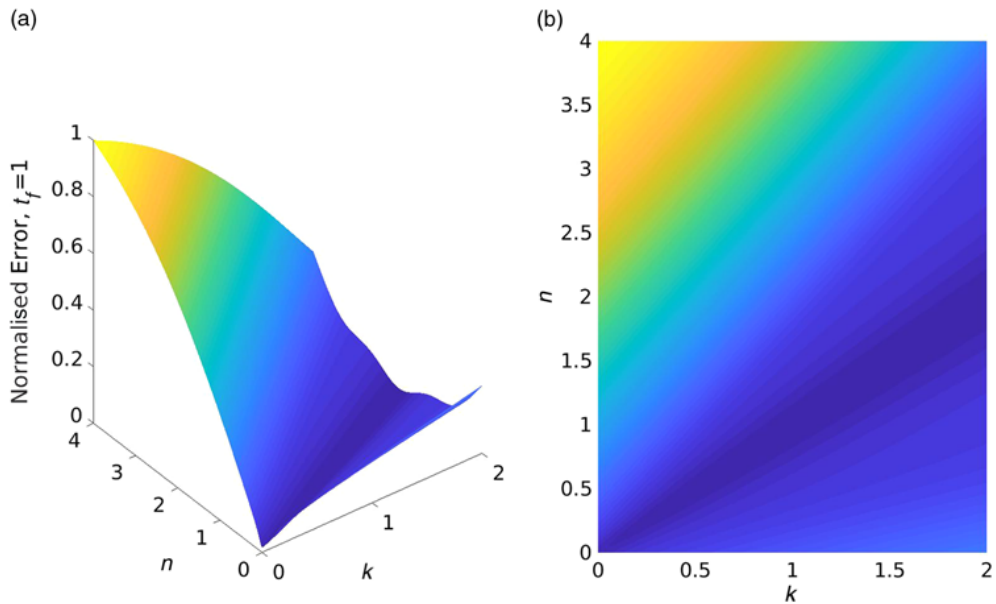
4.3 Haldane nonlinear stochastic equation

Consider next the SDE of (2.3) with the Haldane kind nonlinear drift coefficient of the form [19]

$$\mu(x) = -\frac{V_m x}{K_m + x + \frac{x^2}{K_i}}. \quad (4.5)$$

Analytical solutions for nonlinear stochastic differential equations

11

FIGURE 7. Example 4.2 objective function of (3.15) for $t_f = 1$.

This kind of modelling has been widely used to describe substrate inhibition kinetics and biodegradation of inhibitory substrates [19]. In (4.5), V_m and K_m denote the limiting rate and Michaelis constant, respectively, and K_i is the inhibition constant, while the process under consideration denotes the substrate concentration. In the following, the initial condition $X_0 = 10$ is considered and the parameter values $\sigma^2 = 2\pi S_0 = 0.01$ and $V_m = 1$, $K_m = 1$, $K_i = 20$, in accordance with [19]. Taking into account that $M(x) = -(5\sqrt{5} + 10) \log(x + 4\sqrt{5} + 10) - (5\sqrt{5} + 10) \log(x - 4\sqrt{5} + 10)$, the PDF $\hat{p}_{(k,n)}$ of (3.9) takes the form

$$\hat{p}_{(k,n)}(x_f, t_f | 10, 0) = F(t_f | 10, 0) \exp \left(-\frac{k (x_f - 10)^2 + 2n (-M(x_f) + M(10)) t_f}{2t_f \sigma^2} \right). \quad (4.6)$$

In Figures 7–9, the objective functions of (3.14) are plotted for time instants $t_f = 1$, $t_f = 5$ and $t_f = 10$, respectively, while in Table 3, the computed values of k and n are shown. In Figure 10, the approximate PDF $\hat{p}_{(k,n)}$ of (4.6) as well as the basic approximation p_B of (3.6) are plotted and compared with MCS-based estimated PDFs. It is seen that although the accuracy of the basic approximation of (3.6) deteriorates for larger time instants t_f , the accuracy of the enhanced approximation of (3.9) remains in excellent agreement as compared to pertinent MCS data.

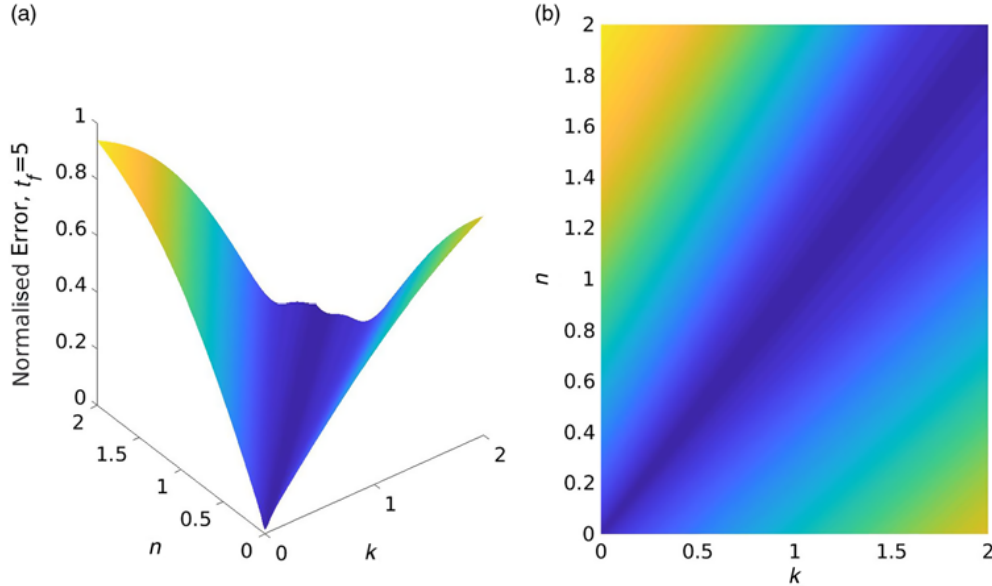
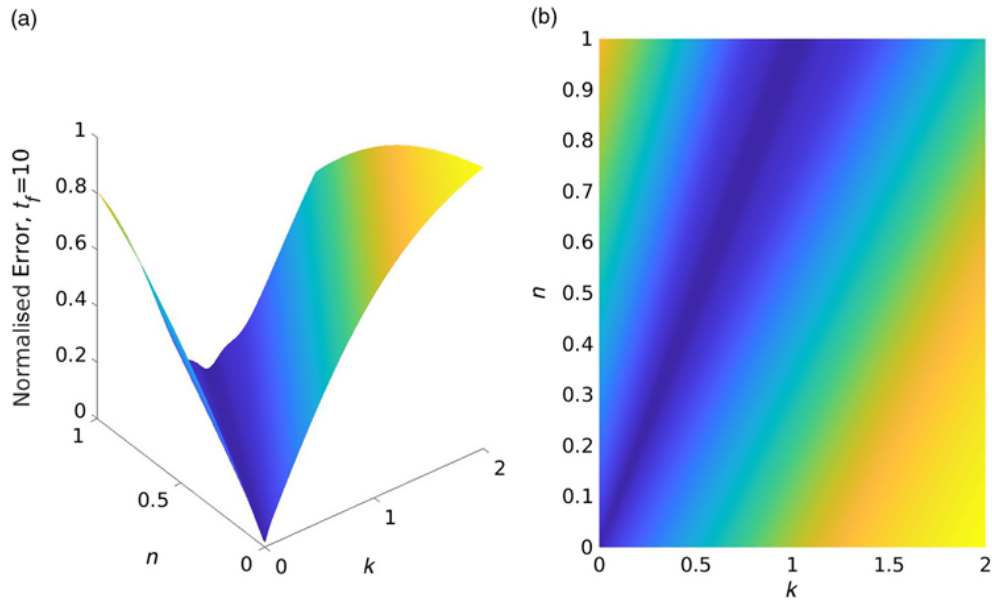
4.4 Oscillators with nonlinear damping

Consider a single degree-of-freedom oscillator with nonlinear damping whose motion is governed by

$$\ddot{y} + \beta \dot{y} + \omega_0^2 y + f(\dot{y}) = v(t), \quad (4.7)$$

12

A. T. Meimaris et al.

FIGURE 8. Example 4.2 objective function of (3.15) for $t_f = 5$.FIGURE 9. Example 4.2 objective function of (3.15) for $t_f = 10$.

where $f(\dot{y})$ is a nonlinear function depending on the response velocity and β is a linear damping coefficient, where $\beta = 2\zeta_0\omega_0$; ζ_0 is the ratio of critical damping and ω_0 is the natural frequency of the corresponding linear oscillator.

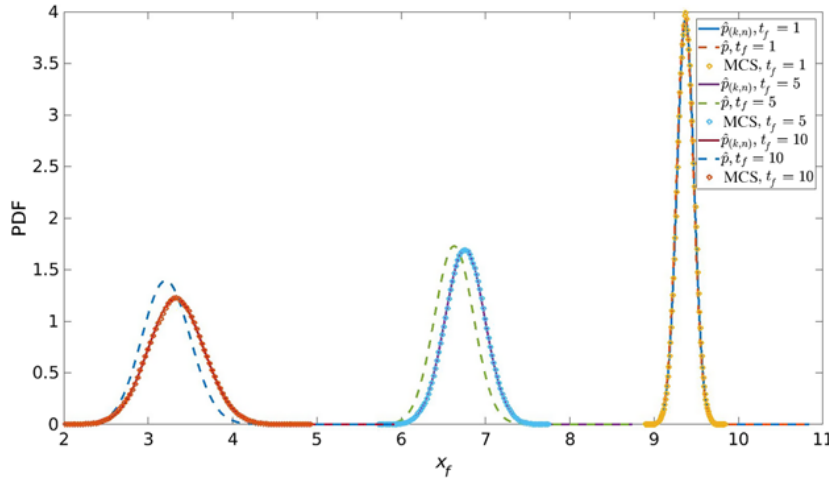
As shown in [10], a stochastic averaging/linearisation treatment can be applied to (4.7) and reduce the second-order SDE into a first-order SDE of the form of (2.3) governing the evolution in time of the response amplitude. Specifically, adopting the assumption of light damping, it can

Analytical solutions for nonlinear stochastic differential equations

13

Table 3. Computed (k, n) values for various final time instants t_f and starting point $(1, 1)$ for example 4.3

	$t_f = 1$	$t_f = 5$	$t_f = 10$
k	0.9876	0.9698	0.7851
n	0.9787	0.9350	0.7688

FIGURE 10. Approximate response PDF $\hat{p}_{(k,n)}$ and \hat{p} for a Haldane kind nonlinear SDE and comparisons with the MCS-based (100,000 realisations) PDF estimates.

be argued that the nonlinear oscillator (4.7) exhibits a pseudo-harmonic behaviour described by the equations

$$y(t) = x \cos[\omega_0 t + \phi(t)] \quad (4.8)$$

and

$$\dot{y} = -\omega_0 x \sin[\omega_0 t + \phi(t)]. \quad (4.9)$$

In (4.8) and (4.9), x denotes the response amplitude defined as

$$x = \sqrt{y^2 + \dot{y}^2 / \omega_0^2}, \quad (4.10)$$

whereas $\phi(t)$ denotes the response phase.

Assuming next that x is a slowly varying function with respect to time, a statistical linearisation treatment (e.g. [18]) yields an equivalent to (4.7) oscillator of the form

$$\ddot{y} + \beta(x)\dot{y} + \omega_0^2 y = v(t), \quad (4.11)$$

where

$$\beta(x) = \beta + \frac{-\frac{1}{\pi} \int_0^{2\pi} \sin[\psi] f(-\omega_0 x \sin \psi) d\psi}{x \omega_0}. \quad (4.12)$$

Further, resorting to stochastic averaging (e.g. [9]), the response amplitude can be decoupled from the response phase, yielding a first-order SDE for the response amplitude x , i.e.

$$\dot{x} = -\frac{1}{2}\beta(x)x + \frac{\pi S_0}{2x\omega_0^2} + \frac{\sqrt{\pi S_0}}{\omega_0}\eta(t), \quad (4.13)$$

where $\eta(t)$ is a white noise process of unit intensity.

It can be readily seen that (4.13) is an SDE of the form of (2.3) with drift μ and diffusion σ coefficients given by

$$\mu(x) = -\frac{1}{2}\beta(x)x + \frac{\pi S_0}{2x\omega_0^2} \quad (4.14)$$

and

$$\sigma = \frac{\sqrt{\pi S_0}}{\omega_0}, \quad (4.15)$$

respectively. As an illustrative example, the linear plus cubic damping oscillator

$$\ddot{y} + \beta \dot{y}(1 + \epsilon \dot{y}^2) + \omega_0^2 y = v(t) \quad (4.16)$$

is considered next. For this case, (4.2) becomes

$$\beta(x) = \beta \left(1 + \epsilon \frac{3}{4} \omega_0^2 x^2 \right). \quad (4.17)$$

In (4.17), ϵ is a parameter controlling the nonlinearity magnitude, whereas in the following, the initial conditions, $y(t_i = 0) = 1$, $\dot{y}(t_i = 0) = 0$, and the parameter values ($\omega_0 = 1$, $\zeta_0 = 0.01$, $S_0 = \frac{6}{\pi} \zeta_0$) are considered. Next, taking into account that $M(x) = -\frac{\beta}{2} \left(\frac{x^2}{2} + \epsilon \frac{3}{16} \omega_0^2 x^4 \right) + \frac{\pi S_0}{2\omega_0^2} \log(x)$, the PDF of (3.9) for oscillator response amplitude takes the form

$$\begin{aligned} & \hat{p}_{(k,n)}(x_f, t_f | 1, 0) \\ &= F(t_f | 1, 0) \exp \left(-\frac{k (x_f - 1)^2 + n \left(\beta \left(\frac{x_f^2}{2} + \epsilon \frac{3}{16} \omega_0^2 x_f^4 - \frac{1}{2} - \epsilon \frac{3}{16} \omega_0^2 \right) - \frac{\pi S_0}{\omega_0^2} \log(x_f) \right) t_f}{2t_f \frac{\pi S_0}{\omega_0^2}} \right), \end{aligned} \quad (4.18)$$

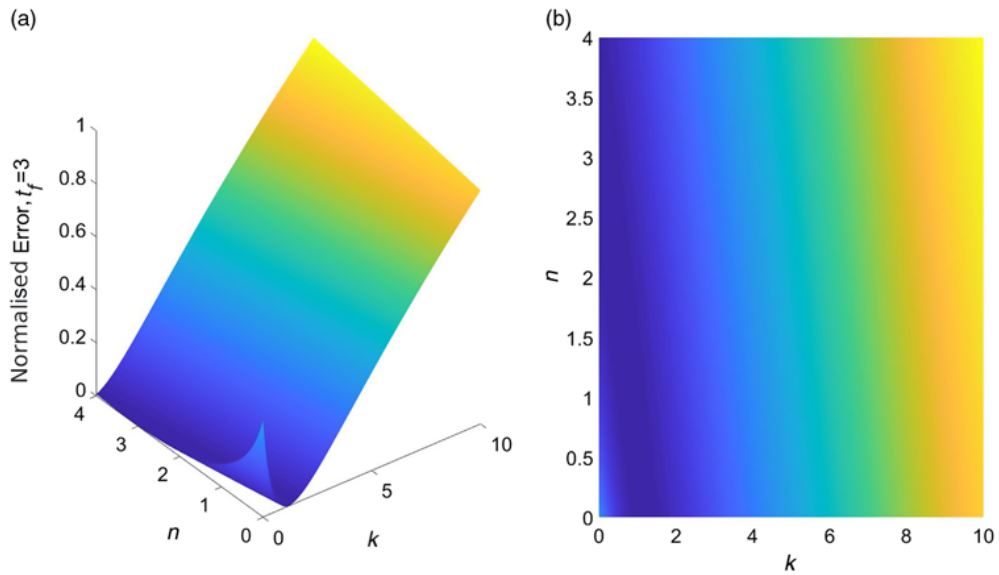
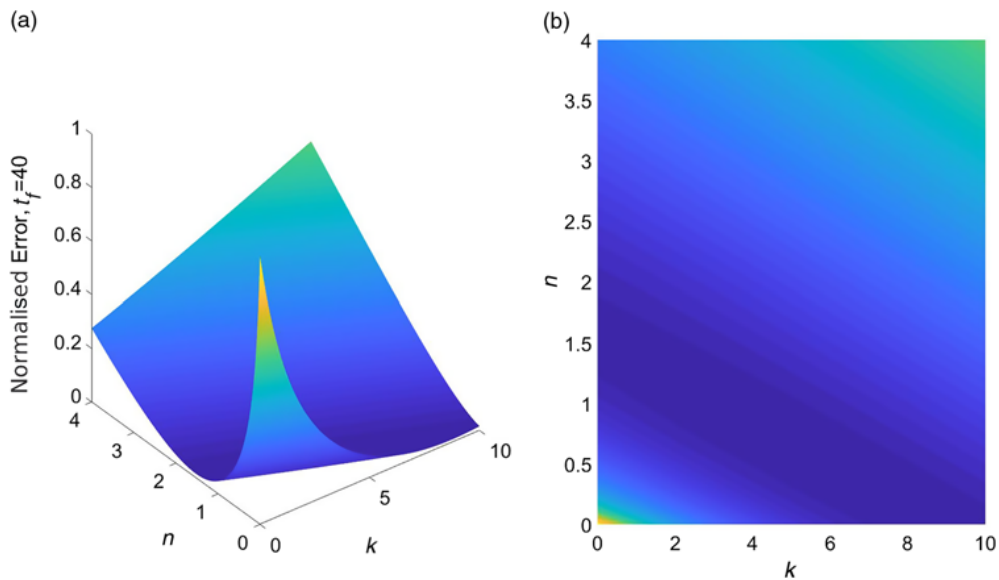
while for the parameter value $\epsilon = 3$, the objective functions of (3.14) are plotted for time instants $t_f = 3$ and $t_f = 40$ in Figures 11 and 12, respectively. In Table 4, the values of k and n as determined by the numerical optimisation scheme are shown, whereas in Figure 13, the approximate PDF $\hat{p}_{(k,n)}$ of (4.18) as well as the basic approximation \hat{p} of (3.6) are plotted and compared with MCS-based estimated PDFs. It is readily seen that even in this relatively challenging case of a linear plus cubic damping oscillator, the herein proposed enhanced approximation is in very good agreement with MCS data and manages to capture the salient features of the PDF.

Analytical solutions for nonlinear stochastic differential equations

15

Table 4. Computed (k, n) values for various final time instants t_f and starting point $(1, 1)$ for example 4.4

	$t_f = 3$	$t_f = 40$
k	0.4076	6.5478
n	2.0611	0.3817

FIGURE 11. Example 4.4 objective function of (3.15) for $t_f = 3$.FIGURE 12. Example 4.4 objective function of (3.15) for $t_f = 40$.

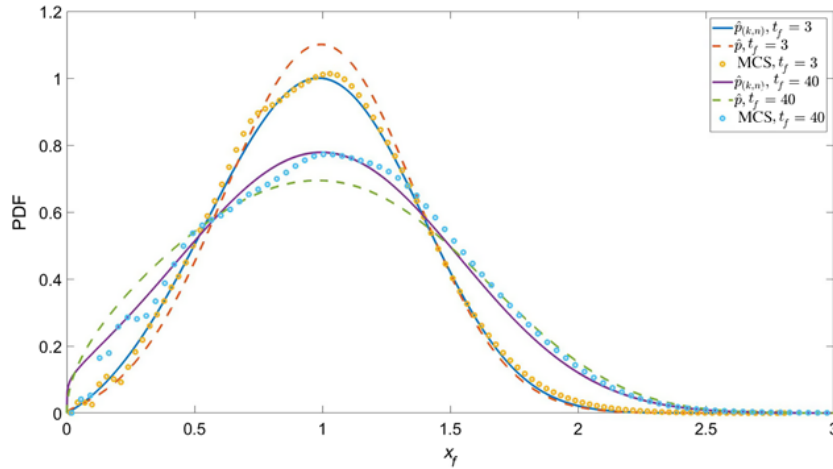


FIGURE 13. Approximate response PDFs $\hat{p}_{(k,n)}$ and \hat{p} for a linear plus cubing damping oscillator and comparisons with the MCS-based (100,000 realisations) PDF estimates.

5 Conclusion

In this paper, an approximate analytical expression for the response transition PDF of a class of SDEs with constant diffusion, but nonlinear drift coefficients, has been derived based on the concept of the WPI and on a Cauchy–Schwarz inequality treatment. This has been done in conjunction with formulating and solving an error minimisation problem by relying on the associated Fokker–Planck equation operator. In comparison to the basic approximation proposed in [14], the herein derived approximate PDF exhibits enhanced accuracy as demonstrated by pertinent MCS data. Overall, a closed form approximate analytical solution PDF has been derived at minimal computational cost, which can serve also as a benchmark for assessing the performance of alternative, more computationally demanding, stochastic dynamics numerical methodologies.

Acknowledgement

I. A. Kougioumtzoglou gratefully acknowledges the support through his CAREER award by the CMMI Division of the National Science Foundation, USA (award number: 1748537).

Conflict of interest

None.

References

- [1] CHAICHIAN, M. & DEMICHEV, A. (2001) *Path Integrals in Physics: Volume I Stochastic Processes and Quantum Mechanics*, CRC Press, Bath, UK.
- [2] DI MATTEO, A., KOUGIOUTZOGLOU, I. A., PIRROTTA, A., SPANOS, P. D. & DI PAOLA, M. (2014) Stochastic response determination of nonlinear oscillators with fractional derivatives elements via the Wiener path integral. *Prob. Eng. Mech.* **38**, 127–135.
- [3] EWING, G. M. (1969) *Calculus of Variations with Applications*, Dover Publications, New York, USA.

Analytical solutions for nonlinear stochastic differential equations

17

- [4] FEYNMAN, R. P. (1948) Space-time approach to non-relativistic quantum mechanics. *Rev. Modern Phys.* **20**(2), 367.
- [5] FORSGREN, A., GILL, P. E. & WRIGHT, M. H. (2002) Interior methods for nonlinear optimization. *SIAM Rev.* **44**(4), 525–597.
- [6] GRIGORIU, M. (2002) *Stochastic Calculus: Applications in Science and Engineering*, Springer Science & Business Media, New York, USA.
- [7] KAY, S. M. (1993) *Fundamentals of Statistical Signal Processing: Estimation Theory*, Prentice Hall PTR.
- [8] KOUGIOUTZOGLOU, I. A. (2017) A Wiener path integral solution treatment and effective material properties of a class of one-dimensional stochastic mechanics problems. *ASCE J. Eng. Mech.* **143**(6), 04017014, 1–12. doi:[10.1061/\(ASCE\)EM.1943-7889.0001211](https://doi.org/10.1061/(ASCE)EM.1943-7889.0001211).
- [9] KOUGIOUTZOGLOU, I. A. & SPANOS, P. D. (2009) An approximate approach for nonlinear system response determination under evolutionary stochastic excitation. *Curr. Sci.* **97**(8), 1203–1211.
- [10] KOUGIOUTZOGLOU, I. A. & SPANOS, P. D. (2012) An analytical Wiener path integral technique for non-stationary response determination of nonlinear oscillators. *Prob. Eng. Mech.* **28**, 125–131.
- [11] KOUGIOUTZOGLOU, I. A. & SPANOS, P. D. (2014) Nonstationary stochastic response determination of nonlinear systems: a Wiener path integral formalism. *ASCE J. Eng. Mech.* **140**(9), 04014064, 1–14. doi:[10.1061/\(ASCE\)EM.1943-7889.0000780](https://doi.org/10.1061/(ASCE)EM.1943-7889.0000780).
- [12] KOUGIOUTZOGLOU, I. A., DI MATTEO, A., SPANOS, P. D., PIRROTTA, A. & DI PAOLA, M. (2015) An efficient Wiener path integral technique formulation for stochastic response determination of nonlinear MDOF systems. *ASME J. Appl. Mech.* **82**(10), 101005.
- [13] LI, J. & CHEN, J. (2009) *Stochastic Dynamics of Structures*, John Wiley & Sons, (Asia) Pte Ltd.
- [14] MEIMARIS, A. T., KOUGIOUTZOGLOU, I. A. & PANTEOUS, A. A. (2018) A closed form approximation and error quantification for the response transition probability density function of a class of stochastic differential equations. *Prob. Eng. Mech.*, **54**, 87–94. doi:[10.1016/j.probengmech.2017.07.005](https://doi.org/10.1016/j.probengmech.2017.07.005).
- [15] MUKHOPADHYAY, N. (2000) *Probability and Statistical Inference*, Marcel Dekker Inc, New York, USA.
- [16] NAESS, A. & JOHNSEN, J. M. (1993) Response statistics of nonlinear, compliant offshore structures by the path integral solution method. *Prob. Eng. Mech.* **8**(2), 91–106.
- [17] NOCEDAL, J. & WRIGHT, S. J. (1999) *Numerical Optimization*, Springer, New York, USA.
- [18] ROBERTS, J. B. & SPANOS, P. D. (2003) *Random Vibration and Statistical Linearization*, Courier Corporation, New York, USA.
- [19] SONNAD, J. R. & GOUDAR, C. T. (2004) Solution of the Haldane equation for substrate inhibition enzyme kinetics using the decomposition method. *Math. Comput. Model.* **40**(5–6), 573–582.
- [20] SPANOS, P. D., KOUGIOUTZOGLOU I. A., DOS SANTOS K. R. M. & BECK A. T. (2018) Stochastic averaging of nonlinear oscillators: Hilbert transform perspective. *ASCE J. Eng. Mech.* **144**(2), 04017173, 1–9.
- [21] STEELE, J. M. (2004) *The Cauchy–Schwarz Master Class: An Introduction to the Art of Mathematical Inequalities*, Cambridge University Press, New York, USA.
- [22] TANIGUCHI, T. & COHEN, E. G. D. (2008) Inertial effects in nonequilibrium work fluctuations by a path integral approach. *J. Stat. Phys.* **130**(1), 1–26.
- [23] TOUCHETTE, H. (2009) The large deviation approach to statistical mechanics. *Phys. Rep.* **478**, 1–69.
- [24] VAN KAMPEN, N. G. (1992) *Stochastic Processes in Physics and Chemistry*, Elsevier, New York, USA.
- [25] WEHNER, M. F. & WOLFER, W. G. (1983) Numerical evaluation of path-integral solutions to Fokker–Planck equations. II. Restricted stochastic processes. *Phys. Rev. A* **28**, 3003.
- [26] WIENER, N. (1921) The average of an analytic functional and the Brownian movement. *Proc. Natl Acad. Sci.* **7**(10), 294–298.

3.2 Discussion

The main focus of this research is the development of a new path integral framework that avoids the computational cost of determining explicitly the most probable path as described in Section 2.3, providing a new analytical (closed-form) approximate solution to SDEs with zero, or near zero, computational cost.

Indeed, this goal was achieved for the case of stochastic processes governed by equations of the form of Eq. (3.1), however, in order to apply the developed technique in the area of option pricing for more complex underlying processes, an extension is required. For instance, interest rate models and volatility models such as the *Cox-Ingersoll-Ross* (CIR) and the *constant elasticity of variance* (CEV) models, respectively, require the underlying process to be modelled in a more general form of Eq. (3.1), specifically

$$dX_t = \mu(X_t) dt + \sigma(X_t) dB_t, \quad (3.2)$$

where now only the restriction of time-homogeneity on the drift and diffusion coefficients is assumed.

Thus, in the following chapter, the method presented in Meimaris, Kougioumtzoglou, and Pantelous, 2018b is revised and enhanced, in order to deal with the more interesting SDEs of the form of Eq. (3.2).

Chapter 4

Approximate solutions for nonlinear Itô SDEs

Based on the arguments given in the previous chapter, we introduce a method of approximating, in an efficient manner, the solution, in a distributional sense, of nonlinear Itô *Stochastic Differential Equations* (SDEs) of the form of Eq. (3.2), i.e., $dX_t = \mu(X_t) dt + \sigma(X_t) dB_t$, where B_t denotes a Wiener process (Standard Brownian motion) and μ (*drift coefficient*), σ (*diffusion coefficient*) are real functions. It is noted that only the restriction of time-homogeneity on the drift and diffusion coefficients is assumed.

This general form of SDEs provides a wide variety of applications, ranging from smart materials and bioengineering to interest rate models and volatility models such as the Cox-Ingersoll-Ross (CIR) and the *constant elasticity of variance* (CEV) models, respectively. Specifically, since option prices are very sensitive to small differences in volatility inputs (e.g. see Figlewski, 1989 for more details), not only computationally efficient, but extremely accurate PDF approximations are necessary to this end.

Thus, in the publication in Section 4.1 we develop the natural extension of the previous chapter's result for Itô SDEs of the form of Eq. (3.2) focusing on failure probability approximations and a smart materials application. Results presenting the applicability of the developed method in a Quantitative Finance framework are included in Section 4.2. Finally, in Section 4.3, a summary leading to the theme of Chapter 5 is presented as well.

4.1 Published Material

An approximate technique for determining in closed-form the response transition probability density function of diverse nonlinear/hysteretic oscillators

Meimaris Antonios, Kougioumtzoglou Ioannis, Pantelous Athanasios and Antonina Pirrotta

Published in the Nonlinear Dynamics journal, Springer Nature (2019)

DOI: 10.1007/s11071-019-05152-w

Reprinted by permission from Springer Nature.

Begins overleaf.



An approximate technique for determining in closed form the response transition probability density function of diverse nonlinear/hysteretic oscillators

Antonios T. Meimaris · Ioannis A. Kougoumtzoglou · Athanasios A. Pantelous · Antonina Pirrotta

Received: 16 April 2019 / Accepted: 17 July 2019
© Springer Nature B.V. 2019

Abstract An approximate analytical technique is developed for determining, in closed form, the transition probability density function (PDF) of a general class of first-order stochastic differential equations (SDEs) with nonlinearities both in the drift and in the diffusion coefficients. Specifically, first, resorting to the Wiener path integral most probable path approximation and utilizing the Cauchy–Schwarz inequality yields a closed-form expression for the system response PDF, at practically zero computational cost. Next, the accuracy of this approximation is enhanced by proposing a more general PDF form with additional parameters to be determined. This is done by relying on the associated Fokker–Planck operator to formulate and solve an error

minimization problem. Besides the mathematical merit of the derived closed-form approximate PDFs, an additional significant advantage of the technique relates to the fact that it can be readily coupled with a stochastic averaging treatment of second-order SDEs governing the dynamics of diverse stochastically excited nonlinear/hysteretic oscillators. In this regard, it is shown that the technique is capable of determining approximately the response amplitude transition PDF of a wide range of nonlinear oscillators, including hysteretic systems following the Preisach versatile modeling. Several numerical examples are considered for demonstrating the reliability and computational efficiency of the technique. Comparisons with pertinent Monte Carlo simulation data are provided as well.

A. T. Meimaris · A. A. Pantelous
Department of Econometrics and Business Statistics,
Monash University, Clayton, VIC 3800, Australia
e-mail: Antonios.Meimaris@monash.edu

A. A. Pantelous
e-mail: Athanasios.Pantelous@monash.edu

I. A. Kougoumtzoglou (✉)
Department of Civil Engineering and Engineering
Mechanics, Columbia University, New York, NY 10027,
USA
e-mail: ikougoum@columbia.edu

A. Pirrotta
Department of Mathematical Sciences, University of
Liverpool, Peach Street, Liverpool L69 7ZL, UK
e-mail: antonina.pirrotta@unipa.it

A. Pirrotta
Dipartimento di Ingegneria, Università degli Studi di Palermo,
Viale delle Scienze, Ed. 8, 90128 Palermo, Italy

Keywords Nonlinear stochastic dynamics · Path integral · Cauchy–Schwarz inequality · Fokker–Planck equation · Stochastic differential equations

1 Introduction

Although Monte Carlo simulation (MCS) has been the most versatile tool for solving stochastic differential equations (SDEs) governing the dynamics of diverse engineering systems and structures (e.g., [1–3]), in many cases it can be computationally prohibitive. Therefore, there is merit in developing alternative numerical and/or analytic solution methodologies. Indicative popular approaches in stochastic engineer-

ing dynamics include moments equations and statistical linearization, stochastic averaging, discrete Chapman–Kolmogorov equation schemes, Fokker–Planck equation solution techniques, (generalized) polynomial chaos expansions, and probability density evolution methods (e.g., [4–6]).

One of the promising semi-analytical techniques relates to the concept of path integral, developed independently by Wiener [7] and by Feynman [8]. Recently, Kougoumtzoglou and co-workers developed Wiener path integral techniques for stochastic response determination and optimization of complex engineering dynamical systems. These techniques are capable of determining the joint response transition probability density function (PDF) of diverse nonlinear systems, even endowed with fractional derivative elements (e.g., [9, 10]). Further, they can account for non-white and non-Gaussian stochastic process modeling [11], while it has been shown that the related computational cost can be reduced drastically by resorting to sparse representations and compressive sampling theory and tools [12]. Nevertheless, the numerical implementation of the technique is still associated with non-negligible computational cost. To address this challenge, a conceptually different solution approach has been pursued recently by the authors [13, 14] by coupling the Wiener path integral formalism with a Cauchy–Schwarz inequality treatment. This has yielded a closed-form approximate expression for the system response transition PDF, whereas the computational cost has been kept at a minimal level. Note, however, that the results in [13, 14] have been restricted to the class of SDEs with nonlinear drift, but constant diffusion coefficients.

In this paper, the technique developed in [13, 14] is extended to account for a more general class of nonlinear SDEs, with nonlinearities appearing both in the drift and in the diffusion coefficients. Specifically, the system response PDF is derived approximately in closed form. This is done by relying on the Wiener path integral “most probable path” approximation and on the Cauchy–Schwarz inequality, in conjunction with formulating and solving an error minimization problem by utilizing the associated Fokker–Planck equation operator. Besides the mathematical merit of this generalization, its relevance to engineering dynamics applications is evident when coupled with a stochastic averaging treatment of the original second-order governing SDE. In this regard, the technique is capable

of determining approximately the response amplitude transition PDF of diverse stochastically excited nonlinear oscillators. Various nonlinear systems are considered in the numerical examples for demonstrating the accuracy and computational efficiency of the developed technique, including hysteretic systems following the Preisach versatile modeling. Comparisons with pertinent MCS data are provided as well.

2 Preliminaries

2.1 Chapman–Kolmogorov and Fokker–Planck equations

This section serves as a brief background on Markov processes, the associated Chapman–Kolmogorov (C–K), and Fokker–Planck (F–P) equations, as well as their relation to the corresponding governing SDE; see also [15, 16] for some indicative standard books on the topic.

Consider a Markov stochastic process, $X_t = X(t)$, for which the C–K equation is satisfied for any $t_3 \geq t_2 \geq t_1$, i.e.,

$$p(x_3, t_3 | x_1, t_1) = \int_{-\infty}^{\infty} p(x_3, t_3 | x_2, t_2) p(x_2, t_2 | x_1, t_1) dx_2, \quad (1)$$

where $p(x_3, t_3 | x_1, t_1)$ denotes the transition PDF of the process X_t . Further, under Lindeberg’s condition, the C–K Eq. (1) leads to the well-known F–P equation governing the evolution in time of the transition PDF (e.g., see [16, 17]), i.e.,

$$\frac{\partial p}{\partial t} = -\frac{\partial (\mu(x, t) p)}{\partial x} + \frac{1}{2} \frac{\partial^2 (\sigma(x, t)^2 p)}{\partial x^2}, \quad (2)$$

where p is the transition PDF of the diffusion process X_t , and $\mu(\cdot, \cdot)$, $\sigma(\cdot, \cdot)$ are real-valued functions denoting the drift and diffusion coefficients, respectively, of the associated governing SDE of the form

$$\dot{x} = \mu(x, t) + \sigma(x, t)\eta(t). \quad (3)$$

In Eq. (3), the dot over a variable denotes differentiation with respect to time t , and $\eta(t)$ is a zero-mean and delta-correlated process of intensity one, i.e., $\mathbf{E}(\eta(t)) = 0$

An approximate technique for determining in closed form

and $\mathbf{E}((\eta(t)\eta(t-\tau)) = \delta_0(\tau)$, where $\delta_0(\cdot)$ is the Dirac delta function.

2.2 Wiener path integral formulation

For completeness, this section reviews the basic elements of a recently developed Wiener path integral stochastic response determination technique, which relies on the machinery of functional integrals and variational calculus; see also [11, 18, 19] for a more detailed presentation. The formulation of the Wiener path integral technique serves as the starting point in the ensuing analysis for deriving a closed-form expression for the system response transition PDF.

In the limit, i.e., $t_2 - t_1 = \Delta t \rightarrow 0$, the transition PDF has been shown to admit a Gaussian distribution of the form (e.g., [17])

$$p(x_2, t_2 | x_1, t_1) = \frac{\exp\left(-\frac{(x_2 - x_1 - \mu(x_1, t_1)\Delta t)^2}{2\sigma(x_1, t_1)^2 \Delta t}\right)}{\sqrt{2\pi\sigma(x_1, t_1)^2 \Delta t}}. \quad (4)$$

Note that the choice of Eq. (4) is not restrictive, and alternative non-Gaussian distributions can also be employed (e.g., [20]). Further, Eq. (4), in conjunction with the C-K Eq. (1), has been the starting point of numerical schemes (typically referred to in the literature as numerical path integral schemes) for propagating the response PDF in short time steps (e.g., [21–23]). Although these schemes have proven to be highly accurate in determining the response transition PDF, they become eventually computationally prohibitive with increasing number of dimensions. This is due to the fact that numerical computation of a multi-dimensional convolution integral is required for each and every time step.

Next, from a Wiener path integral perspective, the probability that x follows a specific path, $x(t)$, can be construed as the probability of a compound event. In particular, it can be expressed (e.g., [11, 18]) as a product of probabilities by utilizing Eq. (4), i.e.,

$$\begin{aligned} P[x(t)] &= \lim_{\Delta t \rightarrow 0, N \rightarrow \infty} \\ &\times \frac{\exp\left(-\sum_{j=0}^{N-1} \frac{(x_{j+1} - x_j - \mu(x_j, t_j)\Delta t)^2}{2\sigma(x_j, t_j)^2 \Delta t}\right)}{\prod_{j=0}^{N-1} \sqrt{2\pi\sigma(x_j, t_j)^2 \Delta t}} \prod_{j=0}^{N-1} dx_j, \end{aligned} \quad (5)$$

where the time has been discretized into N points, Δt apart, and the path $x(t)$ is represented by its values x_j at the discrete time points t_j , for $j \in \{0, \dots, N-1\}$. Also, dx_j denotes the (infinite in number) infinitesimal “gates” through which the path propagates. Loosely speaking, Eq. (5) represents the probability of the process to propagate through the infinitesimally thin tube surrounding $x(t)$. Alternatively, Eq. (5) can be written in the compact form [11, 18]

$$\begin{aligned} P[x(t)] &= \exp\left(-\int_{t_i}^{t_f} \frac{(\dot{x}_j - \mu(x, t))^2}{2\sigma(x, t)^2} dt\right) \prod_{t=t_i}^{t_f} \frac{dx(t)}{\sqrt{2\pi\sigma(x, t)^2 dt}}. \end{aligned} \quad (6)$$

Overall, the total probability that x will start from x_i at time t_i and end up at x_f at time t_f takes the form of a functional integral, which “sums up” the respective probabilities of each and every path that the process can possibly follow (e.g., see [18]). Next, denoting by $C\{x_i, t_i; x_f, t_f\}$ the set of all possible paths starting from x_i at time t_i and ending up at x_f at time t_f , the transition PDF takes the form

$$p(x_f, t_f | x_i, t_i) = \int_{C\{x_i, t_i; x_f, t_f\}} \exp\left(-\int_{t_i}^{t_f} L(x, \dot{x})\right) \mathcal{D}[x(t)]. \quad (7)$$

In Eq. (7), $L(x, \dot{x})$ represents the Lagrangian function equal to

$$L(x, \dot{x}) = \frac{1}{2} \left(\frac{\dot{x} - \mu(x, t)}{\sigma(x, t)} \right)^2, \quad (8)$$

and $\mathcal{D}[x(t)]$ is a functional measure given by

$$\mathcal{D}[x(t)] = \prod_{t=t_i}^{t_f} \frac{dx(t)}{\sqrt{2\pi\sigma(x(t), t)^2 dt}}. \quad (9)$$

2.3 Numerical implementation and computational cost of the Wiener path integral solution technique

It is noted that the formal expression of the path integral in Eq. (7) is of little practical use as its analytical or numerical evaluation is highly challenging. Therefore,

an approximate solution approach is required. In this regard, the “most probable path” approach is employed (e.g., [11, 18, 19]), according to which the largest contribution to the Wiener path integral comes from the path $x_c(t)$ for which the integral in the exponential of Eq. (7) becomes as small as possible. Calculus of variations [24] dictates that this path $x_c(t)$ with fixed end points satisfies the extremality condition

$$\delta \int_{t_i}^{t_f} L(x_c, \dot{x}_c) dt = 0, \quad (10)$$

which yields the Euler–Lagrange (E–L) equation (e.g., see [9, 11, 19])

$$\frac{\partial L}{\partial x_c} - \frac{\partial}{\partial t} \frac{\partial L}{\partial \dot{x}_c} = 0, \quad (11)$$

to be solved in conjunction with the boundary conditions $x_c(t_i) = x_i$, $x_c(t_f) = x_f$. Once the boundary value problem (BVP) of Eq. (11) is solved and $x_c(t)$ is determined, the response transition PDF can be approximated by

$$p(x_f, t_f | x_i, t_i) \approx \Phi \exp \left(- \int_{t_i}^{t_f} L(x_c, \dot{x}_c) dt \right), \quad (12)$$

where Φ is a normalization coefficient; see also [11, 18] for a more detailed presentation.

Although the BVP of Eq. (11) can be solved analytically and yield closed-form solutions for cases of linear systems (e.g., [25, 26]), it is readily seen that a numerical solution treatment is required, in general, to account for arbitrary nonlinearities in the governing Eq. (3), and consequently, in the BVP of Eq. (11). In this regard, note that, due to the fixed boundary conditions, a single point of the response transition PDF is evaluated by solving numerically one BVP of the form of Eq. (11). According to a brute-force solution scheme, and for a given time instant, an effective PDF domain is considered. Following the discretization of the domain into N points x_f , the response PDF values are determined for each point of the mesh. It is worth mentioning that for an m -dimensional version of the SDE of Eq. (3), the number of BVPs to be solved becomes N^m , i.e., the computational cost increases exponentially with the number of dimensions, and becomes prohibitive eventually. To bypass the above bottleneck, Kougiamtzoglou and co-workers have developed recently various

efficient solution techniques by resorting to appropriate response PDF expansions in conjunction with a compressive sampling treatment and group sparsity concepts. The above developments have decreased drastically the associated computational cost as compared both to a standard MCS solution approach and to the N^m BVPs required to be solved numerically by the brute-force Wiener path integral technique implementation; see also [12, 27, 28] for a more detailed presentation and discussion.

Nevertheless, despite the aforementioned efforts toward computational efficiency enhancement of the Wiener path integral technique, the computational cost remains non-trivial as a non-negligible number of BVPs is still required to be solved numerically for determining the response PDF. In this paper, and in the following section in particular, a conceptually different solution approach is pursued, and a closed-form approximate expression is derived for the response transition PDF. This is done in conjunction with the Wiener path integral formalism and by relying on a Cauchy–Schwarz inequality treatment, whereas the computational cost is kept at a minimal level.

3 Main results

In this section, a novel closed-form approximate expression is derived for the response transition PDF of SDEs with nonlinear drift and nonlinear diffusion coefficients of arbitrary form. In this regard, attention is directed in the ensuing analysis to a version of Eq. (3) with time-invariant nonlinear coefficients; that is,

$$\dot{x} = \mu(x) + \sigma(x)\eta(t). \quad (13)$$

Specifically, resorting to a Wiener path integral variational formulation and employing the Cauchy–Schwarz inequality yields an analytical expression for the transition PDF, whose determination requires practically zero computational cost. Further, the accuracy of the above approximation is enhanced by proposing a more versatile closed-form expression with additional “degrees of freedom,” i.e., parameters to be evaluated. To this aim, an error minimization approach based on the corresponding F–P equation is formulated and solved, at the expense of some modest computational cost. The herein developed technique can be construed as an extension of earlier work by Meimaris

An approximate technique for determining in closed form

et al. [13, 14] to account for a more general class of nonlinear SDEs, with nonlinearities appearing both in the drift and in the diffusion coefficients. Besides the mathematical merit of the aforementioned generalization, its relevance to engineering dynamics applications is significant. In particular, as shown in the numerical examples section, when coupled with a stochastic averaging treatment of the original second-order governing SDE, the technique is capable of determining approximately (at minimal, however, computational cost) the response amplitude transition PDF of diverse stochastically excited nonlinear oscillators. Systems exhibiting complex hysteretic response behaviors such as those following the Preisach versatile modeling can also be readily accounted for under the same solution framework.

3.1 Approximate closed-form transition PDF for SDEs with nonlinear drift and nonlinear diffusion coefficients

In this section, a closed-form analytical approximation is derived for the solution PDF of Eq. (13) based on a Cauchy–Schwarz inequality treatment. In this regard, the approximation can be used not only as a direct SDE response PDF estimate that requires practically zero computational effort for its determination, but also as a starting point in the optimization approach developed in the ensuing section toward enhancing the accuracy of the original, rather crude, approximation.

Specifically, following the derivation provided in “Appendix A” and taking into account Eqs. (12) and (73), an approximation for the response transition PDF of Eq. (13) is given by

$$\hat{p}(x_f, t_f | x_i, t_i) = \mathcal{N}(t_f | x_i, t_i) \exp(-G(x_f, t_f | x_i, t_i)), \quad (14)$$

where

$$\begin{aligned} G(x_f, t_f | x_i, t_i) &= \frac{1}{2} \left(\frac{(\mathcal{R}(x_f) - \mathcal{R}(x_i))^2}{t_f - t_i} - (\mathcal{M}(x_f) - \mathcal{M}(x_i)) \right), \\ \mathcal{R}(x) &= \int_{x^*}^x \frac{1}{\sigma(u)} du, \\ \mathcal{M}(x) &= \int_{x^*}^x \frac{2\mu(u)}{\sigma(u)^2} du, \end{aligned} \quad (15)$$

and $x^* \in \mathbb{R}$ an arbitrarily chosen point so that the integrals of Eq. (15) are well defined. Further, the normalization constant \mathcal{N} in Eq. (14) is determined as

$$\mathcal{N}(t_f | x_i, t_i) = \left(\int_{\mathcal{D}} \exp(-G(z, t_f | x_i, t_i)) dz \right)^{-1}, \quad (16)$$

where \mathcal{D} denotes the domain of integration, accounting for any restrictions that $\mathcal{M}(\cdot)$ and $\mathcal{R}(\cdot)$ may impose. Clearly, further manipulation of the closed-form expression of Eqs. (14)–(15) depends on the availability of analytical expressions for the antiderivatives $\mathcal{M}(\cdot)$ and $\mathcal{R}(\cdot)$, which in turn depends on the specific nonlinearity form under consideration.

It can be readily seen that $\hat{p}(\cdot)$ in Eq. (14) can be directly used as an analytical approximation of the response process transition PDF without resorting to the numerical solution of the E–L Eq. (11). Note that the closed-form expression of Eq. (14), which requires essentially zero computational cost for its evaluation, can be construed as a generalization of the expression derived in [13] to account for nonlinearities both in the drift and in the diffusion coefficients of the governing stochastic differential Eq. (13).

3.2 Enhanced accuracy via an error minimization scheme

As demonstrated in [13] for the case of SDEs with nonlinear drift but constant diffusion coefficients, although the approximation of Eq. (14) is capable, in general, of capturing the salient features of the solution PDF, in many cases the degree of accuracy exhibited can be inadequate. To address this limitation, a more general form of the PDF was proposed in [14], by incorporating two additional “degrees of freedom,” i.e., parameters to be determined based on an appropriate optimization scheme. Similarly to [14], and to address the herein considered more challenging case of SDEs with nonlinearities both in the drift and in the diffusion coefficients, a more general form than Eq. (14) is proposed for the transition PDF, that is,

$$\begin{aligned} \hat{p}_{(k,n)}(x_f, t_f | x_i, t_i) &= \mathcal{N}_{(k,n)}(t_f | x_i, t_i) \exp(-G_{(k,n)}(x_f, t_f | x_i, t_i)), \end{aligned} \quad (17)$$

where

$$\begin{aligned} G_{(k,n)}(x_f, t_f | x_i, t_i) \\ = \frac{1}{2} \left(k \frac{(\mathcal{R}(x_f) - \mathcal{R}(x_i))^2}{t_f - t_i} - n (\mathcal{M}(x_f) - \mathcal{M}(x_i)) \right), \end{aligned} \quad (18)$$

and the normalization constant \mathcal{N} in Eq. (17) is given by

$$\mathcal{N}_{(k,n)}(t_f | x_i, t_i) = \left(\int_{\mathcal{D}} \exp(-G_{(k,n)}(z, t_f | x_i, t_i)) dz \right)^{-1}. \quad (19)$$

Note that the additional parameters k and n render the rather crude PDF approximation of Eq. (14) more versatile in capturing diverse response behaviors. In particular, the parameter k relates to optimizing and “tightening” the Cauchy–Schwarz inequality of Eq. (72), whereas the parameter n refers to the overall accuracy of the Wiener path integral approximation of Eq. (12). This generalized PDF form is anticipated to enhance the accuracy exhibited by Eq. (14), at the expense, however, of some modest computational cost related to the determination of k and n .

Specifically, to determine the parameters k and n in Eq. (17), for a given norm ($\|\cdot\|_q$), the error quantity $\|\hat{p}_{(k,n)} - p^*\|_q$ is sought to be minimized, where p^* denotes the exact solution PDF. However, since p^* is unknown, an error minimization scheme based on the F–P equation operator is adopted in the ensuing analysis (see also [14]). In this regard, the exact transition PDF p^* for the SDE of Eq. (13) is given as the solution of the F–P equation [Eq. (2)] associated with Eq. (13), i.e.,

$$\begin{aligned} \frac{\partial p^*(x, t)}{\partial t} &= - \frac{\partial (\mu(x) p^*(x, t))}{\partial x} \\ &+ \frac{1}{2} \frac{\partial^2 (\sigma(x)^2 p^*(x, t))}{\partial x^2}. \end{aligned} \quad (20)$$

Next, denoting the F–P operator as

$$\begin{aligned} \mathcal{L}_{\text{FP}}[p(x, t)] &= \frac{\partial p(x, t)}{\partial t} + \frac{\partial (\mu(x) p(x, t))}{\partial x} \\ &- \frac{1}{2} \frac{\partial^2 (\sigma(x)^2 p(x, t))}{\partial x^2}, \end{aligned} \quad (21)$$

and taking into account that $\mathcal{L}_{\text{FP}}[p^*] = 0$, the error is defined as

$$\begin{aligned} \text{err}_q &= \|\mathcal{L}_{\text{FP}}[\hat{p}_{(k,n)} - p^*]\|_q \\ &= \|\mathcal{L}_{\text{FP}}[\hat{p}_{(k,n)}] - \mathcal{L}_{\text{FP}}[p^*]\|_q \\ &= \|\mathcal{L}_{\text{FP}}[\hat{p}_{(k,n)}]\|_q. \end{aligned} \quad (22)$$

Due to the analytical form of $\hat{p}_{(k,n)}$ in Eq. (17), the error quantity $\text{err}_q = \|\mathcal{L}_{\text{FP}}[\hat{p}_{(k,n)}]\|_q$ in Eq. (22) can be expressed explicitly as a function of k and n ; see also [14]. Further, for a chosen q -norm and final time t_f , the values of k, n are numerically evaluated by solving the optimization problem

$$\hat{z}_q = (\hat{k}, \hat{n})_q = \arg \min_{k, n \in \mathbb{R}} \|\mathcal{L}_{\text{FP}}[\hat{p}_{(k,n)}(\cdot, t_f)]\|_q, \quad (23)$$

and thus, the approximate response PDF of Eq. (17) is determined.

4 Response analysis of stochastically excited nonlinear/hysteretic oscillators

In this section, it is shown that the developed solution technique in Sect. 3 can be readily coupled with a stochastic averaging treatment of the second-order SDEs governing the dynamics of diverse stochastically excited nonlinear/hysteretic oscillators for determining the response transition PDF in a computationally efficient manner. Concisely, the main aspects of stochastic averaging (e.g., [30,31]) relate to a Markovian approximation of an appropriately chosen amplitude of the system response, as well as to a dimension reduction of the original two-dimensional problem to an one-dimensional problem. In particular, the original second-order SDE is cast into a first-order SDE of the form of Eq. (13), and thus, the technique developed in Sect. 3 can be applied in a straightforward manner.

In this regard, consider a nonlinear single-degree-of-freedom oscillator whose motion is governed by

$$\ddot{y} + \beta_0 \dot{y} + g(t, y, \dot{y}) = v(t), \quad (24)$$

where $v(t)$ is a white noise process, i.e., $\mathbf{E}(v(t)) = 0$ and $\mathbf{E}(v(t_1)v(t_2)) = 2\pi S_0 \delta_0(t_1 - t_2)$, $g(\cdot)$ is the restoring force which can be either hysteretic or depend only on the instantaneous values of y and \dot{y} , β_0 is a linear damping coefficient so that $\beta_0 = 2\zeta_0\omega_0$; ζ_0 is

An approximate technique for determining in closed form

the ratio of critical damping, and ω_0 is the natural frequency corresponding to the linear oscillator (i.e., $g(t, y, \dot{y}) = \omega_0^2 y$).

Next, adopting the assumption of light damping (e.g., $\zeta_0 \ll 1$), it can be argued that the oscillator of Eq. (24) exhibits a pseudo-harmonic response behavior described by the equations (e.g., [32])

$$y(t) = x \cos(\omega(x)t + \phi), \quad (25)$$

and

$$\dot{y}(t) = -x\omega(x) \sin(\omega(x)t + \phi). \quad (26)$$

Manipulating Eqs. (25) and (26), the response amplitude x and the response phase ϕ are given by

$$x(t) = \sqrt{y(t)^2 + \dot{y}(t)^2}, \quad (27)$$

and

$$\phi(t) = -\omega(x)t - \tan^{-1} \left(\frac{\dot{y}(t)}{y(t)\omega(x)} \right), \quad (28)$$

respectively. These are considered to be slowly varying functions with respect to time, and approximately constant over one cycle of oscillation; see also [31, 32]. In Eqs. (25) and (26), the equivalent natural frequency $\omega(x)$, to be determined in the following, is approximated as a function of the response amplitude x to account for the effect of nonlinearities in the original system of Eq. (24). Next, a statistical linearization treatment (e.g., [4, 32]) yields an equivalent to Eq. (24) oscillator of the form

$$\ddot{y} + \beta(x)\dot{y} + \omega(x)^2 y = v(t), \quad (29)$$

where

$$\beta(x) = \beta_0 - \frac{\frac{1}{\pi} \int_0^{2\pi} \sin(\psi) g(t, x \cos(\psi), -\omega x \sin(\psi)) d\psi}{x \omega(x)}, \quad (30)$$

and

$$\omega(x)^2 = \frac{\frac{1}{\pi} \int_0^{2\pi} \cos(\psi) g(t, x \cos(\psi), -\omega x \sin(\psi)) d\psi}{x}. \quad (31)$$

Further, resorting to a stochastic averaging treatment (e.g., [32]), the response amplitude x can be decoupled from the response phase ϕ , yielding a first-order stochastic differential equation for x in the form

$$\dot{x} = -\frac{1}{2}\beta(x)x + \frac{\pi S_0}{2x\omega(x)^2} + \frac{\sqrt{\pi S_0}}{\omega(x)}\eta(t). \quad (32)$$

It can be readily seen that Eq. (32) is an SDE of the form of Eq. (13) with drift μ and diffusion σ coefficients given by

$$\mu(x) = -\frac{1}{2}\beta(x)x + \frac{\pi S_0}{2x\omega(x)^2}, \quad (33)$$

and

$$\sigma(x) = \sqrt{\frac{\pi S_0}{\omega(x)^2}}, \quad (34)$$

respectively. Thus, the herein developed solution technique can be applied in a straightforward manner for determining the stochastic response of a wide range of nonlinear/hysteretic oscillators.

5 Numerical examples

In this section, the hardening Duffing and hysteretic Preisach nonlinear oscillators are considered for assessing the reliability of the herein developed technique. In this regard, a standard interior point method [33, 34] using Matlab's *fmincon* built-in function is employed for solving numerically the optimization problem of Eq. (23) in conjunction with the $\|\cdot\|_2$ norm. To this aim, the basic approximation of Eq. (14) with $(k, n) = (1, 1)$ serves as a natural choice for the starting point of the optimization algorithm. In all cases, the algorithm converged in no more than 55 iterations, which translates into a small fraction of a second from a computational cost perspective. The response transition PDF obtained by the closed-form expression of Eq. (32) is compared with pertinent MCS-based PDF estimates produced by numerically integrating the original equation of motion, Eq. (24) (100,000 realizations). A standard computer with 16 GB RAM, Inter(R) Core(TM) i7-6700 CPU @3.40 GHz, is used for the numerical implementations.

5.1 Duffing nonlinear oscillator

In the case of a Duffing oscillator, the equation of motion is governed by Eq. (24), with

$$g(t, y, \dot{y}) = \omega_0^2 (y + \alpha y^3), \quad (35)$$

and α is a parameter controlling the nonlinearity magnitude. Next, utilizing Eqs. (30) and (31) yields

$$\beta(x) = \beta_0, \quad (36)$$

and

$$\omega(x)^2 = \omega_0^2 \left(1 + \frac{3}{4} \alpha x^2 \right). \quad (37)$$

Thus, by employing Eqs. (36–37), the drift and diffusion coefficients of Eqs. (33–34) become

$$\mu(x) = -\frac{1}{2} \beta_0 x + \frac{\pi S_0}{2x \omega_0^2 (1 + \frac{3}{4} \alpha x^2)}, \quad (38)$$

and

$$\sigma(x) = \sqrt{\frac{\pi S_0}{\omega_0^2 (1 + \frac{3}{4} \alpha x^2)}}, \quad (39)$$

respectively.

Further, the antiderivatives $R(\cdot)$ and $M(\cdot)$ take the form

$$\begin{aligned} & \sqrt{\pi S_0} R(x) \\ &= \omega_0 \left(\frac{\sinh^{-1} \left(\sqrt{\frac{3}{4} \alpha} x \right)}{\sqrt{3\alpha}} + \frac{x \sqrt{\frac{3}{4} \alpha} x^2 + 1}{2} \right), \end{aligned} \quad (40)$$

where $\sinh^{-1}(x) = \ln(x + \sqrt{1+x^2})$ and

$$M(x) = \ln(x) - \frac{\beta_0 \omega_0^2}{2\pi S_0} x^2 - \frac{3\beta_0 \omega_0^2 \alpha}{16\pi S_0} x^4, \quad (41)$$

respectively. Thus, the nonlinear Duffing oscillator response amplitude PDF has been expressed in closed form according to Eq. (17).

In the following numerical example, the parameter values $\omega_0 = 1$, $\zeta_0 = 0.01$, $S_0 = \frac{6}{\pi} \zeta_0$ and the initial

conditions $y(t_i = 0) = 1$, $\dot{y}(t_i = 0) = 0$ are considered. Next, minimizing the error as defined in Eq. (23) for a given time instant yields the values for k and n . Two time instants are considered, the first ($t_f = 2s$) corresponding to the transient phase of the response behavior, and the second ($t_f = 50s$) corresponding effectively to the stationary regime. For $t_f = 2s$ and $t_f = 50s$, the respective objective functions of Eq. (23) are plotted in Figs. 1 and 2, respectively, for nonlinearity magnitude $\alpha = 1$. The computed values of k and n are shown in Table 1 together with the corresponding iterations numbers and CPU times of the optimization algorithm. In Fig. 3, both the basic $\hat{p}_{(1,1)}$ and the enhanced $\hat{p}_{(k,n)}$ approximations are plotted for the above two time instants and compared with pertinent MCS-based PDF estimates. It is seen that for early time instants ($t_f = 2s$) $\hat{p}_{(1,1)}$ manages to capture the basic features of the response amplitude PDF and yields comparable accuracy to $\hat{p}_{(k,n)}$. However, the superior performance of $\hat{p}_{(k,n)}$ over $\hat{p}_{(1,1)}$ becomes evident at $t_f = 50s$ (stationary phase). In fact, comparisons both with MCS data and with the available stationary analytical solution of the F–P Eq. (20) (e.g., [31]), i.e.,

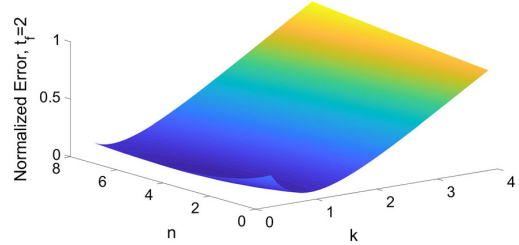


Fig. 1 Objective function of Eq. (23) for a Duffing oscillator with $\alpha = 1$ at $t_f = 2$

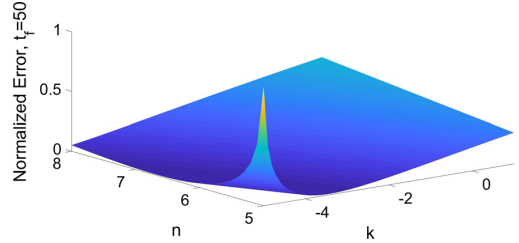


Fig. 2 Objective function of Eq. (23) for a Duffing oscillator with $\alpha = 1$ at $t_f = 50$

An approximate technique for determining in closed form

Table 1 Computed k and n values for various final time instants t_f and starting point $(1, 1)$ for a Duffing oscillator with $\alpha = 1$

	k	n	Iterations	CPU time
$t_f = 2$	0.7949	3.5083	39	0.048
$t_f = 50$ (stationary)	-4.4646	6.1254	54	0.135

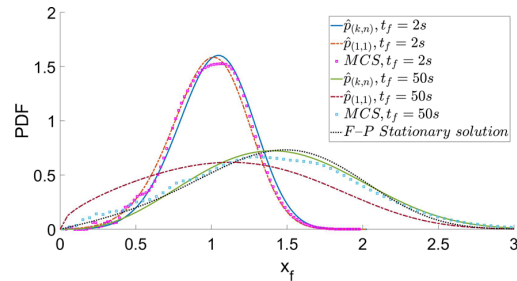


Fig. 3 Approximate response PDFs $\hat{p}_{(k,n)}$ and $\hat{p} = \hat{p}_{(1,1)}$ for various time instants t_f for a Duffing oscillator with $\alpha = 1$; comparisons with MCS-based PDF estimates (100,000 realizations) and with existing analytical stationary PDF expressions

$$p(x_f) = \frac{x_f + \alpha x_f^3}{A^2} \exp\left(-\frac{\left(\frac{1}{2}x_f^2 + \frac{\alpha}{4}x_f^4\right)}{A^2}\right), \quad (42)$$

where

$$A^2 = \frac{\pi S_0}{2\zeta_0\omega_0^3}, \quad (43)$$

indicate a high accuracy degree exhibited by the approximate PDF $\hat{p}_{(k,n)}$. Similar results are shown in Figs. 4, 5 and 6 and Table 2 for nonlinearity magnitude $\alpha = 2$.

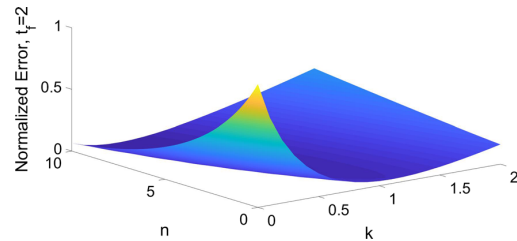


Fig. 4 Objective function of Eq. (23) for a Duffing oscillator with $\alpha = 2$ at $t_f = 2$

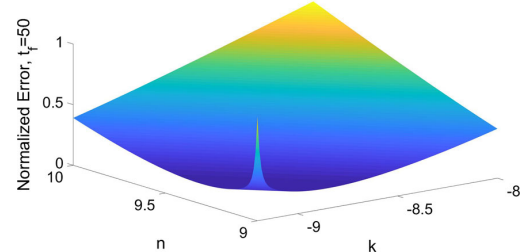


Fig. 5 Objective function of Eq. (23) for a Duffing oscillator with $\alpha = 2$ at $t_f = 50$

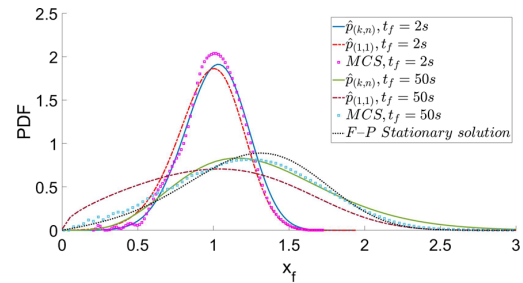


Fig. 6 Approximate response PDFs $\hat{p}_{(k,n)}$ and $\hat{p} = \hat{p}_{(1,1)}$ for various time instants t_f for a Duffing oscillator with $\alpha = 2$; comparisons with MCS-based PDF estimates (100,000 realizations) and with existing analytical stationary PDF expressions

Table 2 Computed k and n values for various final time instants t_f and starting point $(1, 1)$ for a Duffing oscillator with $\alpha = 2$

	k	n	Iterations	CPU time
$t_f = 2$	0.4525	8.6760	42	0.191
$t_f = 50$ (stationary)	-9.0246	9.1555	51	0.157

5.2 Preisach hysteretic oscillator

In the context of engineering dynamics, hysteresis can be construed as a memory-dependent relationship, which describes the dependence of the system restoring force $g(t, y, \dot{y})$ on the time history of the system response. A mathematical description of various hysteretic models can be found in [35, 36]. Recently, the Preisach hysteretic model has been adopted to describe the response behavior of smart materials, such as shape-memory alloys [37, 38]. The model is significantly versatile in representing diverse hysteretic patterns, and even capable of capturing minor loops present in many physical phenomena. A detailed pre-

smentation of the Preisach formalism is given in [39], while indicative contributions toward determining the stochastic response and assessing the reliability of systems endowed with Preisach elements can be found in [32, 40–46].

Following the notation adopted in [41], the Preisach hysteretic restoring force, $f(t)$, is given by

$$f(t) = \iint_{a \geq b} \mu(a, b) \gamma(x, t) da db, \quad (44)$$

where $\gamma(x, t)$ is a relay operator or hysteron. Although the model of Eq. (44) can represent various hysteretic behaviors by appropriately identifying the weight function $\mu(a, b)$ (see also [37]), the one corresponding to the Iwan–Jenkins model is utilized in the following. Specifically, the equation of motion [Eq. (24)] becomes

$$\ddot{y} + \beta_0 \dot{y} + \bar{\omega}^2 y + f_H(t) = v(t), \quad (45)$$

where

$$\bar{\omega}^2 = \omega_0^2 + \omega_j^2 = \omega_j^2(\varphi + 1) = k_j(1 + \varphi), \quad (46)$$

i.e., $k_j = \omega_j^2$ and $\varphi = \frac{\omega_0^2}{\omega_j^2}$. In Eqs. (45–46), it is seen that the Preisach restoring force is divided into a linear part and a nonlinear one monitoring the memory of the system, while φ quantifies the contribution of the Preisach linear part as compared to the stiffness of the corresponding linear oscillator. Next, introducing the parameter

$$\psi = \frac{\bar{\omega}^2}{f_y^\star}, \quad (47)$$

Equation (45) can be cast in the form

$$\ddot{y} + \beta_0 \dot{y} + \bar{\omega}^2 (y + \psi d_H(t)) = v(t), \quad (48)$$

where $d_H(t)$ denotes the scaled hysteretic restoring force. Further, for the case

$$\frac{f_{y,\max} - f_{y,\min}}{f_{y,\max} + f_{y,\min}} = 1, \quad (49)$$

where f_y is the yielding force, utilizing Eqs. (30) and (31) yields

$$\beta(x) = \beta_0 + \frac{\psi \bar{\omega}^2 x}{3\pi (1 + \varphi)^2 \sqrt{\bar{\omega}^2 - \frac{\psi \bar{\omega}^2 x}{4(1+\varphi)^2}}}, \quad (50)$$

and

$$\omega(x)^2 = \bar{\omega}^2 - \frac{\psi \bar{\omega}^2 x}{4(1 + \varphi)^2}. \quad (51)$$

Thus, by employing Eqs. (50–51), the drift and diffusion coefficients of Eqs. (33–34) become

$$\begin{aligned} \mu(x) = & -\frac{\beta_0}{2}x - \frac{\psi \bar{\omega}^2 x^2}{6\pi (1 + \varphi)^2 \sqrt{\bar{\omega}^2 - \frac{\psi \bar{\omega}^2 x}{4(1+\varphi)^2}}} \\ & + \frac{\pi S_0}{2x \left(\bar{\omega}^2 - \frac{\psi \bar{\omega}^2 x}{4(1+\varphi)^2} \right)}, \end{aligned} \quad (52)$$

and

$$\sigma(x) = \sqrt{\frac{\pi S_0}{\bar{\omega}^2 - \frac{\psi \bar{\omega}^2 x}{4(1+\varphi)^2}}}, \quad (53)$$

respectively. The reader is also directed to [41, 43] for more details on stochastic averaging of Preisach oscillators.

Further, the antiderivatives $R(\cdot)$ and $M(\cdot)$ take the form

$$\mathcal{R}(x) = -\frac{\bar{\omega}^2 A_{\varphi, \psi}(x)^2 \sqrt{\frac{\pi S_0 (\varphi+1)^2}{\bar{\omega}^2 A_{\varphi, \psi}(x)}}}{3\pi S_0 \psi (\varphi + 1)^2}, \quad (54)$$

and

$$\begin{aligned} \mathcal{M}(x) = & \log(x) \\ & + \frac{\frac{\beta_0 \bar{\omega}^6 A_{\varphi, \psi}(x)^3}{24} + \frac{\beta_0 \bar{\omega}^6 \psi x A_{\varphi, \psi}(x)^2}{8}}{\pi S_0 \bar{\omega}^4 \psi^2 (\varphi + 1)^2} \\ & + \frac{\frac{8 \bar{\omega}^7 A_{\varphi, \psi}(x)^{7/2}}{315} + \frac{4 \bar{\omega}^7 \psi x A_{\varphi, \psi}(x)^{5/2}}{45} + \frac{\bar{\omega}^7 \psi^2 x^2 A_{\varphi, \psi}(x)^{3/2}}{9}}{\pi S_0 \bar{\omega}^4 \psi^2 \pi (\varphi + 1)^3}, \end{aligned} \quad (55)$$

respectively, where $A_{\varphi, \psi}(x) = (4\varphi^2 + 8\varphi - \psi x + 4)$. Thus, the nonlinear hysteretic Preisach oscillator response amplitude PDF has been expressed in closed form according to Eq. (17).

An approximate technique for determining in closed form

In the numerical example, the parameter values $\bar{\omega} = 1$, $\xi_0 = 0.01$, $S_0 = \frac{2}{\pi}\xi_0$ with $\psi = 1$ are used together with the initial conditions $y(t_i = 0) = 1$, $\dot{y}(t_i = 0) = 0$. Next, minimizing the error in Eq. (23) for a given time instant yields the values for k and n . In a similar manner as in Sect. 5.1, two time instants are considered, the first ($t_f = 5s$) corresponding to the transient phase of the response behavior, and the second ($t_f = 50s$) corresponding effectively to the stationary regime. For $t_f = 5s$ and $t_f = 50s$ the objective functions of Eq. (23) are plotted in Figs. 7 and 8, respectively, for nonlinearity magnitude $\varphi = 1$. The computed values of k and n are shown in Table 3 together with the corresponding iterations numbers and CPU times of the optimization algorithm. In Fig. 9, both the basic $\hat{p}_{(1,1)}$ and the enhanced $\hat{p}_{(k,n)}$ approximations are plotted for the above two time instants and compared

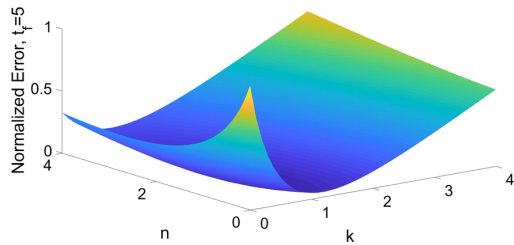


Fig. 7 Objective function of Eq. (23) for a Preisach oscillator with $\varphi = 1$ at $t_f = 5$

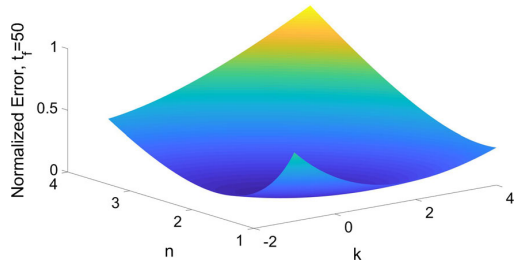


Fig. 8 Objective function of Eq. (23) for a Preisach oscillator with $\varphi = 1$ at $t_f = 50$

Table 3 Computed k and n values for various final time instants t_f and starting point $(1, 1)$ for a Preisach oscillator with $\varphi = 1$

	k	n	Iterations	CPU time
$t_f = 5$	0.9440	1.2226	33	0.023
$t_f = 50$ (stationary)	0.1928	1.9673	48	0.053

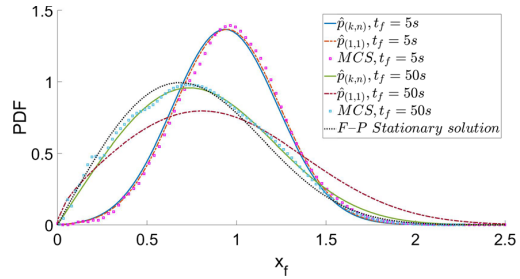


Fig. 9 Approximate response PDFs $\hat{p}_{(k,n)}$ and $\hat{p} = \hat{p}_{(1,1)}$ for various time instants t_f for a Preisach oscillator with $\varphi = 1$; comparisons with MCS-based PDF estimates (100,000 realizations) and with existing analytical stationary PDF expressions

with pertinent MCS-based PDF estimates. It is seen that for early time instants ($t_f = 5s$) $\hat{p}_{(1,1)}$ manages to capture the salient features of the response amplitude PDF and appears to be almost indistinguishable from $\hat{p}_{(k,n)}$. This is also seen by observing the values for k and n in Table 3, which are relatively close to 1. Further, the enhanced accuracy of $\hat{p}_{(k,n)}$ as compared to $\hat{p}_{(1,1)}$ becomes evident at $t_f = 50s$ (stationary phase). In fact, comparisons both with MCS data and with the available stationary analytical solution of the F–P Eq. (20) (e.g., [41]), i.e.,

$$p(x_f) = C(\lambda)x_f \left(\frac{2\xi_0}{1 - \lambda x_f} \right)^{-1/2} \exp \left(-\frac{x_f^2}{2} + \frac{\lambda x_f^3}{12} + \frac{(128 + 48\lambda x_f + 15\lambda^2 x_f^2)(4 - \lambda x_f)^{3/2}}{630\pi\xi_0\lambda^2} \right), \quad (56)$$

where

$$\lambda = \frac{\psi}{(1 + \phi)^2}, \quad (57)$$

and $C(\lambda)$ is a normalization coefficient, indicate a satisfactory level of agreement. Similar results are shown in Figs. 10, 11 and 12 and Table 4 for nonlinearity magnitude $\varphi = 2$.

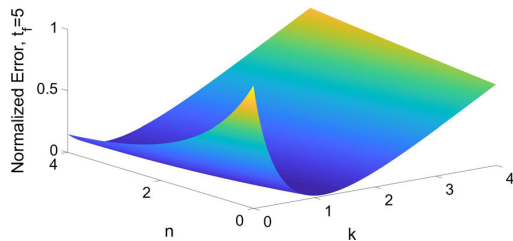


Fig. 10 Objective function of Eq. (23) for a Preisach oscillator with $\varphi = 2$ at $t_f = 5$

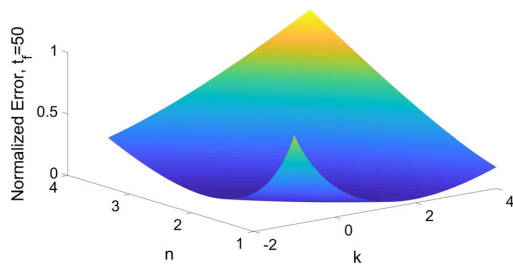


Fig. 11 Objective function of Eq. (23) for a Preisach oscillator with $\varphi = 2$ at $t_f = 50$

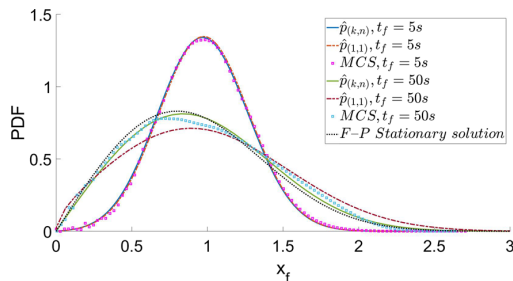


Fig. 12 Approximate response PDFs $\hat{p}_{(k,n)}$ and $\hat{p} = \hat{p}_{(1,1)}$ for various time instants t_f for a Preisach oscillator with $\varphi = 2$; comparisons with MCS-based PDF estimates (100,000 realizations) and with existing analytical stationary PDF expressions

Table 4 Computed k and n values for various final time instants t_f and starting point $(1, 1)$ for a Preisach oscillator with $\varphi = 2$

	k	n	Iterations	CPU time
$t_f = 5$	0.9358	1.3059	27	0.042
$t_f = 50$ (stationary)	0.2215	1.9201	51	0.051

6 Concluding remarks

In this paper, an approximate analytical technique has been developed for determining, in closed form and at minimal computational cost, the transition PDF of a wide range of nonlinear first-order SDEs. This has been done by relying on the Wiener path integral “most probable path” approximation and on the Cauchy–Schwarz inequality, in conjunction with formulating and solving an error minimization problem by utilizing the associated Fokker–Planck equation operator. The technique can be construed as an extension of the results in [13, 14] to account for a more general class of SDEs with nonlinearities both in the drift and in the diffusion coefficients. Besides the mathematical merit of this generalization, the technique can serve also as a benchmark for assessing the performance of alternative, more computationally demanding, stochastic dynamics numerical methodologies. Further, its relevance to engineering dynamics applications has been demonstrated by determining approximately the response amplitude transition PDF of diverse stochastically excited nonlinear oscillators, including hysteretic systems following the Preisach versatile modeling. Comparisons with pertinent MCS data have demonstrated a satisfactory accuracy degree.

Acknowledgements I. A. Kougioumtzoglou gratefully acknowledges the support through his CAREER award by the CMMI Division of the National Science Foundation, USA (Award No. 1748537).

Compliance with ethical standards

Conflict of interest The authors have declared that no conflict of interest exists, and this paper has been approved by all authors for publication.

Appendix A: Derivation of Eq. (14)

Employing the Wiener path integral approximate solution technique and substituting the associated Lagrangian function of Eq. (8) into the E–L Eq. (11) yields

An approximate technique for determining in closed form

$$\begin{aligned} & \frac{\ddot{x}_c - \frac{\partial \mu(x_c)}{\partial x_c} \dot{x}_c}{\sigma(x_c)^2} - 2 \frac{(\dot{x}_c - \mu(x_c)) \frac{\partial \sigma(x_c)}{\partial x_c} \dot{x}_c}{\sigma(x_c)^3} \\ &= - \frac{(\dot{x}_c - \mu(x_c)) \frac{\partial \mu(x_c)}{\partial x_c}}{\sigma(x_c)^2} - \frac{(\dot{x}_c - \mu(x_c))^2 \frac{\partial \sigma(x_c)}{\partial x_c}}{\sigma(x_c)^3}. \end{aligned} \quad (58)$$

Equation (58) can be further manipulated into

$$\ddot{x}_c - \mu(x_c) \frac{\partial \mu(x_c)}{\partial x_c} = \frac{\frac{\partial \sigma(x_c)}{\partial x_c}}{\sigma(x_c)} (\dot{x}_c^2 - \mu(x_c)^2), \quad (59)$$

in conjunction with the boundary conditions $x_c(t_i) = x_i$, $x_c(t_f) = x_f$. Equivalently, Eq. (59) can be cast into the form

$$\begin{aligned} & \ddot{x}_c - \frac{\frac{\partial \sigma(x_c)}{\partial x_c}}{\sigma(x_c)} \dot{x}_c^2 = \mu(x_c) \frac{\partial \mu(x_c)}{\partial x_c} - \frac{\mu(x_c)^2 \frac{\partial \sigma(x_c)}{\partial x_c}}{\sigma(x_c)} \\ &= \frac{\mu(x_c)}{\sigma(x_c)} \left(\sigma(x_c) \frac{\partial \mu(x_c)}{\partial x_c} - \mu(x_c) \frac{\partial \sigma(x_c)}{\partial x_c} \right), \end{aligned} \quad (60)$$

and multiplying both sides by $\frac{2\dot{x}_c}{\sigma(x_c)^2}$ yields

$$\begin{aligned} & \frac{2\dot{x}_c \ddot{x}_c}{\sigma(x_c)^2} - \frac{2 \frac{\partial \sigma(x_c)}{\partial x_c}}{\sigma(x_c)^3} \dot{x}_c^3 \\ &= 2 \frac{\mu(x_c)}{\sigma(x_c)} \left(\frac{\sigma(x_c) \frac{\partial \mu(x_c)}{\partial x_c} - \mu(x_c) \frac{\partial \sigma(x_c)}{\partial x_c}}{\sigma(x_c)^2} \right) \dot{x}_c. \end{aligned} \quad (61)$$

Next, taking into account that

$$\begin{aligned} & \frac{\partial}{\partial x_c} \left(\left(\frac{\mu(x_c)}{\sigma(x_c)} \right)^2 \right) \\ &= 2 \frac{\mu(x_c)}{\sigma(x_c)} \left(\frac{\sigma(x_c) \frac{\partial \mu(x_c)}{\partial x_c} - \mu(x_c) \frac{\partial \sigma(x_c)}{\partial x_c}}{\sigma(x_c)^2} \right), \end{aligned} \quad (62)$$

in conjunction with the chain rule of differentiation, i.e., $\frac{d}{dt} \left(\left(\frac{\mu(x_c)}{\sigma(x_c)} \right)^2 \right) = \frac{\partial}{\partial x_c} \left(\left(\frac{\mu(x_c)}{\sigma(x_c)} \right)^2 \right) \dot{x}_c$, Eq. (61) becomes

$$\frac{2\dot{x}_c \ddot{x}_c}{\sigma(x_c)^2} - \frac{2 \frac{\partial \sigma(x_c)}{\partial x_c}}{\sigma(x_c)^3} \dot{x}_c^3 = \frac{d}{dt} \left(\left(\frac{\mu(x_c)}{\sigma(x_c)} \right)^2 \right). \quad (63)$$

Further, it can be readily verified that

$$\frac{d}{dt} \left(\frac{\dot{x}_c^2}{\sigma(x_c)^2} \right) = \frac{2\dot{x}_c \ddot{x}_c}{\sigma(x_c)^2} - \frac{2 \frac{\partial \sigma(x_c)}{\partial x_c}}{\sigma(x_c)^3} \dot{x}_c^3. \quad (64)$$

Utilizing Eq. (64), Eq. (63) becomes

$$\frac{d}{dt} \left(\frac{\dot{x}_c^2}{\sigma(x_c)^2} \right) = \frac{d}{dt} \left(\left(\frac{\mu(x_c)}{\sigma(x_c)} \right)^2 \right), \quad (65)$$

or, alternatively,

$$\frac{\dot{x}_c^2}{\sigma(x_c)^2} = \left(\frac{\mu(x_c)}{\sigma(x_c)} \right)^2 + b, \quad (66)$$

where b is a constant, dependent on the boundary conditions, i.e., $x_c(t_i) = x_i$, $x_c(t_f) = x_f$. Considering next Eq. (8), and expanding, leads to

$$L(x_c, \dot{x}_c) = \frac{1}{2} \left(\frac{\dot{x}_c^2 - 2\dot{x}_c \mu(x_c) + \mu(x_c)^2}{\sigma(x_c)^2} \right), \quad (67)$$

whereas substituting Eq. (66) into Eq. (67) yields

$$L(x_c, \dot{x}_c) = \frac{1}{2} \left(\frac{2\dot{x}_c^2 - 2\dot{x}_c \mu(x_c)}{\sigma(x_c)^2} - b \right). \quad (68)$$

Next, integrating Eq. (68) leads to

$$\begin{aligned} & \int_{t_i}^{t_f} L(x_c, \dot{x}_c) dt \\ &= \frac{1}{2} \left(2 \int_{t_i}^{t_f} \frac{\dot{x}_c^2}{\sigma(x_c)^2} dt - \int_{t_i}^{t_f} \frac{2\dot{x}_c \mu(x_c)}{\sigma(x_c)^2} dt \right. \\ &\quad \left. - b (t_f - t_i) \right). \end{aligned} \quad (69)$$

Furthermore, for arbitrary functions $f(\cdot)$, $g(\cdot)$, the Cauchy–Schwarz inequality (e.g., [29]) states that

$$\left(\int_a^b f(t) g(t) dt \right)^2 \leq \int_a^b f(t)^2 dt \int_a^b g(t)^2 dt. \quad (70)$$

Clearly, setting $f \equiv 1$ yields the special case

$$\int_a^b g(t)^2 dt \geq \frac{1}{b-a} \left(\int_a^b g(t) dt \right)^2. \quad (71)$$

Next, denoting by $\mathcal{M}(\cdot)$ an antiderivative of $\frac{2\mu(\cdot)}{\sigma(\cdot)^2}$ and by $\mathcal{R}(\cdot)$ an antiderivative of $\frac{1}{\sigma(\cdot)}$, and applying Eq. (71) to the term $2 \int_{t_i}^{t_f} \frac{\dot{x}_c^2}{\sigma(x_c)^2} dt$ in Eq. (69) yields

$$\begin{aligned} 2 \int_{t_i}^{t_f} \frac{\dot{x}_c^2}{\sigma(x_c)^2} dt &\geq \int_{t_i}^{t_f} \frac{\dot{x}_c^2}{\sigma(x_c)^2} dt \\ &\geq \frac{\left(\int_{t_i}^{t_f} \frac{\dot{x}_c}{\sigma(x_c)} dt \right)^2}{t_f - t_i} \\ &= \frac{(\mathcal{R}(x_f) - \mathcal{R}(x_i))^2}{t_f - t_i}. \end{aligned} \quad (72)$$

Considering Eq. (72), Eq. (69) becomes

$$\begin{aligned} \int_{t_i}^{t_f} L(x_c, \dot{x}_c) dt &\geq -\frac{b(t_f - t_i)}{2} \\ &+ \frac{1}{2} \left(\frac{(\mathcal{R}(x_f) - \mathcal{R}(x_i))^2}{t_f - t_i} - (\mathcal{M}(x_f) - \mathcal{M}(x_i)) \right). \end{aligned} \quad (73)$$

Thus, taking into account Eqs. (12) and (73) an approximation for the response transition PDF of Eq. (13) is given by

$$\hat{p}(x_f, t_f | x_i, t_i) = \mathcal{N}(t_f | x_i, t_i) \exp(-G(x_f, t_f | x_i, t_i)), \quad (74)$$

where

$$\begin{aligned} G(x_f, t_f | x_i, t_i) \\ = \frac{1}{2} \left(\frac{(\mathcal{R}(x_f) - \mathcal{R}(x_i))^2}{t_f - t_i} - (\mathcal{M}(x_f) - \mathcal{M}(x_i)) \right), \end{aligned} \quad (75)$$

and \mathcal{N} in Eq. (74) serves as the normalization constant, which is determined as

$$\mathcal{N}(t_f | x_i, t_i) = \left(\int_{\mathcal{D}} \exp(-G(z, t_f | x_i, t_i)) dz \right)^{-1}, \quad (76)$$

where \mathcal{D} denotes the domain of integration, accounting for any restrictions that $\mathcal{M}(\cdot)$ and $\mathcal{R}(\cdot)$ may impose.

References

- Grigoriu, M.: Applied Non-Gaussian Processes: Examples, Theory, Simulation, Linear Random Vibration, and Matlab Solutions. Prentice Hall, Englewood Cliffs (1995)
- Spanos, P.D., Zeldin, B.A.: Monte Carlo treatment of random fields: a broad perspective. *Appl. Mech. Rev.* **51**(3), 219–237 (1998)
- Vanmarcke, E.: Random Fields: Analysis and Synthesis (Revised and Expanded New Edition). World Scientific, Singapore (2010)
- Roberts, J.B., Spanos, P.D.: Random Vibration and Statistical Linearization. Courier Corporation, New York (2003)
- Li, J., Chen, J.: Stochastic Dynamics of Structures. Wiley, New York (2009)
- Grigoriu, M.: Stochastic Systems: Uncertainty Quantification and Propagation. Springer, London (2012)
- Wiener, N.: The average of an analytic functional and the Brownian movement. *Proc. Natl. Acad. Sci.* **7**(10), 294–298 (1921)
- Feynman, R.P.: Space-time approach to non-relativistic quantum mechanics. *Rev. Mod. Phys.* **20**(2), 367–387 (1948)
- Di Matteo, A., Kougoumtzoglou, I.A., Pirrotta, A., Spanos, P.D., Di Paola, M.: Stochastic response determination of nonlinear oscillators with fractional derivatives elements via the Wiener path integral. *Probab. Eng. Mech.* **38**, 127–135 (2014)
- Petromichelakis, I., Psaros, A.F., Kougoumtzoglou, I.A.: Stochastic response determination and optimization of a class of nonlinear electromechanical energy harvesters: a Wiener path integral approach. *Probab. Eng. Mech.* **53**, 116–125 (2018)
- Psaros, A.F., Brudastova, O., Malara, G., Kougoumtzoglou, I.A.: Wiener path integral based response determination of nonlinear systems subject to non-white, non-Gaussian, and non-stationary stochastic excitation. *J. Sound Vib.* **433**, 314–333 (2018)
- Psaros, A.F., Kougoumtzoglou, I.A., Petromichelakis, I.: Sparse representations and compressive sampling for enhancing the computational efficiency of the Wiener path integral technique. *Mech. Syst. Signal Process.* **111**, 87–101 (2018)
- Meimaris, A.T., Kougoumtzoglou, I.A., Pantelous, A.A.: A closed form approximation and error quantification for the response transition probability density function of a class of stochastic differential equations. *Probab. Eng. Mech.* **54**, 87–94 (2018)
- Meimaris, A.T., Kougoumtzoglou, I.A., Pantelous, A.A.: Approximate analytical solutions for a class of nonlinear stochastic differential equations. *Eur. J. Appl. Math.* 1–17 (2018) (In Press)
- Grigoriu, M.: Stochastic Calculus: Applications in Science and Engineering. Springer, New York (2002)
- Gardiner, C.: Stochastic Methods: A Handbook for the Natural and Social Sciences. Springer, New York (2009)
- Risken, H.: The Fokker–Planck Equation: Methods of Solution and Applications. Springer, New York (1996)

An approximate technique for determining in closed form

18. Chaichian, M., Demichev, A.: Path Integrals in Physics: Volume I Stochastic Processes and Quantum Mechanics. CRC Press, Bath (2001)
19. Kougioumtzoglou, I.A., Spanos, P.D.: An analytical Wiener path integral technique for non-stationary response determination of nonlinear oscillators. *Probab. Eng. Mech.* **28**, 125–131 (2012)
20. Naess, A., Moe, V.: Stationary and non-stationary random vibration of oscillators with bilinear hysteresis. *Int. J. Non-Linear Mech.* **31**(5), 553–562 (1996)
21. Wehner, M.F., Wolfer, W.G.: Numerical evaluation of path-integral solutions to Fokker–Planck equations. II. Restricted stochastic processes. *Phys. Rev. A* **28**(5), 3003–3011 (1983)
22. Naess, A., Johnsen, J.M.: Response statistics of nonlinear, compliant offshore structures by the path integral solution method. *Probab. Eng. Mech.* **8**(2), 91–106 (1993)
23. Alevras, P., Yurchenko, D.: GPU computing for accelerating the numerical Path integration approach. *Comput. Struct.* **171**, 46–53 (2016)
24. Ewing, G.M.: Calculus of Variations with Applications. Dover Publications, New York (1969)
25. Kougioumtzoglou, I.A., Spanos, P.D.: Nonstationary stochastic response determination of nonlinear systems: a Wiener path integral formalism. *ASCE J. Eng. Mech.* **140**(9), 04014064: 1–14 (2014)
26. Kougioumtzoglou, I.A.: A Wiener path integral solution treatment and effective material properties of a class of one-dimensional stochastic mechanics problems. *ASCE J. Eng. Mech.* **143**(6), 04017014: 1–12 (2017)
27. Kougioumtzoglou, I.A., Di Matteo, A., Spanos, P.D., Pirrotta, A., Di Paola, M.: An efficient Wiener path integral technique formulation for stochastic response determination of nonlinear MDOF systems. *J. Appl. Mech.* **82**(10), 101005: 1–7 (2015)
28. Psaros, A.F., Petromichelakis, I., Kougioumtzoglou, I.A.: Wiener path integrals and multi-dimensional global bases for non-stationary stochastic response determination of structural systems. *Mech. Syst. Signal Process.* (Under Review) (2019)
29. Steele, J.M.: The Cauchy–Schwarz Master Class: An Introduction to the Art of Mathematical Inequalities. Cambridge University Press, New York (2004)
30. Roberts, J.B., Spanos, P.D.: Stochastic averaging: an approximate method of solving random vibration problems. *Int. J. Non-Linear Mech.* **21**(2), 314–333 (1986)
31. Spanos, P.D., Kougioumtzoglou, I.A., dos Santos, K.R.M., Beck, A.T.: Stochastic averaging of nonlinear oscillators: Hilbert transform perspective. *ASCE J. Eng. Mech.* **144**(2), 04017173: 1–9 (2018)
32. Kougioumtzoglou, I.A., Spanos, P.D.: An approximate approach for nonlinear system response determination under evolutionary stochastic excitation. *Curr. Sci.* **97**(8), 1203–1211 (2009)
33. Forsgren, A., Philip, E., Gill, P.E., Wright, M.H.: Interior methods for nonlinear optimization. *SIAM Rev.* **44**(4), 525–597 (2002)
34. Nocedal, J., Wright, S.J.: Numerical Optimization. Springer, New York (1999)
35. Macki, J.W., Nistri, P., Zecca, P.: Mathematical models for hysteresis. *SIAM Rev.* **35**(1), 94–123 (1993)
36. Bertotti, G., Mayergoyz, I.D.: The Science of Hysteresis: Mathematical Modeling and Applications, vol. I. Elsevier, New York (2003)
37. Ktena, A., Fotiadis, D.I., Spanos, P.D., Massalas, C.V.: A Preisach model identification procedure and simulation of hysteresis in ferromagnets and shape-memory alloys. *Phys. B Condens. Matter* **306**(1–4), 84–90 (2001)
38. Spanos, P.D., Cacciola, P., Red-Horse, J.: Random vibration of SMA systems via Preisach formalism. *Nonlinear Dyn.* **36**(2–4), 405–419 (2004)
39. Mayergoyz, I.D.: Mathematical Models of Hysteresis and Their Applications. Elsevier, New York (2003)
40. Ni, Y.Q., Ying, Z.G., Ko, J.M.: Random response analysis of Preisach hysteretic systems with symmetric weight distribution. *ASME J. Appl. Mech.* **69**(2), 171–178 (2002)
41. Spanos, P.D., Cacciola, P., Muscolino, G.: Stochastic averaging of Preisach hysteretic systems. *ASCE J. Eng. Mech.* **130**(11), 1257–1267 (2004)
42. Wang, Y., Ying, Z.G., Zhu, W.Q.: Stochastic averaging of energy envelope of Preisach hysteretic systems. *J. Sound Vib.* **321**(3–5), 976–993 (2009)
43. Kougioumtzoglou, I.A., Spanos, P.D.: Response and first-passage statistics of nonlinear oscillators via a numerical path integral approach. *ASCE J. Eng. Mech.* **139**, 1207–1217 (2013)
44. Kougioumtzoglou, I.A.: Stochastic joint time-frequency response analysis of nonlinear structural systems. *J. Sound Vib.* **332**, 7153–7173 (2013)
45. Spanos, P.D., Kougioumtzoglou, I.A.: Survival probability determination of nonlinear oscillators subject to evolutionary stochastic excitation. *ASME J. Appl. Mech.* **81**, 051016: 1–9 (2014)
46. Di Matteo, A., Spanos, P.D., Pirrotta, A.: Approximate survival probability determination of hysteretic systems with fractional derivative elements. *Probab. Eng. Mech.* **54**, 138–146 (2018)

Publisher's Note Springer Nature remains neutral with regard to jurisdictional claims in published maps and institutional affiliations.

4.2 Quantitative Finance Applications

In this section, the Tanaka Equation and the CEV model are considered for assessing the reliability of the developed method in Quantitative Finance applications. Specifically, using the same set-up as in the numerical examples of Meimaris et al., 2019, the Tanaka Equation is used as a case illustrating that the basic approximation coincides with the known exact solution even when discontinuities are considered, whereas the CEV model is used for pricing Bermuda call options. Comparisons with MCS-based (100,000 simulations) option prices and the exact *Fokker-Planck* (F-P) equation PDF solution based prices are included.

Special Case: The Tanaka Equation

In the special case of constant zero drift and diffusion coefficient being equal to the generalized signum function, i.e.

$$\sigma(x) := \begin{cases} +1 & \text{if } x \geq 0, \\ -1 & \text{if } x < 0, \end{cases} \quad (4.1)$$

Eq. (3.2) becomes

$$dX_t = \sigma(X_t) dB_t, \quad (4.2)$$

which is typically called the Tanaka Equation when $x_i = t_i = 0$ (see also Shiryaev, 1999 for more details). In this special case, since $\frac{1}{\sigma(x)} = \sigma(x)$ and $\sigma(x)^2 = 1$ everywhere, the approximate basic PDF \hat{p} (see Eq. (14) in Published Material Section 4.1) takes the form

$$\hat{p}(x_f, t_f | 0, 0) = \mathcal{N}(t_f | 0, 0) \exp\left(-\frac{(|x_f|)^2}{2t_f}\right) = \mathcal{N}(t_f | 0, 0) \exp\left(-\frac{x_f^2}{2t_f}\right), \quad (4.3)$$

where the fact that the signum function is the derivative of the absolute value function almost everywhere, under the generalised notion of differentiation in distribution theory, was utilized. The PDF of Eq. (4.3) can be construed as the distribution of a standard Brownian motion process, which, notably, coincides with the already known result from Shiryaev, 1999, i.e. $\hat{p} = p^*$. Since, it can be readily seen that $\mathcal{L}_{FP}[\hat{p}] = \mathcal{L}_{FP}[p^*] = 0$, for this case the calibration of the parameters k and n is redundant, i.e. $\hat{p}_{(\hat{k}, \hat{n})} = \hat{p}_{(1, 1)} = \hat{p} = p^*$.

Pricing Bermuda Calls Under drift-less CEV

The drift-less constant elasticity of variance (CEV) model (e.g. see Hull, 2018 for more details) describes a process which evolves according to the following SDE

$$dS_t = \sigma S_t^\gamma dB_t. \quad (4.4)$$

In Fig. 4.1¹, using the values $S_0 = 2800$, $\sigma = 0.14$ and $\gamma = 0.87$, the PDFs based on the basic approximation \hat{p} (Eq. (14) in Published Material Section 4.1) are compared with the exact solution from a F-P PDE solver for quarterly dates in a year.

Since, the end goal of this application is the efficient pricing of a Bermuda call option with quarterly exercise dates in a year, the PDF of $X = \max(S_{\frac{62}{250}}, S_{\frac{125}{250}}, S_{\frac{187}{250}}, S_1)$ needs to be determined in order to calculate $\mathbb{E}_X [\max(X - K, 0)]$. However, as seen in Fig. 4.2, minor inaccuracies in approximating the PDFs of S_t , lead to greater inaccuracies when approximating the PDF of the random variable X . Thus, the proposed enhanced PDF (Eq. (17) in Published Material Section 4.1) is utilized in the following. Specifically, in Table 4.1, the computed calibrated values of k are shown together with the corresponding iterations numbers for each date; CPU times are included as well for the different methodologies.

¹For this and all following figures of this section, the x -axis is kept the same for comparison purposes.

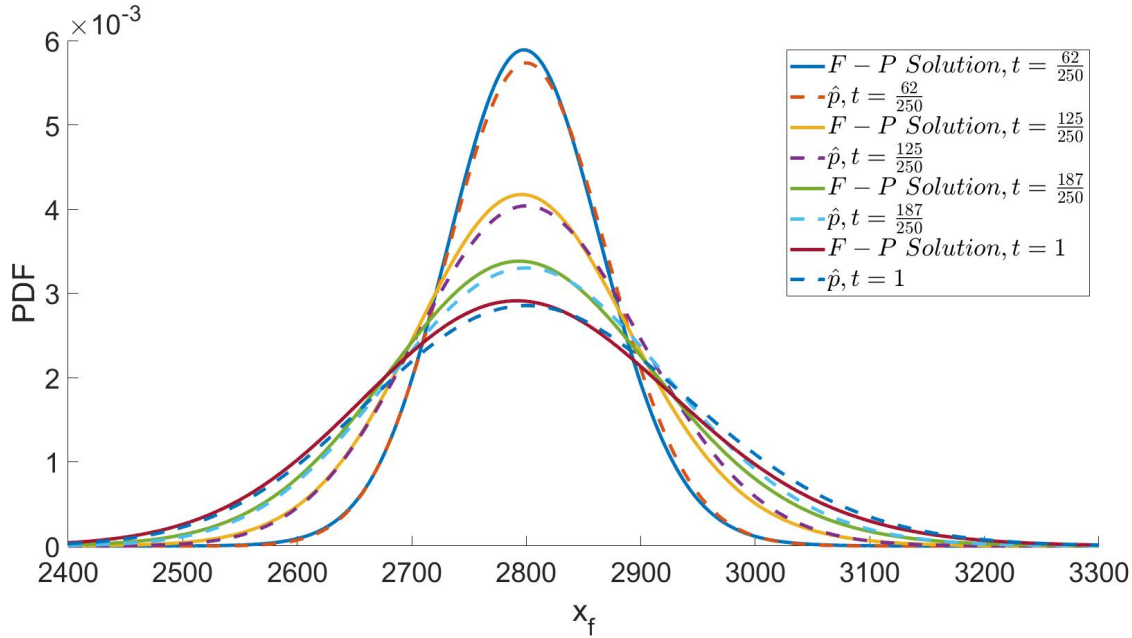


FIGURE 4.1: Approximate basic PDFs \hat{p} for various time instants t_f for a CEV model; comparisons with exact F-P based PDF solutions.

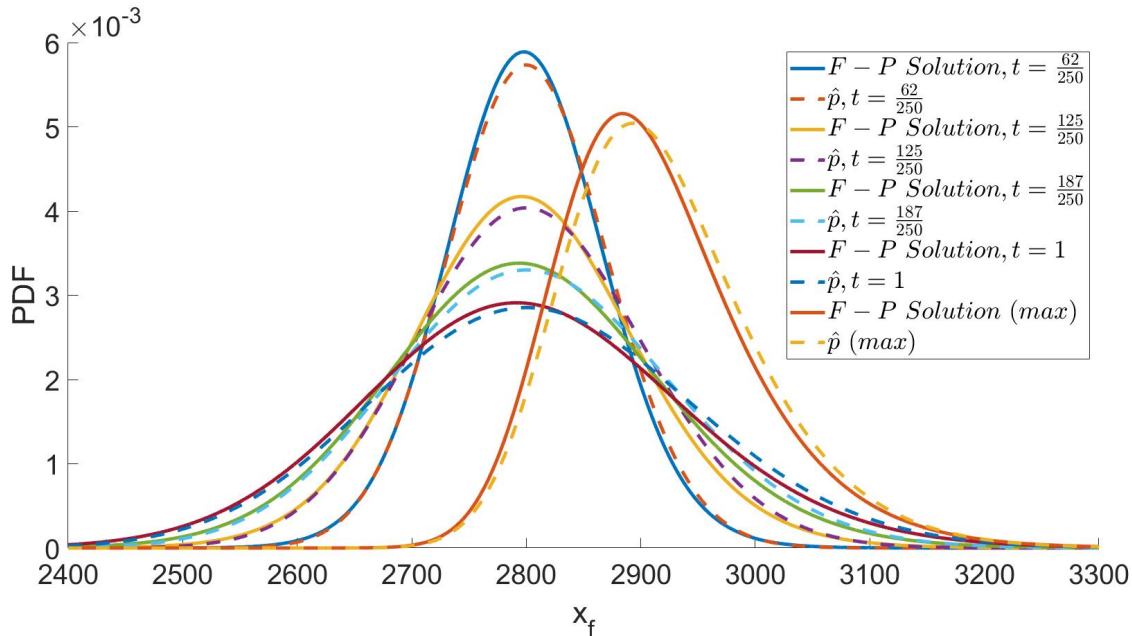


FIGURE 4.2: PDF approximations for the random variable $X = \max\left(S_{\frac{62}{250}}, S_{\frac{125}{250}}, S_{\frac{187}{250}}, S_1\right)$ based on the approximate basic PDFs \hat{p} and the exact F-P based PDF solutions; comparison with Figure 4.1 plots.

In Fig. 4.3, the approximate enhanced PDFs $\hat{p}_{(k,n)} = \hat{p}_k$, can capture the dynamics of the different random variables, i.e., $S_{\frac{62}{250}}, S_{\frac{125}{250}}, S_{\frac{187}{250}}, S_1$, with a high degree of accuracy. As presented in Fig. 4.4, minor deviations from the exact solution PDFs, result in a less accurate, however, still satisfactory, approximation of the distribution of the maximum of those considered random variables, i.e., X .

Regarding the pricing of the Bermunda call and associated errors, depicted in Figs. 4.5

TABLE 4.1: Computed k values for various final time instants t_f and starting point 1 for a drift-less CEV model

	$t_f = \frac{62}{250}$	$t_f = \frac{125}{250}$	$t_f = \frac{187}{250}$	$t_f = 1$
k	1.050	1.057	1.040	1.031
Iterations	14	14	14	14
CPU time	0.205	0.085	0.049	0.033
MCS CPU time	NA	NA	NA	8.869
F-P PDE solver CPU time	NA	NA	NA	17.921

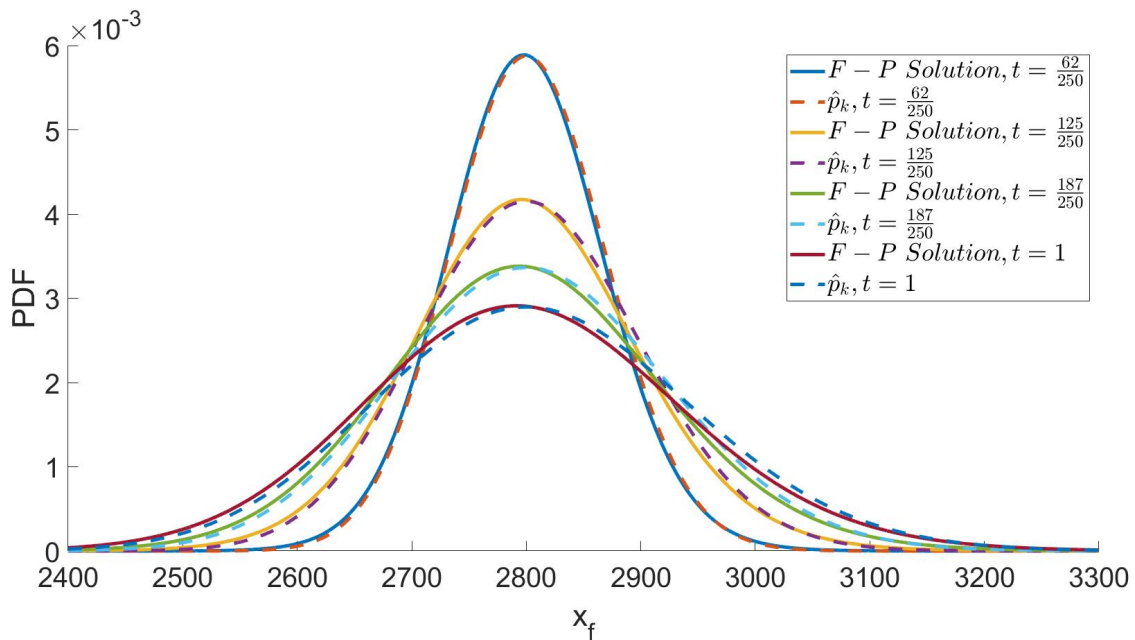


FIGURE 4.3: Approximate enhanced PDFs $\hat{p}_{(k,n)} = \hat{p}_k$ for various time instants t_f for a CEV model; comparisons with exact F-P based PDF solutions.

and 4.6, respectively, the prices given from the computationally efficient approximate solution methods are closer to the exact theoretical values produced by solving the F-P partial differential equation, than the more time consuming 100,000 MCS realized prices.

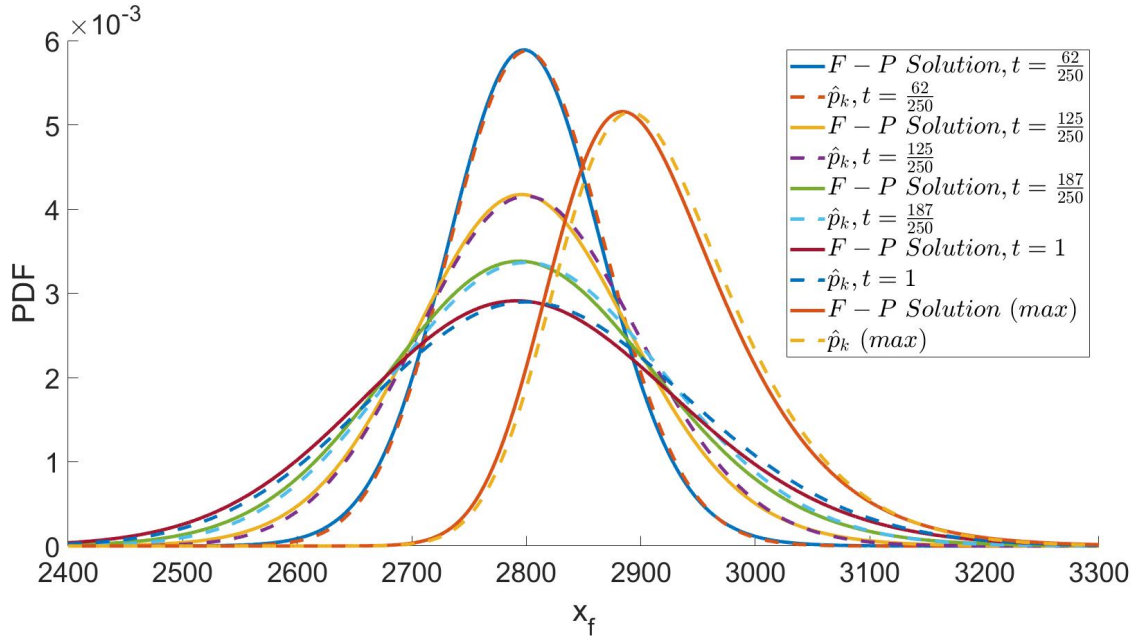


FIGURE 4.4: PDF approximations for the random variable $X = \max\left(S_{\frac{62}{250}}, S_{\frac{125}{250}}, S_{\frac{187}{250}}, S_1\right)$ based on the approximate enhanced PDFs $\hat{p}_{(k,n)} = \hat{p}_k$ and the exact F-P based PDF solutions; comparison with Figure 4.3 plots.

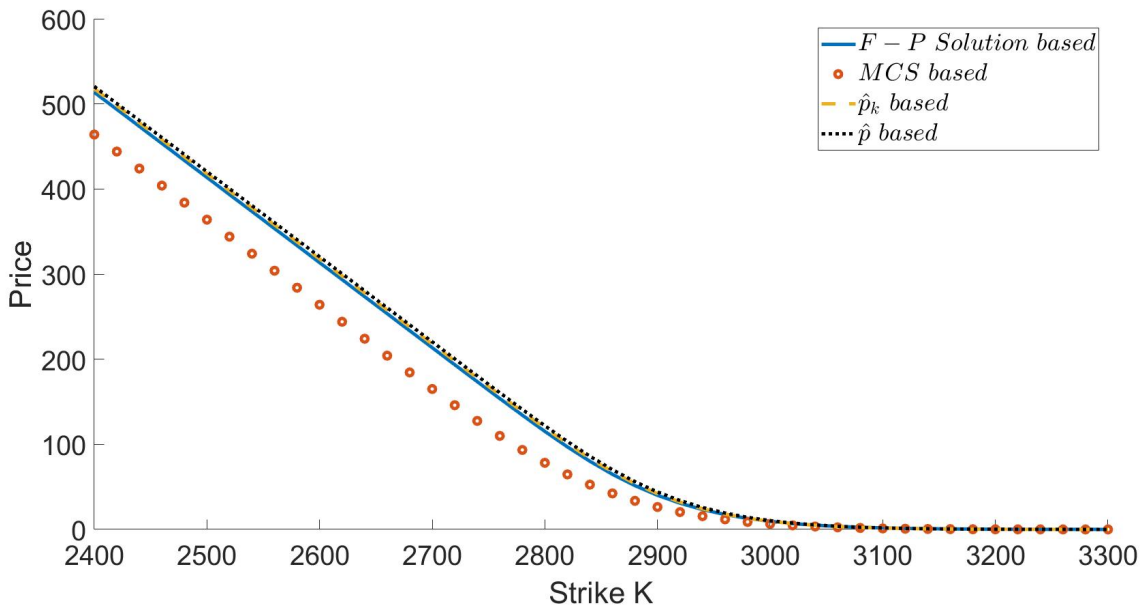


FIGURE 4.5: Approximate Bermuda call prices based on basic \hat{p} and enhanced PDFs $\hat{p}_{(k,n)} = \hat{p}_k$ for various strike values K for a CEV model; comparisons with MCS based prices (100,000 realizations) and with F-P based prices (exact).

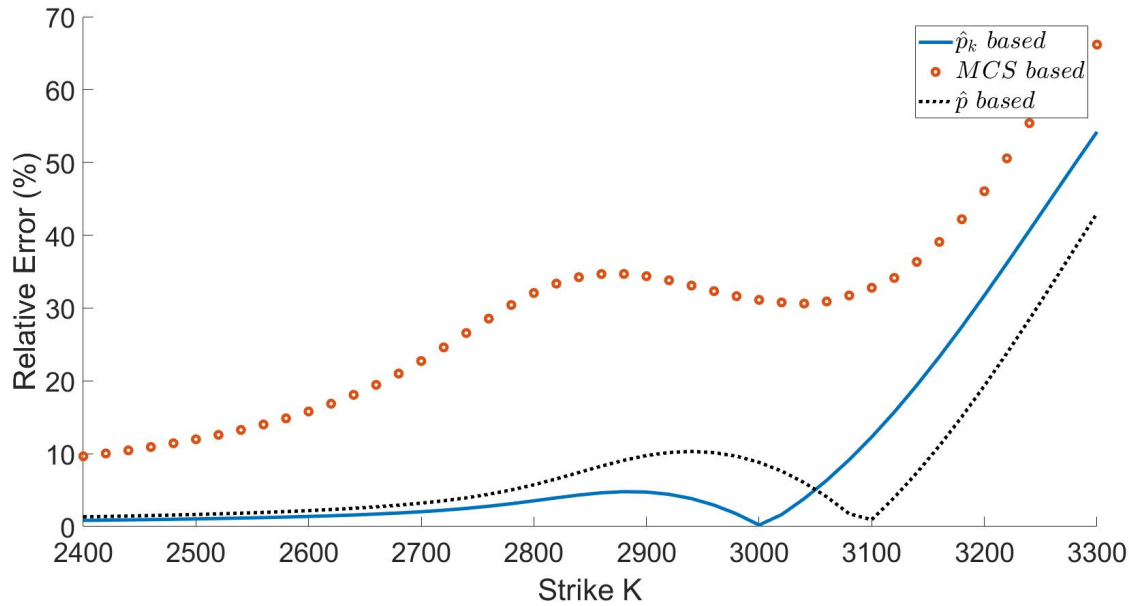


FIGURE 4.6: Relative error comparison for the Bermuda call prices based on basic \hat{p} and enhanced PDFs $\hat{p}_{(k,n)} = \hat{p}_k$ and MCS based prices (100,000 realizations) with exact F-P based prices.

4.3 Summary

To conclude, an analytical closed form approximation for SDEs with time-homogeneous nonlinear drift and diffusion coefficients has been derived based on a WPI formulation, which can serve as an alternative for assessing the performance of other numerical stochastic dynamics methodologies, at minimal computational cost. Regarding the applicability of the aforementioned technique, a variety of models from different disciplines were considered. Examples from both engineering dynamics (smart materials) and Quantitative Finance (option pricing) were presented and demonstrated a high degree of accuracy.

Chapter 5

Approximate solutions for a case of coupled Itô SDEs

The aim of the previous chapters was the development of an efficient approximation technique for a class of one-dimensional nonlinear Itô SDEs, namely of the form of Eq. (3.2), i.e., $dX_t = \mu(X_t) dt + \sigma(X_t) dB_t$. It is noted that the first crucial step for this derivation was the analysis of the simpler case, i.e., SDEs of the form of Eq. (3.1), where the diffusion coefficient was assumed to be constant.

The most general case of one-dimensional nonlinear Itô SDEs, i.e., equations of the form of Eq. (2.3), can be written in the following system of coupled SDEs, i.e.,

$$\begin{aligned} dX_t &= \mu(X_t, Y_t) dt + \sigma(X_t, Y_t) dB_t \\ dY_t &= dt, \quad Y_0 = 0, \end{aligned} \tag{5.1}$$

equivalently. Thus, if the derivation of efficient approximations for the even more general case of coupled nonlinear N -dimensional SDEs, i.e.,

$$dX_t^{(j)} = \mu_j(\mathbf{X}_t) dt + \sigma(\mathbf{X}_t) dB_t^{(j)}, \quad \forall j \in \{1, 2, \dots, N\} \equiv [N], \tag{5.2}$$

where $\mu(\mathbf{X}_t) = (\mu_1(\mathbf{X}_t), \mu_2(\mathbf{X}_t), \dots, \mu_N(\mathbf{X}_t))^T$ denotes the nonlinear drift coefficient vector and $\sigma(\mathbf{X}_t) = (\sigma_1(\mathbf{X}_t), \sigma_2(\mathbf{X}_t), \dots, \sigma_N(\mathbf{X}_t))^T$ is the nonlinear diffusion coefficient vector, is achieved, then, as a special case, approximations for SDEs of the form of Eq. (2.3) will also become available.

However, the approach which was used in the previous chapters cannot work immediately in this general case of coupled SDEs of the form of Eq. (5.2), as noted in Section 2.3, due to the indeterminacy about the exact form of the associated Lagrangian, L , function which needs to be used for the consequent derivations. Thus, this chapter sets the course towards deriving approximate solutions for SDEs of the form of Eq. (2.3) and Eq. (5.2), by dealing with the case of N -dimensional coupled SDEs of the following form

$$dX_t^{(j)} = \mu_j(\mathbf{X}_t) dt + \sigma dB_t^{(j)}, \quad \forall j \in \{1, 2, \dots, N\} \equiv [N], \tag{5.3}$$

where μ denotes the nonlinear drift coefficient vector and σ is the constant diffusion coefficient.

This kind of modeling is then used in the publication in Section 5.1 to study chemical and complex ecological applications which have clear connections with finance & economics as discussed in Chapter 1. The two-dimensional version of the labyrinth model, which was cut from Meimaris, Kougoumtzoglou, and Pantelous, 2020, is presented in Section 5.2 for completeness. Note that some information contained in the publication is repeated to achieve a mostly self-consistent write-up.

5.1 Published Material

Closed-form approximate solutions for a class of coupled nonlinear stochastic differential equations

Meimaris Antonios, Kougioumtzoglou Ioannis and Pantelous Athanasios

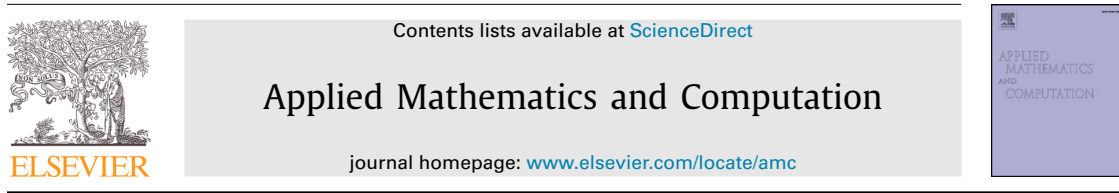
Published in the Applied Mathematics and Computation journal, Elsevier (2020)

DOI: 10.1016/j.amc.2019.124669

With kind permission of the Applied Mathematics and Computation journal, Elsevier.

Begins overleaf.

Applied Mathematics and Computation 364 (2020) 124669



Closed-form approximate solutions for a class of coupled nonlinear stochastic differential equations



Antonios T. Meimaris^a, Ioannis A. Kougioumtzoglou^b, Athanasios A. Pantelous^{a,*}

^aDepartment of Econometrics and Business Statistics, Monash Business School, Monash University, 20 Chancellors Walk, Wellington Rd, Clayton, VIC 3800, Australia

^bDepartment of Civil Engineering and Engineering Mechanics, The Fu Foundation School of Engineering and Applied Science, Columbia University, 500 West 120th Street, New York, NY 10027, USA

ARTICLE INFO

Keywords:

Nonlinear stochastic dynamics
Path Integral
Error quantification
Cauchy–Schwarz inequality
Fokker–Planck equation
Stochastic differential equations

ABSTRACT

An approximate solution technique is developed for a class of coupled multi-dimensional stochastic differential equations with nonlinear drift and constant diffusion coefficients. Relying on a Wiener path integral formulation and employing the Cauchy–Schwarz inequality, an approximate closed-form expression for the joint response process transition probability density function is determined. Next, the accuracy of the approximation is further enhanced by proposing a more versatile closed-form expression with additional “degrees of freedom”; that is, parameters to be determined. To this aim, an error minimization problem related to the corresponding Fokker–Planck equation is formulated and solved. Several diverse numerical examples are considered for demonstrating the reliability of the herein developed solution technique, which requires minimal computational cost for determining the joint response transition probability density function and exhibits satisfactory accuracy as compared with pertinent Monte Carlo simulation data.

© 2019 Elsevier Inc. All rights reserved.

1. Introduction

Systems of coupled nonlinear ordinary stochastic differential equations (SDEs) are widely used for modeling the dynamics of diverse systems. In this regard, several solution methodologies have been developed in the literature, with Monte Carlo (MC) simulation techniques [1,2] being among the most widely utilized numerical approaches. Nevertheless, in certain situations MC techniques can be computationally highly intensive, and thus, a need for developing alternative approximate solution methodologies arises; see, for instance, some indicative work in the field of chemical processes (e.g., [3,4]). Further, based on preliminary work in [5], Naess and co-workers developed a stochastic response determination numerical scheme by utilizing a discrete version of the Chapman–Kolmogorov equation, and by propagating the response probability density function (PDF) in short time steps [6,7]. Nevertheless, although the scheme exhibits excellent accuracy in predicting even the tails of the system response PDF, it becomes eventually computationally prohibitive with increasing dimensionality. This is due to the fact that a multi-convolution integral needs to be computed for each and every time step, while the time increment is required to be short. The reader is also referred to [8,9] for other alternative approximate techniques for solving SDEs modelling the random vibrations of diverse structural and mechanical systems.

* Corresponding author.

E-mail addresses: Antonios.Meimaris@monash.edu (A.T. Meimaris), ikougioum@columbia.edu (I.A. Kougioumtzoglou), Athanasios.Pantelous@monash.edu (A.A. Pantelous).

Recently, Kougioumtzoglou and co-workers developed a semi-analytical technique based on the concept of the Wiener path integral (WPI) [10,11] for determining the joint response PDF of coupled nonlinear SDEs describing the dynamics of multi-degree-of-freedom structural systems subject to stochastic excitation [12–15]. In general, although the WPI technique has exhibited both versatility and relatively high accuracy in addressing a wide range of engineering problems (e.g. [16–18]), its implementation relates, unfortunately, to non-negligible computational cost; see [15,19] for more details and some recent enhancements of the technique regarding computational efficiency. Motivated by the above challenge, and relying on a WPI formulation, as well as on a Cauchy–Schwarz inequality treatment, the authors derived recently in [20,21] closed-form approximate expressions for the response PDF of a class of one-dimensional nonlinear SDEs. Due to the analytical nature of the solution techniques, minimal computational effort is required, while the approximate PDF has demonstrated satisfactory accuracy as compared to pertinent Euler–Maruyama MC simulation data.

In this paper, the approximations proposed in [20,21] are generalized to account for multi-dimensional stochastic processes related to systems of coupled nonlinear Itô SDEs. Specifically, first, a basic approximation is derived for the joint response transition PDF, which is enhanced further by introducing additional “degrees-of-freedom”, i.e., parameters to be determined. To this aim, an error minimization problem associated with the corresponding Fokker–Planck equation is formulated and solved. This enhancement aims at “tightening” the Cauchy–Schwarz inequality as well as increasing the overall accuracy of the basic approximation. Several diverse numerical examples are considered for demonstrating the reliability of the approximation, while comparisons with Euler–Maruyama MC data demonstrate a satisfactory degree of accuracy.

The outline of the paper is as follows: In Section 2, the basic aspects of the WPI technique are delineated, while a note regarding the Cauchy–Schwarz inequality is included as well. In Section 3, a closed-form approximate joint response transition PDF for a class of multi-dimensional coupled SDEs with nonlinear drift and constant diffusion coefficients is derived, which is supplemented by an error quantification analysis as well. This, in turn, facilitates the development of an enhanced approximate joint PDF by proposing a more versatile closed-form expression with additional parameters to be determined by resorting to an appropriate error minimization scheme. Section 4 corresponds to the numerical examples, while concluding remarks are provided in Section 5.

2. Preliminaries

Let $(\Omega, \mathcal{F}, \mathcal{F}_{t \geq 0}, \mathbb{P})$ be a complete filtered probability space on which a scalar standard Brownian motion $(B_t, t \geq 0)$ is defined, and \mathcal{F}_t is the augmentation of $\sigma\{B_s | 0 \leq s \leq t\}$ by all the \mathbb{P} -null sets of \mathcal{F} .

2.1. Wiener path integral overview

In general, for an N -dimensional stochastic process $\mathbf{X}_t = (X^{(1)}(t), X^{(2)}(t), \dots, X^{(N)}(t))$ the joint transition PDF $p(\mathbf{x}_f, t_f | \mathbf{x}_i, t_i)$ from a point in state space \mathbf{x}_i at time t_i to a point \mathbf{x}_f at time t_f , where $t_f > t_i$, can be expressed as a functional integral over the space of all possible paths $C[\mathbf{x}_i, t_i; \mathbf{x}_f, t_f]$ in the form (e.g., see [15])

$$p(\mathbf{x}_f, t_f | \mathbf{x}_i, t_i) = \int_{\{\mathbf{x}_i, t_i\}}^{\{\mathbf{x}_f, t_f\}} \mathbb{E}[\mathbf{x}(t)] [d\mathbf{x}(t)]. \quad (1)$$

In Eq. (1), $\mathbb{E}[\mathbf{x}(t)]$ represents the probability density functional, which can be explicitly determined in closed-form only for relatively simple cases of stochastic processes, and $[d\mathbf{x}(t)]$ represents a functional measure. For instance, for a Gaussian white noise process vector $\mathbf{w}(t)$ possessing a diagonal power spectrum matrix

$$\mathbf{S} = \begin{bmatrix} S_0 & & \\ & \ddots & \\ & & S_0 \end{bmatrix}, \quad (2)$$

$\mathbb{E}[\mathbf{x}(t)]$ is given by [22]

$$\mathbb{E}[\mathbf{w}(t)] = \exp \left[- \int_{t_i}^{t_f} \frac{1}{4\pi} \mathbf{w}(t)^T \mathbf{S}^{-1} \mathbf{w}(t) dt \right]. \quad (3)$$

Without loss of generality and for notation simplicity, it has been assumed that the constant entries of the power spectrum matrix of Eq. (2) are identical, and equal to S_0 . A detailed derivation and discussion of Eq. (3) can be found in standard path integral related books such as [23]. In the ensuing analysis, the following system of coupled nonlinear Itô stochastic differential equations is considered, i.e.,

$$dX_t^{(j)} = \mu_j(\mathbf{X}_t) dt + \sigma dB_t^{(j)}, \quad \forall j \in \{1, 2, \dots, N\} \equiv \lceil N \rceil, \quad (4)$$

where $\mu(\mathbf{X}_t) = (\mu_1(\mathbf{X}_t), \mu_2(\mathbf{X}_t), \dots, \mu_N(\mathbf{X}_t))^T$ denotes the nonlinear drift coefficient vector, $\sigma^2 = 2\pi S_0$ is the constant diffusion coefficient, and dB/dt represents the formal time-derivative of a white noise process of unit intensity. In this regard, Eq. (4) can be substituted into Eq. (3), yielding for the transition PDF of the response process \mathbf{X}_t the expression (e.g., see

[12–16])

$$p(\mathbf{x}_f, t_f | \mathbf{x}_i, t_i) = \int_{\{\mathbf{x}_i, t_i\}}^{\{\mathbf{x}_f, t_f\}} \exp \left(- \int_{t_i}^{t_f} L(\mathbf{x}, \dot{\mathbf{x}}) dt \right) [d\mathbf{x}(t)], \quad (5)$$

where $L(\mathbf{x}, \dot{\mathbf{x}})$ represents the Lagrangian function associated with the dynamical system of Eq. (4), and is given by

$$L(\mathbf{x}, \dot{\mathbf{x}}) = \frac{1}{2\sigma^2} \sum_{j=1}^N (\dot{x}^{(j)} - \mu_j(\mathbf{x}))^2. \quad (6)$$

As noted earlier, the constant diffusion coefficients in Eq. (5) are taken all equal to σ for convenience and notation simplicity. It is rather straightforward to consider non-equal values for the diffusion coefficients in Eq. (5) (corresponding to non-equal entries in the power spectrum matrix of Eq. (2)) and adjust accordingly Eq. (6). Further, although the assumption of constant diffusion coefficients appears rather restrictive, it is often possible to transform more general cases with state-dependent/nonlinear diffusion coefficients into the form of Eq. (5); see for instance [24], as well as the herein considered example in Section 4.3. Furthermore, the assumption of constant diffusion may be quite reasonable for various engineering dynamics applications. Indicatively, the SDE governing the dynamics of a class of oscillators with nonlinear damping subject to stochastic excitation can be approximated via a stochastic averaging treatment by Eq. (4); see, for instance, the numerical examples in [12] for more details. Extending the herein developed solution technique for the more general and significantly more challenging case of nonlinear drift and nonlinear diffusion coefficients is identified as future work.

Next, it is readily seen that, in general, the analytical evaluation of the WPI, Eq. (5), is at least a rather challenging, if not impossible, task. Thus, seeking for an approximate solution technique, it is observed that the greatest contribution to the WPI comes from the trajectory for which the integral in the exponential of Eq. (5) becomes as small as possible. According to calculus of variations [25], this trajectory with fixed end points satisfies the extremality condition

$$\delta \int_{t_i}^{t_f} L(\mathbf{x}_c, \dot{\mathbf{x}}_c) dt = 0, \quad (7)$$

where \mathbf{x}_c denotes the “most probable path” to be determined by the functional optimization problem

$$\text{Min}(\text{Max}) \quad J[\mathbf{x}_c(t)] = \int_{t_i}^{t_f} L(\mathbf{x}_c, \dot{\mathbf{x}}_c) dt, \quad (8)$$

together with the boundary conditions $\mathbf{x}_c(t_i) = \mathbf{x}_i$ and $\mathbf{x}_c(t_f) = \mathbf{x}_f$. Further, $\mathbf{x}_c(t)$ can be determined either by deriving and solving a system of Euler–Lagrange (E–L) equations associated with Eq. (7) (e.g., see [13,15]), i.e.

$$\frac{\partial L}{\partial \mathbf{x}_c^{(k)}} - \frac{\partial}{\partial t} \frac{\partial L}{\partial \dot{\mathbf{x}}_c^{(k)}} = 0, \forall k \in [N], \quad (9)$$

in conjunction with the boundary conditions $\mathbf{x}_c(t_i) = \mathbf{x}_i$, $\mathbf{x}_c(t_f) = \mathbf{x}_f$, or alternatively, by treating directly the deterministic boundary value problem (BVP) of Eq. (8) (e.g. [14,16]). Once $\mathbf{x}_c(t)$ is determined, the joint transition PDF can be approximated by

$$p(\mathbf{x}_f, t_f | \mathbf{x}_i, t_i) \approx \Phi \exp \left(- \int_{t_i}^{t_f} L(\mathbf{x}_c, \dot{\mathbf{x}}_c) dt \right), \quad (10)$$

where Φ is a normalization coefficient.

2.2. Cauchy–Schwarz inequality

For completeness, the integral form of the Cauchy–Schwarz inequality is included below, whereas a detailed presentation of the topic can be found in [26].

Lemma 2.1. Let f and g be real functions that are continuous on the closed interval $[a, b]$. Then

$$\left(\int_a^b f(t)g(t)dt \right)^2 \leq \int_a^b f(t)^2 dt \int_a^b g(t)^2 dt. \quad (11)$$

Clearly, setting $g = 1$ yields the special case

$$\int_a^b f(t)^2 dt \geq \frac{1}{b-a} \left(\int_a^b f(t)dt \right)^2, \quad (12)$$

which will be used in Section 3.1 for proving Lemma 3.1.

3. Main results

3.1. A closed-form approximate solution for stochastically driven nonlinear dynamical systems with constant diffusion

Although the approximate expression of Eq. (10) has exhibited a significant degree of accuracy (as compared to pertinent MC simulation data) in several applications such as those pertaining to engineering dynamical systems [14,15,20], there is a considerable computational cost associated with solving numerically the BVPs of Eq. (8); see for instance [19] for a recent work towards enhancing the computational efficiency of the WPI. In this section, a closed-form approximate expression for the joint response transition PDF of Eq. (4) is derived by relying on a Cauchy–Schwarz inequality treatment. The approximate solution, which can be construed as a generalization of the results of [20] to account for multi-dimensional processes \mathbf{x}_t , not only requires essentially zero computational effort, but also facilitates an error quantification analysis (see Section 3.2).

Regarding the system of coupled nonlinear SDEs of Eq. (4), the following Lemma is proved next, which will be instrumental in deriving the approximate joint response PDF.

Lemma 3.1. Let $M^{(j)}(\cdot)$ be an antiderivative of $\mu_j(\cdot)$ w.r.t the j th coordinate, i.e.,

$$\frac{\partial M^{(j)}(\mathbf{x})}{\partial x^{(j)}} = \mu_j(\mathbf{x}) \quad \forall j. \quad (13)$$

Then, the integral of the Lagrangian function, $\int_{t_i}^{t_f} L(\mathbf{x}_c, \dot{\mathbf{x}}_c) dt$, is bounded by

$$\int_{t_i}^{t_f} L(\mathbf{x}_c, \dot{\mathbf{x}}_c) dt \geq \frac{1}{2\sigma^2} \left(\sum_{j=1}^N \frac{(\chi^{(j)})^2}{\tau} - b\tau - 2 \sum_{j=1}^N (M^{(j)}(\mathbf{x}_f) - M^{(j)}(\mathbf{x}_i)) \right), \quad (14)$$

where $\chi^{(j)} = x_f^{(j)} - x_i^{(j)}$, $\tau = t_f - t_i$ and b is a constant, depending on the boundary conditions $\mathbf{x}_c(t_i) = \mathbf{x}_i$, $\mathbf{x}_c(t_f) = \mathbf{x}_f$.

Proof. Substituting the Lagrangian function of Eq. (6) corresponding to the system of SDEs of Eq. (4) into the E-L Eq. (9), and manipulating, yields

$$-\frac{1}{\sigma^2} \sum_{j=1}^N (\dot{x}_c^{(j)} - \mu_j(\mathbf{x}_c)) \frac{\partial \mu_j(\mathbf{x}_c)}{\partial x_c^{(k)}} - \frac{1}{\sigma^2} \left(\ddot{x}_c^{(k)} - \sum_{j=1}^N \frac{\partial \mu_k(\mathbf{x}_c)}{\partial x_c^{(j)}} \dot{x}_c^{(j)} \right) = 0, \quad \forall k \in [N], \quad (15)$$

together with the boundary conditions $\mathbf{x}_c(t_i) = \mathbf{x}_i$, $\mathbf{x}_c(t_f) = \mathbf{x}_f$. Further, Eq. (15) can be cast in the form

$$\ddot{x}_c^{(k)} = \sum_{j=1}^N \dot{x}_c^{(j)} \left(\frac{\partial \mu_k(\mathbf{x}_c)}{\partial x_c^{(j)}} - \frac{\partial \mu_j(\mathbf{x}_c)}{\partial x_c^{(k)}} \right) + \sum_{j=1}^N \mu_j(\mathbf{x}_c) \frac{\partial \mu_j(\mathbf{x}_c)}{\partial x_c^{(k)}}, \quad \forall k \in [N], \quad (16)$$

or equivalently written as

$$\frac{\partial}{\partial t} \left((\dot{x}_c^{(k)})^2 \right) = 2 \sum_{j=1}^N \dot{x}_c^{(j)} \left(\frac{\partial \mu_k(\mathbf{x}_c)}{\partial x_c^{(j)}} - \frac{\partial \mu_j(\mathbf{x}_c)}{\partial x_c^{(k)}} \right) \dot{x}_c^{(k)} + \sum_{j=1}^N 2 \mu_j(\mathbf{x}_c) \frac{\partial \mu_j(\mathbf{x}_c)}{\partial x_c^{(k)}} \dot{x}_c^{(k)}, \quad \forall k \in [N]. \quad (17)$$

Considering Eq. (17), and summing over all k indexes yields

$$\sum_{k=1}^N \frac{\partial}{\partial t} \left((\dot{x}_c^{(k)})^2 \right) = 2 \sum_{k=1}^N \sum_{j=1}^N \dot{x}_c^{(j)} \left(\frac{\partial \mu_k(\mathbf{x}_c)}{\partial x_c^{(j)}} - \frac{\partial \mu_j(\mathbf{x}_c)}{\partial x_c^{(k)}} \right) \dot{x}_c^{(k)} + \sum_{k=1}^N \sum_{j=1}^N 2 \mu_j(\mathbf{x}_c) \frac{\partial \mu_j(\mathbf{x}_c)}{\partial x_c^{(k)}} \dot{x}_c^{(k)}, \quad (18)$$

or equivalently,

$$\sum_{k=1}^N \frac{\partial}{\partial t} \left((\dot{x}_c^{(k)})^2 \right) = \sum_{j=1}^N 2 \mu_j(\mathbf{x}_c) \sum_{k=1}^N \frac{\partial \mu_j(\mathbf{x}_c)}{\partial x_c^{(k)}} \dot{x}_c^{(k)}, \quad (19)$$

since by symmetry,

$$\sum_{k=1}^N \sum_{j=1}^N \dot{x}_c^{(j)} \left(\frac{\partial \mu_k(\mathbf{x}_c)}{\partial x_c^{(j)}} - \frac{\partial \mu_j(\mathbf{x}_c)}{\partial x_c^{(k)}} \right) \dot{x}_c^{(k)} = 0. \quad (20)$$

Taking into account the chain rule of differentiation, Eq. (19) becomes

$$\sum_{k=1}^N \frac{\partial}{\partial t} \left((\dot{x}_c^{(k)})^2 \right) = \sum_{j=1}^N 2 \mu_j(\mathbf{x}_c) \frac{\partial}{\partial t} \mu_j(\mathbf{x}_c) = \sum_{j=1}^N \frac{\partial}{\partial t} (\mu_j(\mathbf{x}_c)^2), \quad (21)$$

or equivalently,

$$\frac{\partial}{\partial t} \left(\sum_{k=1}^N (\dot{x}_c^{(k)})^2 \right) = \frac{\partial}{\partial t} \left(\sum_{j=1}^N \mu_j(\mathbf{x}_c)^2 \right), \quad (22)$$

which yields

$$\sum_{k=1}^N (\dot{x}_c^{(k)})^2 = \sum_{j=1}^N \mu_j(\mathbf{x}_c)^2 + b. \quad (23)$$

In Eq. (23) b is a constant, depending on the boundary conditions $\mathbf{x}_c(t_i) = \mathbf{x}_i$, $\mathbf{x}_c(t_f) = \mathbf{x}_f$. Expanding next the square in Eq. (6), and substituting Eq. (23) yields

$$L(\mathbf{x}_c, \dot{\mathbf{x}}_c) = \frac{1}{2\sigma^2} \left(2 \sum_{j=1}^N (\dot{x}_c^{(j)})^2 - b - 2 \sum_{j=1}^N \mu_j(\mathbf{x}_c) \dot{x}_c^{(j)} \right). \quad (24)$$

Next, the integral of Eq. (24) is given by

$$\int_{t_i}^{t_f} L(\mathbf{x}_c, \dot{\mathbf{x}}_c) dt = \frac{1}{2} \left(\frac{\sum_{j=1}^N 2 \int_{t_i}^{t_f} (\dot{x}_c^{(j)})^2 dt - b\tau - 2 \sum_{j=1}^N \int_{t_i}^{t_f} \mu_j(\mathbf{x}_c) d\dot{x}_c^{(j)}}{\sigma^2} \right), \quad (25)$$

or equivalently, by utilizing the $M^{(j)}$ antiderivatives of Eq. (13)

$$\int_{t_i}^{t_f} L(\mathbf{x}_c, \dot{\mathbf{x}}_c) dt = \frac{1}{2} \left(\frac{\sum_{j=1}^N 2 \int_{t_i}^{t_f} (\dot{x}_c^{(j)})^2 dt - b\tau - 2 \sum_{j=1}^N (M^{(j)}(\mathbf{x}_f) - M^{(j)}(\mathbf{x}_i))}{\sigma^2} \right). \quad (26)$$

Further, employing the Cauchy–Schwarz inequality of Eq. (12), the quantity $2 \int_{t_i}^{t_f} (\dot{x}_c^{(j)})^2 dt$ is bounded by

$$2 \int_{t_i}^{t_f} (\dot{x}_c^{(j)})^2 dt \geq \int_{t_i}^{t_f} (\dot{x}_c^{(j)})^2 dt \geq \frac{(x_f^{(j)} - x_i^{(j)})^2}{\tau} = \frac{(\chi^{(j)})^2}{\tau}. \quad (27)$$

Combining Eqs. (26) and (27), Eq. (14) is derived. \square

In the following, the main result of the present section is stated and proved.

Theorem 3.2. Let

$$G(\mathbf{x}_f, t_f | \mathbf{x}_i, t_i) = \frac{\sum_{j=1}^N (\chi^{(j)})^2 + \sum_{j=1}^N (-2M^{(j)}(\mathbf{x}_f) + 2M^{(j)}(\mathbf{x}_i))\tau}{2\tau\sigma^2}, \quad (28)$$

then an approximate joint transition PDF for Eq. (4) is given by $\hat{p} : \mathcal{D}(M) \times (t_i, +\infty) \times \{\mathbf{x}_i\} \times \{t_i\} \rightarrow \mathbb{R}$, where $\mathcal{D}(M) = \mathcal{D}(M^{(1)}) \times \mathcal{D}(M^{(2)}) \times \dots \times \mathcal{D}(M^{(N)})$, defined as

$$\hat{p}(\mathbf{x}_f, t_f | \mathbf{x}_i, t_i) = F(t_f) \exp(-G(\mathbf{x}_f, t_f | \mathbf{x}_i, t_i)), \quad (29)$$

where $F(t_f)$ is a normalization constant.

Proof. The proof follows in a straightforward manner from Lemma 3.1 and Eqs. (10) and (14). Thus, it can be readily seen that a closed-form approximate solution for the joint transition PDF can be given by Eq. (29), where $F(t_f) = (\int_{\mathcal{D}(M)} \exp(-G(\mathbf{x}, t_f | \mathbf{x}_i, t_i)) d\mathbf{x})^{-1}$. Note that the arbitrary term $\exp(\frac{-b\tau}{2\sigma^2})$ has been included in the constant $F(t_f)$. \square

3.2. Error quantification

The transition PDF of Eq. (29) derived herein constitutes an approximate solution of the coupled system of nonlinear SDEs of Eq. (4). Naturally, the next step is to quantify the accuracy of the derived approximation and estimate its error. In this regard, for a given norm $(\|\cdot\|_q)$, the error quantity $\|\hat{p} - p^*\|_q$ can be defined, where p^* is the exact transition PDF. Clearly, however, the error quantity $\|\hat{p} - p^*\|_q$ cannot be determined explicitly as p^* is unknown. Thus, an alternative error definition, also adopted in [20,21], is utilized in the ensuing analysis. Specifically, the transition PDF p^* for the SDEs of Eq. (4) is given as the solution of the associated Fokker–Planck equation [27], i.e.,

$$\exists p^* : \frac{\partial p^*(\mathbf{x}, t)}{\partial t} = - \sum_{j=1}^N \frac{\partial (\mu_j(\mathbf{x}) p^*(\mathbf{x}, t))}{\partial x^{(j)}} + \frac{\sigma^2}{2} \sum_{j=1}^N \sum_{k=1}^N \frac{\partial^2 p^*(\mathbf{y}, t)}{\partial x^{(j)} \partial x^{(k)}}. \quad (30)$$

Let us denote the Fokker–Planck operator as follows

$$\mathcal{L}_{FP}[p(\mathbf{x}, t)] = \frac{\partial p(\mathbf{x}, t)}{\partial t} + \sum_{j=1}^N \frac{\partial(\mu_j(\mathbf{x})p(\mathbf{x}, t))}{\partial x^{(j)}} - \frac{\sigma^2}{2} \sum_{j=1}^N \sum_{k=1}^N \frac{\partial^2 p(\mathbf{x}, t)}{\partial x^{(j)} \partial x^{(k)}}. \quad (31)$$

From Eq. (30), it follows that $L_{FP}[p^*] = 0$. Thus, the error is defined as $\|\mathcal{L}_{FP}[\hat{p} - p^*]\|_q = \|\mathcal{L}_{FP}[\hat{p}] - \mathcal{L}_{FP}[p^*]\|_q = \|\mathcal{L}_{FP}[\hat{p}]\|_q$ (see also [20,21]).

Clearly, utilizing the Fokker–Planck operator in the above error definition (see also [28–30]) facilitates the evaluation via $\|\mathcal{L}_{FP}[\hat{p}]\|_q$ of the error incurred by using \hat{p} as an approximation to the exact PDF p^* . In particular, substituting the approximate transition PDF of Eq. (29) into Eq. (31) and manipulating yields

$$\mathcal{L}_{FP}[\hat{p}] = \hat{p} \left(\frac{\dot{F}}{F} - \frac{\partial G}{\partial t} + \sum_{j=1}^N \left(\frac{\mu_j}{\partial x^{(j)}} - \mu_j \frac{\partial G}{\partial x^{(j)}} \right) - \frac{\sigma^2}{2} \sum_{j=1}^N \sum_{k=1}^N \left(-\frac{\partial^2 G}{\partial x^{(j)} \partial x^{(k)}} + \left(\frac{\partial G}{\partial x^{(j)}} \right) \left(\frac{\partial G}{\partial x^{(k)}} \right) \right) \right). \quad (32)$$

Differentiating Eq. (28) leads to

$$-\frac{\partial G}{\partial t} \Big|_{\mathbf{x}=\mathbf{x}_f, t=t_f} = \frac{1}{2\sigma^2} \sum_{j=1}^N \left(\frac{\chi^{(j)}}{\tau} \right)^2, \quad (33)$$

$$\frac{\partial G}{\partial x^{(j)}} \Big|_{\mathbf{x}=\mathbf{x}_f, t=t_f} = \frac{\frac{x_f^{(j)} - x_i^{(j)}}{\tau} - \mu_j(\mathbf{x}_f)}{\sigma^2}, \quad (34)$$

$$\frac{\partial^2 G}{\partial x^{(j)} \partial x^{(k)}} \Big|_{\mathbf{x}=\mathbf{x}_f, t=t_f} = \left(\frac{\partial}{\partial x^{(j)}} \left(\frac{\partial G}{\partial x^{(k)}} \right) \right) \Big|_{\mathbf{x}=\mathbf{x}_f, t=t_f} = \frac{\mathbf{1}_{j=k} - \frac{\partial}{\partial x^{(j)}} \mu_k(\mathbf{x}_f) \tau}{\tau \sigma^2}. \quad (35)$$

Next, substituting Eqs. (33) to (35) into Eq. (32), and manipulating, yields

$$\begin{aligned} \mathcal{L}_{FP}[\hat{p}] &= \frac{\hat{p}(\mathbf{x}_f, t_f | \mathbf{x}_i, t_i)}{2} \left(2 \frac{\dot{F}(t_f)}{F(t_f)} + \frac{N}{\tau} + \frac{1}{\sigma^2} \sum_{j=1}^N \mu_j(\mathbf{x}_f)^2 + \sum_{j=1}^N \frac{\partial \mu_j(\mathbf{x}_f)}{\partial x^{(j)}} \right. \\ &\quad \left. - \sum_{j \neq k} \frac{\partial \mu_k(\mathbf{x}_f)}{\partial x^{(j)}} - \frac{1}{\sigma^2} \sum_{j \neq k} \left(\frac{\chi^{(j)}}{\tau} - \mu_j(\mathbf{x}_f) \right) \left(\frac{\chi^{(k)}}{\tau} - \mu_k(\mathbf{x}_f) \right) \right). \end{aligned} \quad (36)$$

Utilizing Eq. (36), the error function, $err(\mathbf{x}_f, t_f | \mathbf{x}_i, t_i)$, and its normalized version are given by

$$\begin{aligned} err(\mathbf{x}_f, t_f | \mathbf{x}_i, t_i) &= \left\| \frac{\hat{p}(\mathbf{x}_f, t_f | \mathbf{x}_i, t_i)}{2} \left(2 \frac{\dot{F}(t_f)}{F(t_f)} + \frac{N}{\tau} + \sum_{j=1}^N \frac{\partial \mu_j(\mathbf{x}_f)}{\partial x^{(j)}} - \sum_{j \neq k} \frac{\partial \mu_k(\mathbf{x}_f)}{\partial x^{(j)}} \right. \right. \\ &\quad \left. \left. + \frac{1}{\sigma^2} \sum_{j=1}^N \mu_j(\mathbf{x}_f)^2 - \frac{1}{\sigma^2} \sum_{j \neq k} \left(\frac{\chi^{(j)}}{\tau} - \mu_j(\mathbf{x}_f) \right) \left(\frac{\chi^{(k)}}{\tau} - \mu_k(\mathbf{x}_f) \right) \right) \right\|_q \end{aligned} \quad (37)$$

and

$$\widetilde{err}(\mathbf{x}_f, t_f | \mathbf{x}_i, t_i) = \frac{err(\mathbf{x}_f, t_f | \mathbf{x}_i, t_i)}{\sup_{\substack{\mathbf{x}_f \in \mathcal{D}(M) \\ t_f \in [t_i^+, +\infty)}} err(\mathbf{x}_f, t_f | \mathbf{x}_i, t_i)}, \quad (38)$$

where $\sup(\cdot)$ denotes the supremum operator.

Overall, the normalized error of Eq. (38) can be estimated for a given system of SDEs of Eq. (4) for assessing the relative accuracy of the approximate response transition PDF both for various x_f values, and for various time instants t_f .

3.3. SDEs with constant drift and diffusion coefficients: an exact analytical solution case

For the special case of constant drift coefficients, the system of coupled SDEs of Eq. (4) degenerates to

$$dX_t^{(j)} = \mu_j dt + \sigma dB_t^{(j)}, \quad \forall j \in [N]. \quad (39)$$

Eq. (39) represents a system of uncoupled SDEs, which has been used, for instance, to model the motion of particles [31]. In this regard, the approximate PDF of Eq. (29) takes the form (see also [20])

$$\hat{p}(\mathbf{x}_f, t_f | \mathbf{x}_i, t_i) = F(t_f) \exp \left(-\frac{\sum_{j=1}^N (\chi^{(j)})^2 + \sum_{j=1}^N (-2\mu x_f^{(j)} + 2\mu x_i^{(j)})\tau}{2\tau\sigma^2} \right), \quad (40)$$

or equivalently,

$$\hat{p}(\mathbf{x}_f, t_f | \mathbf{x}_i, t_i) = \tilde{F}(t_f) \exp\left(-\sum_{j=1}^N \frac{(\chi^{(j)} - \mu\tau)^2}{2\tau\sigma^2}\right), \quad (41)$$

where the term $\exp\left(\frac{N\mu^2\tau^2}{2\tau\sigma^2}\right)$ has been merged with the normalization coefficient $\tilde{F}(t_f)$. Note that for the SDEs of Eq. (39), an exact response PDF for the process $\mathbf{X}(t)$ is available (e.g., [32]) which, notably, coincides with Eq. (41). Also, it can be readily seen that substituting Eq. (41) into Eq. (37) yields $\text{err}(\mathbf{x}_f, t_f | \mathbf{x}_i, t_i) = 0$, and thus, as anticipated, the error of approximating the exact PDF of Eq. (39) with the approximate one of Eq. (29) is zero, since in that case the two PDFs coincide as discussed earlier.

3.4. Enhanced accuracy via an error minimization scheme

It can be readily seen that \hat{p} in Eq. (29) can be directly used as an analytical approximation of the joint response process PDF without resorting to the numerical solution of the E-L Eq. (9). Thus, essentially zero computational effort is required for the determination of the joint response transition PDF. However, as demonstrated in [20] for the one-dimensional case, although the approximation of Eq. (29) is capable, in general, of capturing the salient features of the solution PDF, in many cases the degree of accuracy exhibited can be inadequate. To address this limitation, a more general form of the PDF was proposed in [21], by incorporating two additional “degrees-of-freedom”; that is, parameters to be determined based on an appropriate optimization scheme.

In this section, a more general form than Eq. (29) is proposed for the joint solution PDF of the system of coupled SDEs of Eq. (4). This can be construed as a generalization of the results of [21] to account for multi-dimensional processes \mathbf{X}_t . Specifically, the joint response transition PDF is expressed in the form

$$\hat{p}_{(\mathbf{k}, \mathbf{n})}(\mathbf{x}_f, t_f | \mathbf{x}_i, t_i) = F_{(\mathbf{k}, \mathbf{n})}(t_f) \exp(-G_{(\mathbf{k}, \mathbf{n})}(\mathbf{x}_f, t_f | \mathbf{x}_i, t_i)), \quad (42)$$

where

$$(\mathbf{k}, \mathbf{n}) = (k_1, \dots, k_N, n_1, \dots, n_N), \quad (43)$$

and

$$G_{(\mathbf{k}, \mathbf{n})}(\mathbf{x}_f, t_f | \mathbf{x}_i, t_i) = \frac{\sum_{j=1}^N k_j (\chi^{(j)})^2 + \sum_{j=1}^N n_j (-2M^{(j)}(\mathbf{x}_f) + 2M^{(j)}(\mathbf{x}_i))\tau}{2\tau\sigma^2}. \quad (44)$$

The constant F in Eq. (42) is determined as

$$F_{(\mathbf{k}, \mathbf{n})}(t_f) = \left(\int_{\mathcal{D}(M)} \exp(-G_{(\mathbf{k}, \mathbf{n})}(\mathbf{y}, t_f | \mathbf{x}_i, t_i)) d\mathbf{y} \right)^{-1}. \quad (45)$$

Note that in comparison to Eq. (29), the general solution form in Eq. (42) has $2N$ additional “degrees-of-freedom”; that is, the parameters \mathbf{k} and \mathbf{n} to be determined based on an appropriate optimization scheme. The rationale behind this choice relates to utilizing available knowledge and integrating it in an optimization scheme for determining Eq. (42), and thus, enhancing the overall accuracy of Eq. (29). In particular, the parameter \mathbf{k} relates to optimizing and “tightening” the Cauchy-Schwarz inequality of Eq. (27), whereas the parameter \mathbf{n} refers to the overall accuracy of the WPI approximation of Eq. (10). In comparison to Eq. (29) it is anticipated that the approximation of Eq. (42) will exhibit higher accuracy, at the expense of course of some added modest computational cost related to the optimization algorithm. In this regard, it is emphasized that exploiting a priori available information in many problems, such as obvious symmetries, can reduce significantly the effective size of the vector of unknown parameters (\mathbf{k}, \mathbf{n}) . As seen also in many of the following numerical examples, the size of (\mathbf{k}, \mathbf{n}) can be considerably smaller than $2N$; thus, reducing the complexity and computational cost of the associated optimization problem.

Next, to determine the parameters \mathbf{k} and \mathbf{n} in Eq. (42), for a given norm ($\|\cdot\|_q$), the error quantity of Eq. (37) is sought to be minimized; see also [21]. In fact, due to the closed-form expression of $\hat{p}_{(\mathbf{k}, \mathbf{n})}$, the error quantity $\text{err} = \|\mathcal{L}_{FP}[\hat{p}_{(\mathbf{k}, \mathbf{n})}]\|_q$ can be explicitly determined as a function of \mathbf{k} and \mathbf{n} . Further, for a chosen q -norm and final time t_f , the values of \mathbf{k} , \mathbf{n} are numerically evaluated by solving the optimization problem

$$\hat{\mathbf{z}}_q = \left(\hat{\mathbf{k}}, \hat{\mathbf{n}} \right)_q = \arg \min_{(\mathbf{k}, \mathbf{n}) \in \mathbb{R}^{2N}} \text{err} = \arg \min_{(\mathbf{k}, \mathbf{n}) \in \mathbb{R}^{2N}} \|\mathcal{L}_{FP}[\hat{p}_{(\mathbf{k}, \mathbf{n})}(\cdot, t_f)]\|_q, \quad (46)$$

and, thus, the approximate response PDF of Eq. (42), is determined. Note that in comparison to Section 3.3, in this section the closed-form expression of Eq. (37) is used not as an error estimate, but rather as a tool within the optimization scheme for enhancing the accuracy of the joint response PDF.

Table 1
Computed (\mathbf{k}, \mathbf{n}) values for various final time instants t_f and starting point $(1,1,1)$ for Example 4.1.

	$k_1 = k_2$	$n_1 = n_2$	Iterations
$t_f = 0.1$	0.9848	0.4411	24
$t_f = 0.5$	1.0595	0.6001	36
$t_f = 1$	1.3648	0.8180	39
$t_f = 3$	3.4699	1.0824	36

Table 2
Error estimates and CPU times for Example 4.1.

	$\epsilon \times 10^{-4}$	ϵ_{ratio}	MCS CPU time (100,000 realizations)	$\hat{p}_{(\mathbf{k}, \mathbf{n})}$ CPU time
$t_f = 0.1$	3.42	8.18	126 s	0.068 s
$t_f = 0.5$	3.92	23.20	534 s	0.081 s
$t_f = 1$	10	14.20	931 s	0.058 s
$t_f = 3$	17	23.23	2,313 s	0.051 s

4. Numerical examples

In the ensuing numerical examples, a standard interior point method [33,34] using Matlab's *fmincon* built-in function is employed to solve the unconstrained optimization problem of Eq. (46), in conjunction with the $\|\cdot\|_2$ norm (i.e., $q = 2$). To this aim, the basic approximation of Eq. (29) with $(\mathbf{k}, \mathbf{n}) = (1, \dots, 1) \in \mathbb{R}^{2N}$ serves as a natural choice for the initial starting point of the algorithm.

In most of the numerical examples, the algorithm converged in less than a hundred iterations, which translates into less than a tenth of a second from a computational cost perspective for the examples considered. The accuracy of the approximate PDF of Eq. (42) is demonstrated by comparisons to the PDF estimated based on pertinent Euler-Maruyama MC simulation data (100,000 realizations) produced by numerically integrating the original Eq. (4) with $\Delta t = 10^{-2}$ on a computer with 16GB RAM, Inter(R) Core(TM) i7-6700 CPU @3.40GHz. Further, the error metric $\epsilon = \|\hat{p}_{(\mathbf{k}, \mathbf{n})} - \text{MCS PDF}\|_2$ is employed for quantifying the accuracy of the approximate PDF as compared to the MC simulation based estimate. Also, the additional error quantity $\epsilon_{ratio} = \frac{\|\hat{p}_{(\mathbf{k}, \mathbf{n})} - \text{MCS PDF}\|_2}{\|\hat{p}_{(1, \dots, 1)} - \text{MCS PDF}\|_2}$ is utilized for demonstrating how much better the enhanced approximation $\hat{p}_{(\mathbf{k}, \mathbf{n})}$ is in comparison to the basic one of \hat{p} .

4.1. Duffing kind nonlinearity: bimodal response PDF

In this example, a 2-dimensional Duffing nonlinear system with bimodal response PDF (e.g. [19]) of the form

$$\begin{cases} dX_t = (Y_t - X_t^3)dt + \sigma dB_t^{(1)} \\ dY_t = (X_t - Y_t^3)dt + \sigma dB_t^{(2)}, \end{cases} \quad (47)$$

is considered. Next, assuming zero initial conditions, and taking into account that $M_1(x, y) = xy - \frac{1}{4}x^4$ and $M_2(x, y) = M_1(y, x)$ the PDF of Eq. (42) takes the form

$$\hat{p}_{(\mathbf{k}, \mathbf{n})}(x_f, y_f, t_f | 0, 0, 0) = F(t_f) \exp \left(-\frac{k_1 x_f^2 + k_2 y_f^2 - t_f(n_1(2x_f y_f - \frac{1}{2}x_f^4) + n_2(2x_f y_f - \frac{1}{2}y_f^4))}{2t_f \sigma^2} \right). \quad (48)$$

Utilizing the parameter value $\sigma = 1$, and applying the numerical optimization scheme of Eq. (46) based on the $\|\cdot\|_2$ norm, yields the values for (\mathbf{k}, \mathbf{n}) . Specifically, exploiting the symmetry of Eqs. (47) and (48) the number of the unknown parameters is reduced from four to two by setting $k_1 = k_2$ and $n_1 = n_2$. The computed values are shown in Table 1 along with the iterations number of the optimization algorithm, whereas in Table 2 error estimates and CPU times are presented as well. In Figs. 1–4 the approximate PDFs $\hat{p}_{(\mathbf{k}, \mathbf{n})}$ of Eq. (48) are plotted for various time instants and compared both with the closed-form PDFs of Eq. (29) and with MCS based estimated PDFs. It is seen that the herein proposed enhanced PDF approximation of Eq. (48) is in very good agreement with MCS data, and yields improved performance as compared to the basic approximation of Eq. (29). Specifically, the closed-form basic approximation of Eq. (29) exhibits satisfactory accuracy at relatively early time instants, which deteriorates as t_f increases.

A.T. Meimaris, I.A. Kougioumtzoglou and A.A. Pantelous / Applied Mathematics and Computation 364 (2020) 124669

9

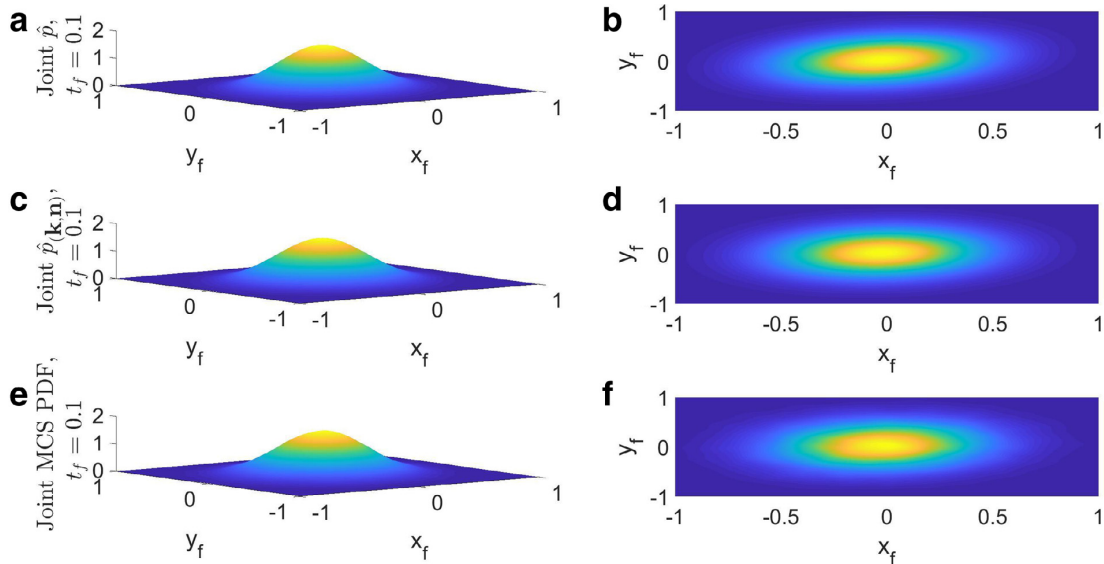


Fig. 1. Joint response PDF at $t_f = 0.1$ for a coupled system of SDEs with Duffing nonlinearity and bimodal response PDF: basic approximate PDF \hat{p} (a) and (b); Enhanced approximate PDF $\hat{p}_{(k,n)}$ (c) and (d); MCS based PDF (100,000 realizations) (e) and (f).

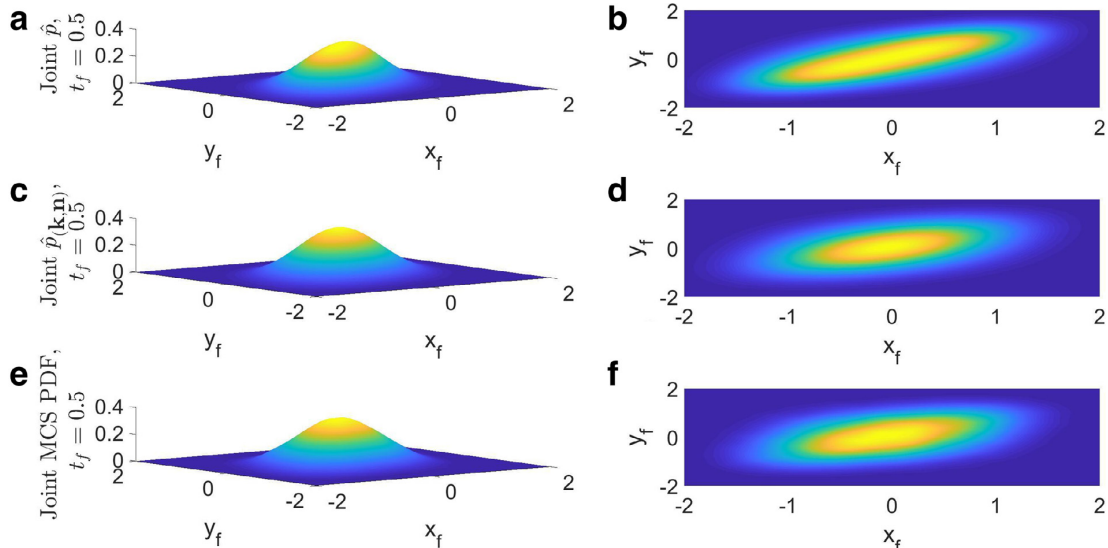


Fig. 2. Joint response PDF at $t_f = 0.5$ for a coupled system of SDEs with Duffing nonlinearity and bimodal response PDF: basic approximate PDF \hat{p} (a) and (b); enhanced approximate PDF $\hat{p}_{(k,n)}$ (c) and (d); MCS based PDF (100,000 realizations) (e) and (f).

4.2. The “labyrinth” model

Let

$$s(i) = (i + 1)\text{mod}N, \quad \forall i \in \mathbb{N}_0, \quad (49)$$

denote a circular shift permutation (rotation) operator of the natural numbers. The N -dimensional circulant system of the form

$$dX_t^{(j)} = \phi\left(X_t^{s^j(0)}, X_t^{s^j(1)}, \dots, X_t^{s^j(N-1)}\right)dt + \sigma dB_t^{(j)}, \quad \forall j \in [N]. \quad (50)$$

10

A.T. Meimaris, I.A. Kougioumtzoglou and A.A. Pantelous / Applied Mathematics and Computation 364 (2020) 124669

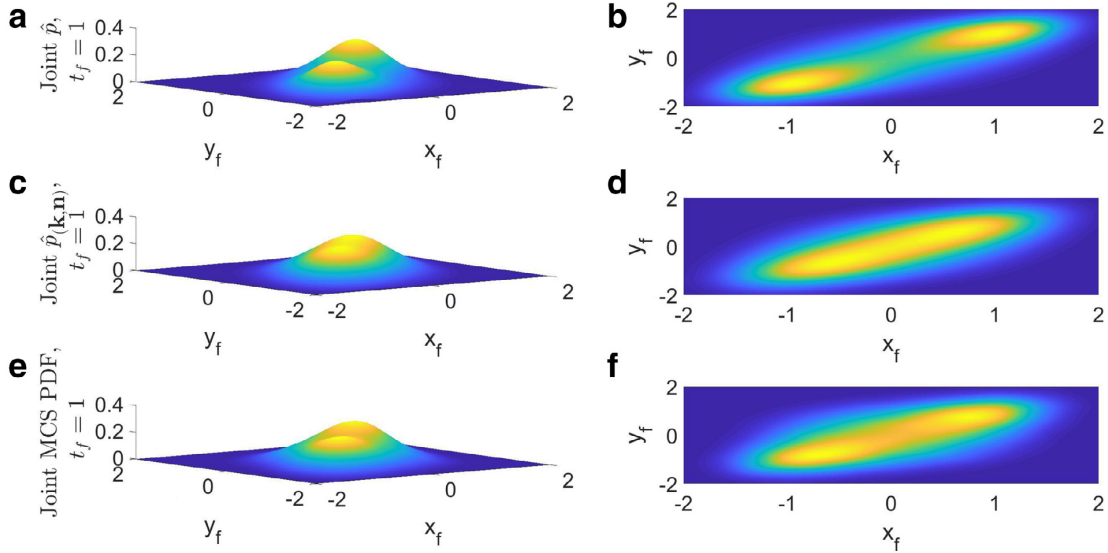


Fig. 3. Joint response PDF at $t_f = 1$ for a coupled system of SDEs with Duffing nonlinearity and bimodal response PDF: basic approximate PDF \hat{p} (a) and (b); Enhanced approximate PDF $\hat{p}_{(k,n)}$ (c) and (d); MCS based PDF (100,000 realizations) (e) and (f).

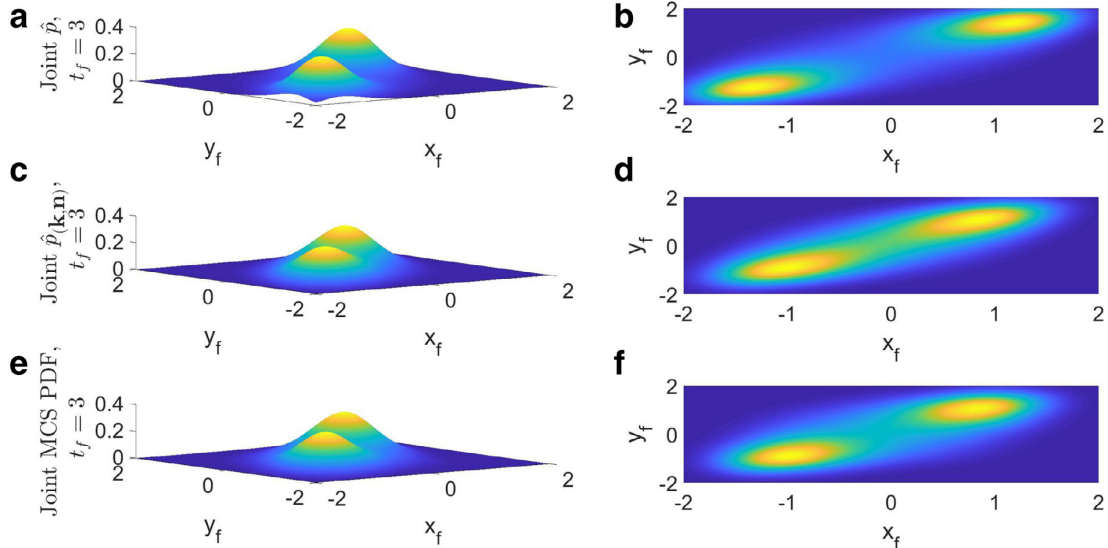


Fig. 4. Joint response PDF at $t_f = 3$ for a coupled system of SDEs with Duffing nonlinearity and bimodal response PDF: basic approximate PDF \hat{p} (a) and (b); Enhanced approximate PDF $\hat{p}_{(k,n)}$ (c) and (d); MCS based PDF (100,000 realizations) (e) and (f).

where $s^{\circ j} = \overbrace{s \circ s \circ \dots \circ s}^{j\text{-times}}$, for $\phi(a_1, a_2, \dots, a_N) = \sin(a_2)$, is typically called the labyrinth model [35–37], and has been used extensively in diverse applications [38–40] for representing auto-catalytic systems.

In the following example, a three-dimensional version of the labyrinth model given by Sprott [36]

$$\begin{cases} dX_t = \sin(Y_t)dt + \sigma dB_t^{(1)} \\ dY_t = \sin(Z_t)dt + \sigma dB_t^{(2)} \\ dZ_t = \sin(X_t)dt + \sigma dB_t^{(3)} \end{cases} \quad (51)$$

Table 3
Computed (\mathbf{k}, \mathbf{n}) values for various final time instants t_f and starting point $(1,1,1,1,1)$ for Example 4.2.

	$k_1 = k_2 = k_3$	$n_1 = n_2 = n_3$	Iterations
$t_f = 0.5$	0.9594	0.2616	39
$t_f = 1$	0.8912	0.2680	27
$t_f = 10$	0.4376	0.0235	48
$t_f = 25$	0.4498	0.0068	57

Table 4
Error estimates and CPU times for Example 4.2.

	$\epsilon \times 10^{-4}$	MCS CPU time (100,000 realizations)	$\hat{p}_{(\mathbf{k}, \mathbf{n})}$ CPU time
$t_f = 0.5$	0.74	974 s	0.036 s
$t_f = 1$	1.32	1687 s	0.025 s
$t_f = 10$	1.07	11,923 s	0.027 s
$t_f = 25$	0.04	28,369 s	0.085 s

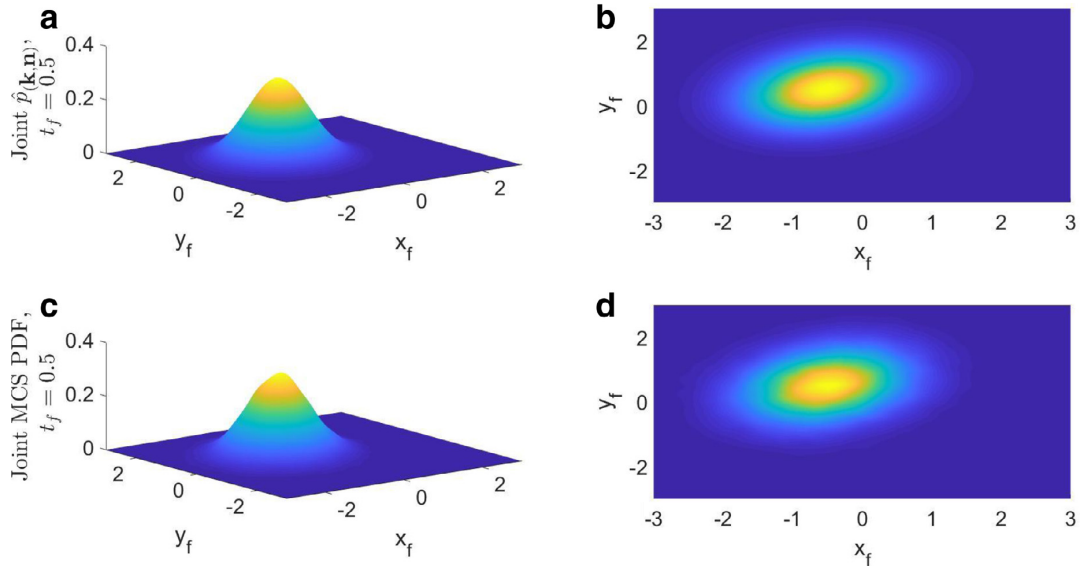


Fig. 5. Joint response PDF at $t_f = 0.5$ for a coupled nonlinear system of SDEs of the “labyrinth” type: Enhanced approximate PDF $\hat{p}_{(\mathbf{k}, \mathbf{n})}$ (a) and (b); MCS based PDF (100,000 realizations) (c) and (d).

is utilized to assess the accuracy of the approximate response PDF of Eq. (42). Next, considering Eq. (51) and zero initial conditions, the PDF of Eq. (42) takes the form

$$\hat{p}_{(\mathbf{k}, \mathbf{n})}(x_f, y_f, z_f, t_f | 0, 0, 0, 0) = F(t_f) \exp \left(-\frac{k_1 x_f^2 + k_2 y_f^2 + k_3 z_f^2 + (-2n_1 x_f \sin(y_f) - 2n_2 y_f \sin(z_f) - 2n_3 z_f \sin(x_f))t_f}{2t_f \sigma^2} \right). \quad (52)$$

In the following, utilizing the parameter value $\sigma = 1$, and applying the numerical optimization scheme of Eq. (46) based on the $\|\cdot\|_2$ norm, yields the values for (\mathbf{k}, \mathbf{n}) . Specifically, exploiting the symmetry of Eqs. (51) and (52) the number of the unknown parameters is reduced from six to two by setting $k_1 = k_2 = k_3$ and $n_1 = n_2 = n_3$. The computed values are shown in Table 3 along with the iterations taken by the optimization algorithm to converge, whereas in Table 4 error estimates and CPU times are included as well. In Figs. 5–8 the joint PDFs of X_t and Y_t are plotted for various time instants based on the

12

A.T. Meimaris, I.A. Kougioumtzoglou and A.A. Pantelous / Applied Mathematics and Computation 364 (2020) 124669

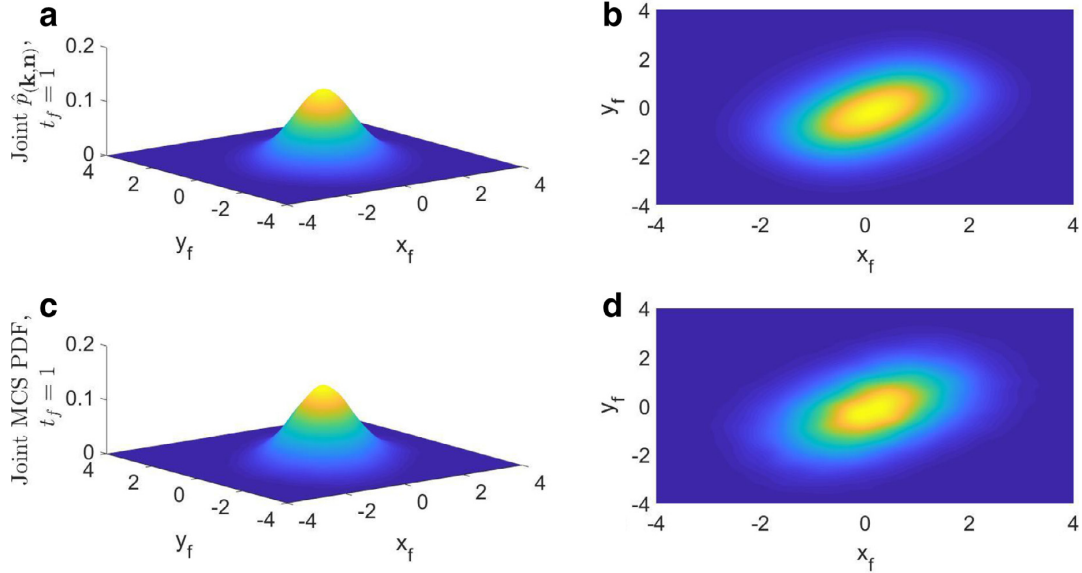


Fig. 6. Joint response PDF at $t_f = 1$ for a coupled nonlinear system of SDEs of the “labyrinth” type: Enhanced approximate PDF $\hat{p}_{(k,n)}$ (a) and (b); MCS based PDF (100,000 realizations) (c) and (d).

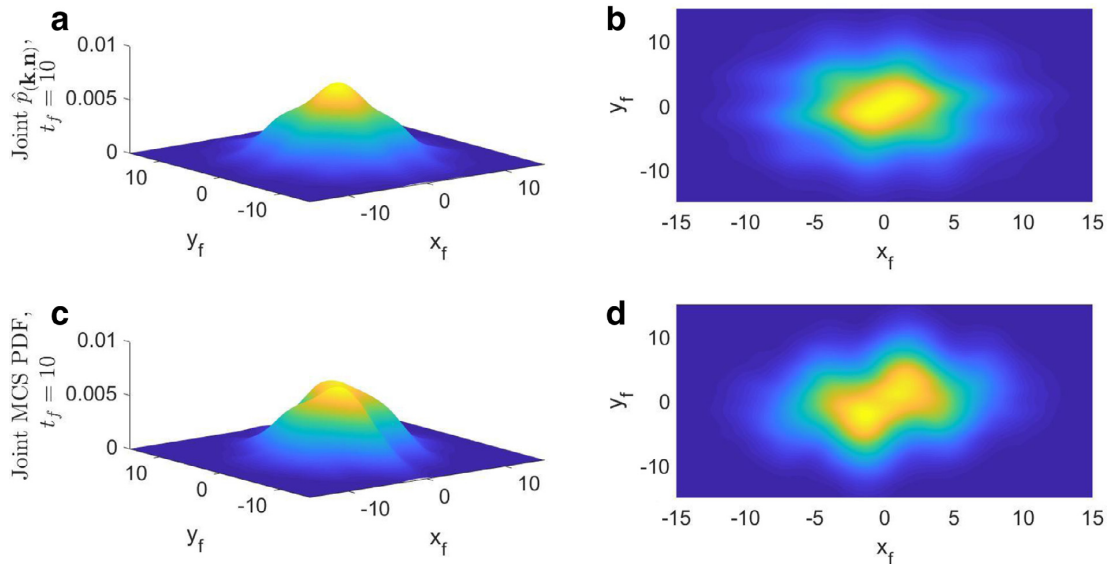


Fig. 7. Joint response PDF at $t_f = 10$ for a coupled nonlinear system of SDEs of the “labyrinth” type: Enhanced approximate PDF $\hat{p}_{(k,n)}$ (a) and (b); MCS based PDF (100,000 realizations) (c) and (d).

approximate PDFs $\hat{p}_{(k,n)}$ of Eq. (52) and compared with MCS based estimated PDFs. Additional results are shown in Fig. 9 corresponding to the marginal PDF of Z_t . It is seen that the herein proposed enhanced PDF approximation of Eq. (52) is in very good agreement with MC simulation data.

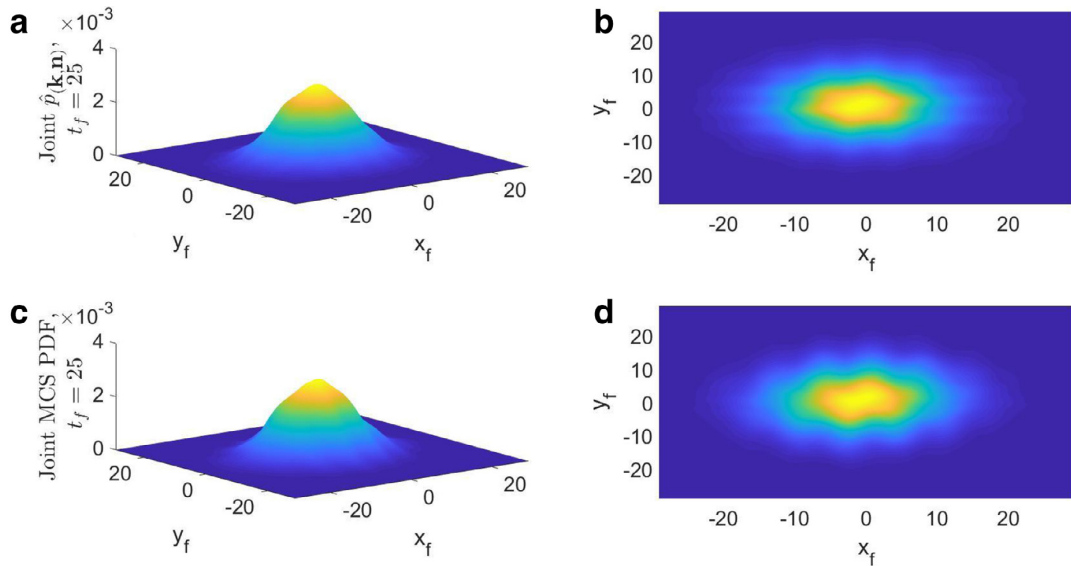


Fig. 8. Joint response PDF at $t_f = 25$ for a coupled nonlinear system of SDEs of the “labyrinth” type: Enhanced approximate PDF $\hat{p}_{(k,n)}$ (a) and (b); MCS based PDF (100,000 realizations) (c) and (d).

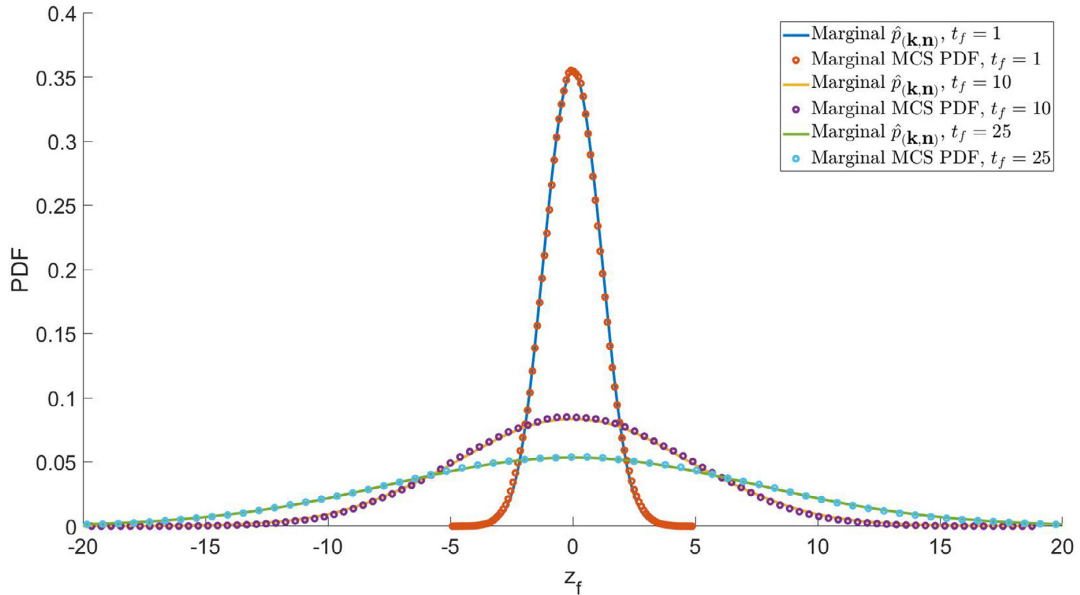


Fig. 9. Enhanced approximate marginal response PDFs $\hat{p}_{(k,n)}$ for various time instants t_f for a coupled nonlinear system of SDEs of the “labyrinth” type; comparisons with MCS based PDF estimates (100,000 realizations).

4.3. The predator-prey model

Various predator-prey mathematical models have been developed in ecology to describe the dynamics of species populations [41]. In this regard, a rather general predator-prey model is given by

$$\begin{cases} \dot{x}(t) = ax(t) - \phi(x(t))y(t) \\ \dot{y}(t) = -by(t) + c\phi(x(t))y(t), \end{cases} \quad (53)$$

Table 5
Computed (\mathbf{k}, \mathbf{n}) values for various final time instants t_f and starting point $(1,1,1,1)$ for Example 4.3.

	k_1	k_2	n_1	n_2	Iterations
$t_f = 0.1$	0.9628	0.9667	2.8039	1.4113	100
$t_f = 0.5$	0.9406	0.9857	2.7976	1.4448	100
$t_f = 1$	0.9116	1.0421	2.5932	1.5088	120
$t_f = 10$	0.7614	1.5122	0.8480	2.3328	410

Table 6
Error statistics and CPU times for Example 4.3.

	$\epsilon \times 10^{-4}$	MCS CPU time (100,000 realizations)	$\hat{p}_{(\mathbf{k}, \mathbf{n})}$ CPU time
$t_f = 0.1$	3.92	131 s	0.064 s
$t_f = 0.5$	1.44	520 s	0.059 s
$t_f = 1$	1.23	922 s	0.065 s
$t_f = 10$	3.16	13,600 s	0.377 s

where $x(t), y(t)$ represent the population densities of prey and predator, respectively; a, b and c are positive constants denoting the prey's intrinsic growth rate, the prey's death rate and the predator's conversion rate, respectively. Further, various expressions have been proposed in the literature for $\phi(x(t))$, ranging from Lotka–Volterra [41] to Holling-kind nonlinear modeling [42]. Without loss of generality, and following [43], a modified stochastic version of Leslie–Gower functional response and of the Holling-type II for the predator-prey model is given by

$$\begin{cases} dX_t = X_t \left(a - bX_t - \frac{cY_t}{m + X_t} \right) dt + \sigma X_t dB_t^{(1)} \\ dY_t = Y_t \left(r - \frac{fY_t}{m + X_t} \right) dt + \sigma Y_t dB_t^{(2)} \end{cases} \quad (54)$$

together with the initial conditions, $X(0) = X_0 > 0$, $Y(0) = Y_0 > 0$. In Eq. (54), the parameters a, b, c, r, f and m are all positive. These parameters are defined as follows: a is the growth rate of prey X , b measures the strength of competition among individuals of species X , c is the maximum value of the per capita reduction rate of X due to Y , m measures the extent to which the environment provides protection to prey X and to the predator Y , r describes the growth rate of Y and f has a similar meaning to c . The interested reader is referred to [44,45] for indicative generalizations of the model.

Next, setting $X = \exp(U)$ and $Y = \exp(V)$, Eq. (54) is cast in the form of Eq. (4); that is,

$$\begin{cases} dU_t = \left(a - \frac{\sigma^2}{2} - be^{U_t} - \frac{ce^{V_t}}{m + e^{U_t}} \right) dt + \sigma dB_t^{(1)} \\ dV_t = \left(r - \frac{\sigma^2}{2} - \frac{fe^{V_t}}{m + e^{U_t}} \right) dt + \sigma dB_t^{(2)} \end{cases} \quad (55)$$

and the PDF of Eq. (42) takes the form

$$\begin{aligned} \hat{p}_{(\mathbf{k}, \mathbf{n})}(u_f, v_f, t_f | u_0, v_0, 0) &= F(t_f) \exp \left(-\frac{k_1(u_f - u_0)^2 + k_2(v_f - v_0)^2}{2t_f \sigma^2} \right) \\ &\times \exp \left(-\frac{n_1(-M(u_f, v_f) + M(u_0, v_0)) + n_2(-K(u_f, v_f) + K(u_0, v_0))}{\sigma^2} \right), \end{aligned} \quad (56)$$

where $M(u, v) = au - \frac{g^2}{2}u - be^u - \frac{ce^v(u - \log(m+e^u))}{m}$ and $K(u, v) = rv - \frac{\sigma^2}{2}v - \frac{fe^v}{m+e^u}$.

In the numerical example, the parameter values $\sigma = 1$, $a = 0.4$, $b = 0.1$, $c = 0.1$, $r = 0.3$, $f = 0.5$, $m = 0.1$ are considered, together with the initial conditions $x_0 = y_0 = 0.3$. Next, applying the numerical optimization scheme of Eq. (46) based on the $\|\cdot\|_2$ norm yields the values for (\mathbf{k}, \mathbf{n}) , which are shown in Eq. (5) along with the iterations number of the optimization algorithm, whereas in Table 6 error estimates and CPU times are presented for comparison purposes. In Figs. 10–13 the approximate PDFs $\hat{p}_{(\mathbf{k}, \mathbf{n})}$ of Eq. (56) are plotted for various time instants and compared with MCS based estimated PDFs. It can be readily seen that the herein proposed enhanced PDF approximation of Eq. (56) exhibits satisfactory accuracy.

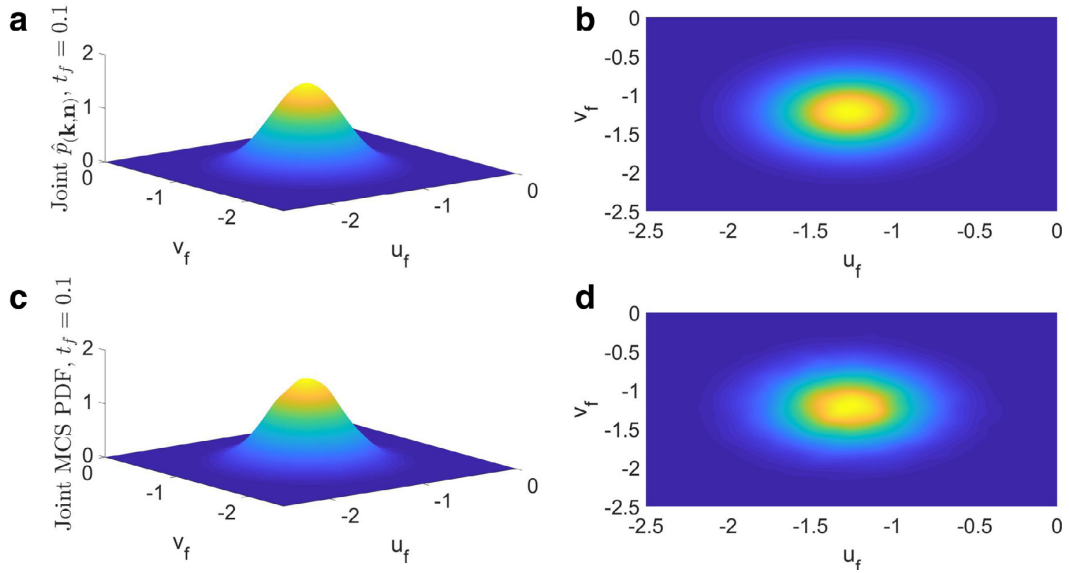


Fig. 10. Joint response PDF at $t_f = 0.1$ for a coupled predator-prey nonlinear system of SDEs: enhanced approximate PDF $\hat{p}_{(k,n)}$ (a) and (b); MCS based PDF (100,000 realizations) (c) and (d).

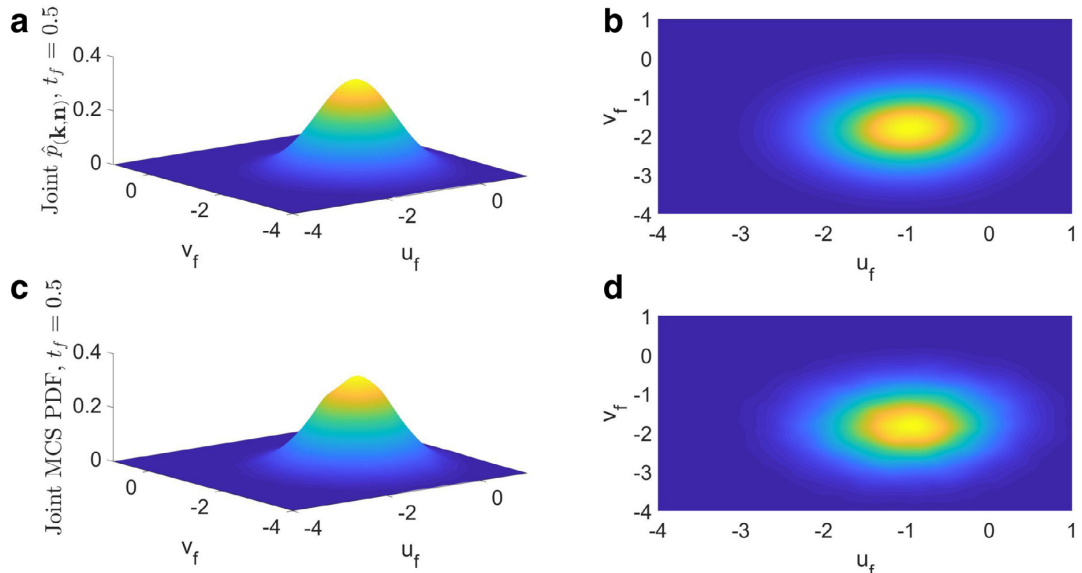


Fig. 11. Joint response PDF at $t_f = 0.5$ for a coupled predator-prey nonlinear system of SDEs: enhanced approximate PDF $\hat{p}_{(k,n)}$ (a) and (b); MCS based PDF (100,000 realizations) (c) and (d).

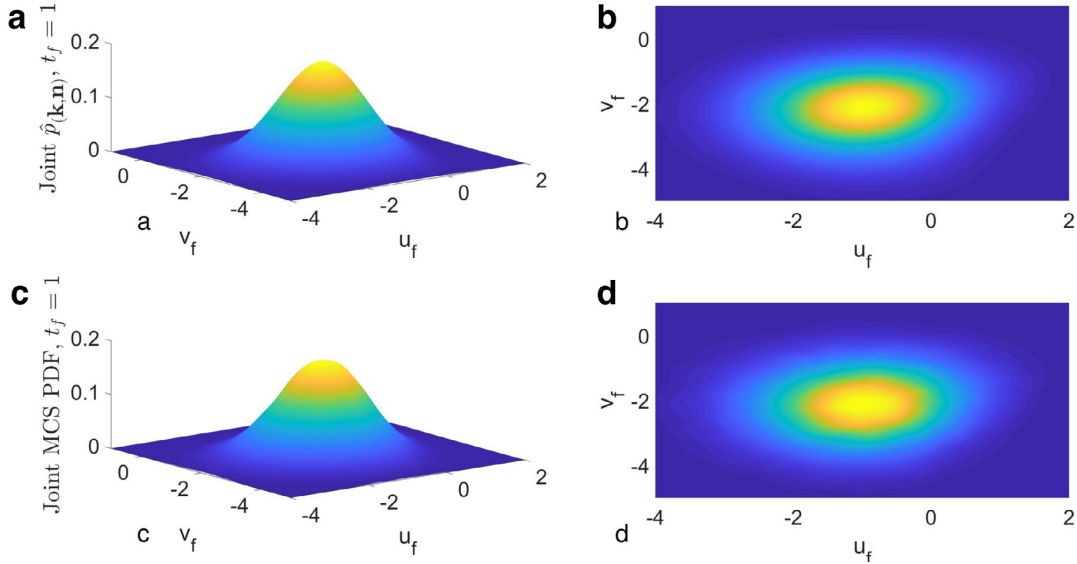


Fig. 12. Joint response PDF at $t_f = 1$ for a coupled predator-prey nonlinear system of SDEs: enhanced approximate PDF $\hat{p}_{(k,n)}$ (a) and (b); MCS based PDF (100,000 realizations) (c) and (d).

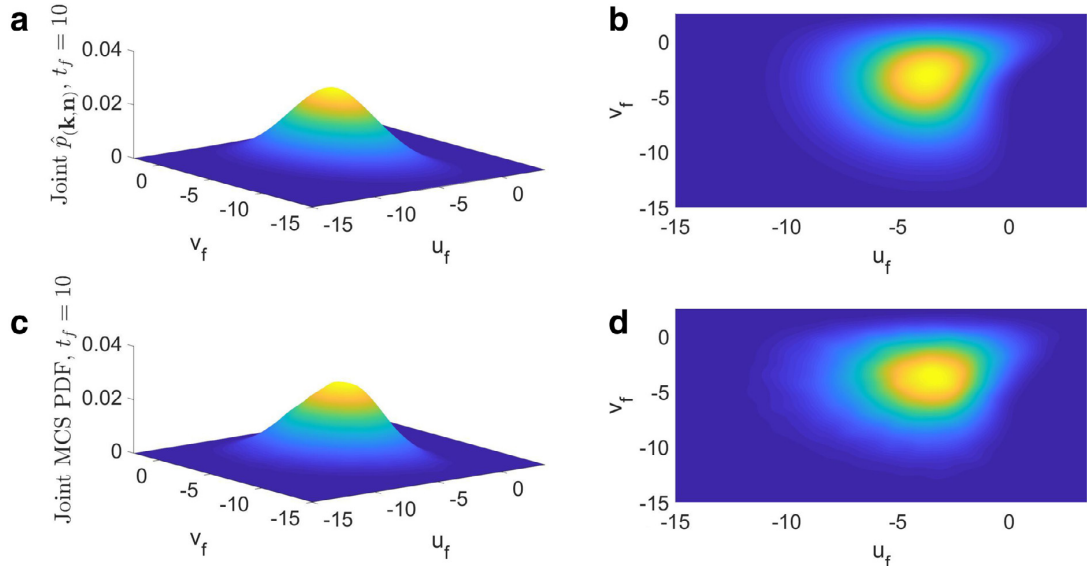


Fig. 13. Joint response PDF at $t_f = 10$ for a coupled predator-prey nonlinear system of SDEs: enhanced approximate PDF $\hat{p}_{(k,n)}$ (a) and (b); MCS based PDF (100,000 realizations) (c) and (d).

5. Conclusion

In this paper, an approximate analytical expression for the joint response transition PDF of a class of coupled SDEs with constant diffusion, but nonlinear drift coefficients, has been derived based on the concept of the Wiener path integral and on a Cauchy-Schwarz inequality treatment. Specifically, first, a basic approximation has been derived that requires essentially zero computational cost for its determination. Next, the approximation has been enhanced from an accuracy perspective by proposing a more general and versatile expression for the joint response transition PDF, which includes additional parameters. These are determined by formulating and solving an appropriate optimization problem related to

the corresponding Fokker–Planck equation. The enhanced PDF has demonstrated significant increase in accuracy, albeit at the expense of some modest computational cost related to the optimization scheme. Several diverse examples have been considered for assessing the reliability and accuracy of the derived approximation as compared to pertinent MC simulation data. In addition to the mathematical merit of the derived closed-form PDF, the approximate solutions can serve also as a benchmark for assessing the performance of alternative, more computationally demanding, stochastic dynamics numerical methodologies.

Acknowledgment

The authors would like to thank the Editor-in-Chief Theodore E. Simos and the anonymous reviewers for their insightful comments that significantly improved the quality of this paper. I. A. Kougioumtzoglou gratefully acknowledges the support through his CAREER award by the CMMI Division of the National Science Foundation, USA (Award number: 1748537).

References

- [1] P.E. Kloeden, E. Platen, *Numerical Solution of Stochastic Differential Equations*, Springer-Verlag Berlin and Heidelberg GmbH & Co. Kg, 1992.
- [2] M. Grigoriu, *Stochastic Calculus: Applications in Science and Engineering*, Springer, New York, USA, 2002.
- [3] S. Tronci, M. Grossi, J. Alvarez, R. Baratti, On the global nonlinear stochastic dynamical behavior of a class of exothermic CSTRs, *J. Process Control* 21 (9) (2011) 1250–1264.
- [4] J. Alvarez, R. Baratti, S. Tronci, M. Grossi, A. Schaum, Global-nonlinear stochastic dynamics of a class of two-state two-parameter non-isothermal continuous stirred tank reactors, *J. Process Control* 72 (2018) 1–16.
- [5] M.F. Wehner, W.G. Wolfer, Numerical evaluation of path-integral solutions to Fokker–Planck equations. II. Restricted stochastic processes, *Phys. Rev. A* 28 (5) (1983) 3003–3011.
- [6] A. Naess, J.M. Johnsen, Response statistics of nonlinear, compliant offshore structures by the path integral solution method, *Probab. Eng. Mech.* 8 (2) (1993) 91–106.
- [7] L. Chen, E.R. Jakobsen, A. Naess, On numerical density approximations of solutions of SDES with unbounded coefficients, *Adv. Comput. Math.* (2017) 1–29.
- [8] J.B. Roberts, P.D. Spanos, *Random Vibration and Statistical Linearization*, Courier Corporation, 2003.
- [9] J. Li, J. Chen, *Stochastic Dynamics of Structures*, John Wiley & Sons (Asia) Pte Ltd, 2009.
- [10] N. Wiener, The average of an analytic functional and the Brownian movement, *Proc. Natl. Acad. Sci.* 7 (10) (1921) 294–298.
- [11] R.P. Feynman, Space-time approach to non-relativistic quantum mechanics, *Rev. Mod. Phys.* 20 (2) (1948) 367.
- [12] I.A. Kougioumtzoglou, P.D. Spanos, An analytical Wiener path integral technique for non-stationary response determination of nonlinear oscillators, *Probab. Eng. Mech.* 28 (2012) 125–131.
- [13] I.A. Kougioumtzoglou, P.D. Spanos, Nonstationary stochastic response determination of nonlinear systems: a Wiener path integral formalism, *ASCE J. Eng. Mech.* 140 (9) (2014) 04014064.
- [14] A. Di Matteo, I.A. Kougioumtzoglou, A. Pirrotta, P.D. Spanos, M. Di Paola, Stochastic response determination of nonlinear oscillators with fractional derivatives elements via the Wiener path integral, *Probab. Eng. Mech.* 38 (2014) 127–135.
- [15] I.A. Kougioumtzoglou, A. Di Matteo, P.D. Spanos, A. Pirrotta, M. Di Paola, An efficient Wiener path integral technique formulation for stochastic response determination of nonlinear MDOF systems, *ASME J. Appl. Mech.* 82 (10) (2015) 101005.
- [16] I.A. Kougioumtzoglou, A Wiener path integral solution treatment and effective material properties of a class of one-dimensional stochastic mechanics problems, *ASCE J. Eng. Mech.* 143 (6) (2017) 04017014.
- [17] I. Petromichelakis, A.F. Psaros, I.A. Kougioumtzoglou, Stochastic response determination and optimization of a class of nonlinear electromechanical energy harvesters: A Wiener path integral approach, *Probab. Eng. Mech.* 53 (2018) 116–125.
- [18] A.F. Psaros, O. Brudastova, G. Malara, I.A. Kougioumtzoglou, Wiener Path Integral based response determination of nonlinear systems subject to non-white, non-Gaussian, and non-stationary stochastic excitation, *J. Sound Vib.* 433 (2018) 314–333.
- [19] A.F. Psaros, I.A. Kougioumtzoglou, I. Petromichelakis, Sparse representations and compressive sampling for enhancing the computational efficiency of the wiener path integral technique, *Mech. Syst. Signal Process.* 111 (2018) 87–101.
- [20] A.T. Meimaris, I.A. Kougioumtzoglou, A.A. Pantelous, A closed form approximation and error quantification for the response transition probability density function of a class of stochastic differential equations, *Probab. Eng. Mech.* 54 (2018) 87–94.
- [21] A.T. Meimaris, I.A. Kougioumtzoglou, A.A. Pantelous, Approximate analytical solutions for a class of nonlinear stochastic differential equations, *Eur. J. Appl. Math.* (2018) 1–17.
- [22] T. Taniguchi, E.G.D. Cohen, Inertial effects in nonequilibrium work fluctuations by a path integral approach, *J. Stat. Phys.* 130 (1) (2008) 1–26.
- [23] M. Chaichian, A. Demichev, *Path Integrals in Physics: Volume I Stochastic Processes and Quantum Mechanics*, CRC Press, 2001.
- [24] R.L. Schilling, L. Partzsch, *Brownian Motion: An Introduction to Stochastic Processes*, Walter de Gruyter GmbH & Co KG, 2012.
- [25] G.M. Ewing, *Calculus of Variations with Applications*, Dover Publications, New York, USA, 2016.
- [26] J.M. Steele, *The Cauchy–Schwarz Master Class: An Introduction to the Art of Mathematical Inequalities*, Cambridge University Press, New York, USA, 2004.
- [27] N.G. Van Kampen, *Stochastic Processes in Physics and Chemistry*, Elsevier, New York, USA, 2007.
- [28] D. Künszenti-Kovács, On the error of Fokker–Planck approximations of some one-step density dependent processes, arXiv:1612.08829, 2016.
- [29] R. Grima, P. Thomas, A.V. Straube, How accurate are the nonlinear chemical Fokker–Planck and chemical Langevin equations? *J. Chem. Phys.* 135 (2011) 084103.
- [30] Q. Yang, F. Liu, I. Turner, Stability and convergence of an effective numerical method for the time-space fractional Fokker–Planck equation with a nonlinear source term, *Int. J. Diff. Eq.* 2010 (2010) 1–22.
- [31] H.A. Kramers, Brownian motion in a field of force and the diffusion model of chemical reactions, *Physica* 7 (4) (1940) 284–304.
- [32] B. Øksendal, *Stochastic Differential Equations: An Introduction with Applications*, Springer-Verlag Berlin and Heidelberg GmbH & Co. Kg, 2010.
- [33] A. Forsgren, P.E. Gill, M.H. Wright, Interior methods for nonlinear optimization, *SIAM Rev.* 44 (4) (2002) 525–597.
- [34] J. Nocedal, S. Wright, *Numerical Optimization*, Springer, New York, USA, 2006.
- [35] R. Thomas, Deterministic chaos seen in terms of feedback circuits: analysis, synthesis, “labyrinth chaos”, *Int. J. Bifurc. Chaos* 9 (10) (1999) 1889–1905.
- [36] J.C. Sprott, *Elegant Chaos: Algebraically Simple Chaotic Flows*, World Scientific, Singapore, 2010.
- [37] S. Vaidyanathan, C. Volos, *Advances and Applications in Chaotic Systems*, Springer-Verlag Berlin and Heidelberg GmbH & Co. Kg, 2016.
- [38] S. Rasmussen, C. Knudsen, R. Feldberg, M. Hindholm, The coreworld: emergence and evolution of cooperative structures in a computational chemistry, *Phys. D: Nonlinear Phenom.* 42 (1–3) (1990) 111–134.
- [39] J.L. Deneubourg, S. Goss, Collective patterns and decision-making, *Ethol. Ecol. Evol.* 1 (1989) 295–311.
- [40] S.A. Kauffman, *The Origins of Order: Self-Organization and Selection in Evolution*, Oxford University Press, USA, 1993.
- [41] H.I. Freedman, *Deterministic Mathematical Models in Population Ecology*, Pure and applied mathematics, Marcel Dekker, Inc., New York, USA, 1980.

- [42] B. Liu, Z. Teng, L. Chen, Analysis of a predator-prey model with Holling II functional response concerning impulsive control strategy, *J. Comput. Appl. Math.* 193 (2006) 347–362.
- [43] C. Ji, D. Jiang, N. Shi, Analysis of a predator-prey model with modified Leslie-Gower and Holling-type II schemes with stochastic perturbation, *J. Math. Anal. Appl.* 359 (2) (2009) 482–498.
- [44] A.F. Nindjin, M.A. Aziz-Alaoui, M. Cadivel, Analysis of a predator-prey model with modified Leslie-Gower and Holling-type II schemes with time delay, *Nonlinear Anal.: Real World Appl.* 7 (2006) 1104–1118.
- [45] H. Guo, X. Song, An impulsive predator-prey system with modified Leslie-Gower and Holling type II schemes, *Chaos Solitons Fractals* 36 (5) (2008) 1320–1331.

5.2 The "labyrinth" model

Let

$$s(i) = (i + 1) \bmod N, \quad \forall i \in \mathbb{N}_0, \quad (5.4)$$

denote a circular shift permutation (rotation) operator of the natural numbers. The N -dimensional circulant system of the form

$$dX_t^{(j)} = \phi \left(X_t^{s^{\circ j}(0)}, X_t^{s^{\circ j}(1)}, \dots, X_t^{s^{\circ j}(N-1)} \right) dt + \sigma dB_t^{(j)}, \quad \forall j \in [N], \quad (5.5)$$

where $s^{\circ j} = \overbrace{s \circ s \circ \dots \circ s}^{j-times}$, for $\phi(a_1, a_2, \dots, a_N) = \sin(a_2)$, is typically called the labyrinth model, and has been used extensively in diverse applications for representing auto-catalytic systems.

In the following example, a two-dimensional version of the labyrinth model given by

$$\begin{cases} dX_t = \sin(Y_t)dt + \sigma dB_t^{(1)} \\ dY_t = \sin(X_t)dt + \sigma dB_t^{(2)} \end{cases} \quad (5.6)$$

is utilized to assess the accuracy of the enhanced approximate response PDF (see Eq. (42) in Published Material Section 5.1). Next, considering Eq. (5.6) and zero initial conditions, the enhanced PDF of Eq. (42) (see Published Material Section 5.1) takes the form

$$\hat{p}_{(\mathbf{k},\mathbf{n})}(x_f, y_f, t_f | 0, 0, 0) = F(t_f) \exp \left(-\frac{k_1 x_f^2 + k_2 y_f^2 + (-2n_1 x_f \sin(y_f) - 2n_2 y_f \sin(x_f)) t_f}{2t_f \sigma^2} \right). \quad (5.7)$$

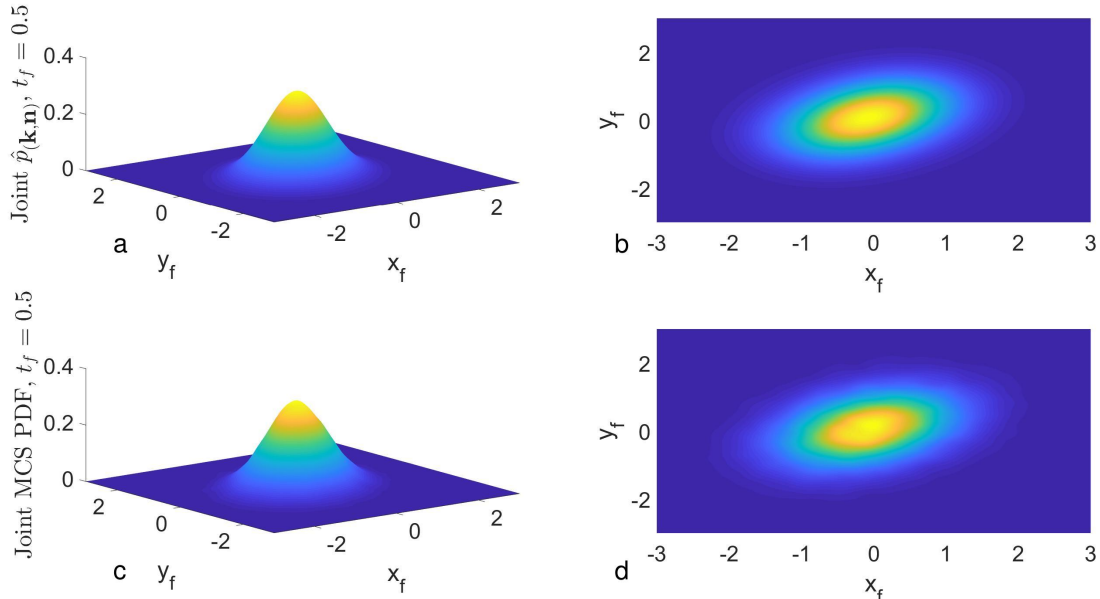
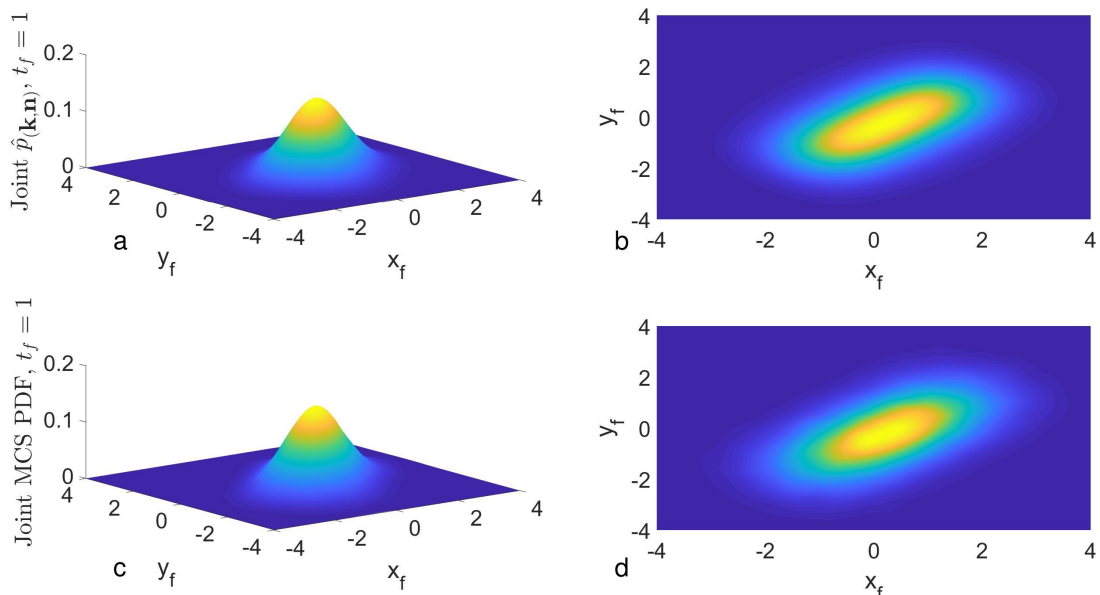
In the following, utilizing the parameter value $\sigma = 1$, and applying the associated numerical optimization scheme of Eq. (46) (see Published Material Section 5.1) based on the $\|\cdot\|_2$ norm, yields the values for (\mathbf{k}, \mathbf{n}) . Specifically, exploiting the symmetry of Eqs. (5.6) and (5.7) the number of the unknown parameters is reduced from four to two by setting $k_1 = k_2$ and $n_1 = n_2$. The computed values are shown in Table 5.1 along with the iterations taken by the optimization algorithm to converge, whereas in Table 5.2 error estimates and CPU times are included as well. In Figs. 5.1 to 5.4 the approximate PDFs $\hat{p}_{(\mathbf{k},\mathbf{n})}$ of Eq. (5.7) are plotted for various time instants and compared with MCS based estimated PDFs. It is seen that the herein proposed enhanced PDF approximation of Eq. (5.7) is in very good agreement with MC simulation data.

TABLE 5.1: Computed (\mathbf{k}, \mathbf{n}) values for various final time instants t_f and starting point $(1, 1, 1, 1)$ for example of Section 5.2

	$k_1 = k_2$	$n_1 = n_2$	Iterations
$t_f = 0.5$	0.9981	0.3887	36
$t_f = 1$	0.9447	0.4017	30
$t_f = 10$	0.4303	0.0348	47
$t_f = 25$	0.4545	0.0114	54

TABLE 5.2: Error estimates and CPU times for example of Section 5.2

	$\epsilon \times 10^{-4}$	MCS CPU time (100,000 realizations)	$\hat{p}_{(k,n)}$ CPU time
$t_f = 0.5$	0.87	500 s	0.138 s
$t_f = 1$	3.21	881 s	0.045 s
$t_f = 10$	0.70	7196 s	0.054 s
$t_f = 25$	0.03	25890 s	0.051 s

FIGURE 5.1: Joint response PDF at $t_f = 0.5$ for a coupled nonlinear system of SDEs of the "labyrinth" type: Enhanced approximate PDF $\hat{p}_{(k,n)}$ (a and b); MCS based PDF (100,000 realizations) (c and d).FIGURE 5.2: Joint response PDF at $t_f = 1$ for a coupled nonlinear system of SDEs of the "labyrinth" type: Enhanced approximate PDF $\hat{p}_{(k,n)}$ (a and b); MCS based PDF (100,000 realizations) (c and d).

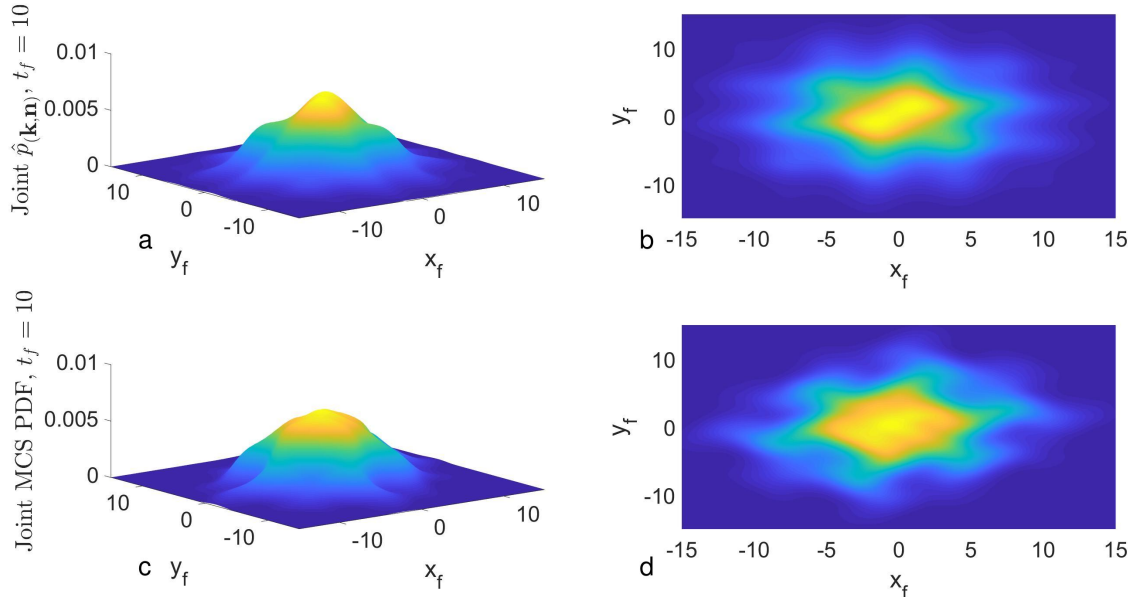


FIGURE 5.3: Joint response PDF at $t_f = 10$ for a coupled nonlinear system of SDEs of the "labyrinth" type: Enhanced approximate PDF $\hat{p}_{(k,n)}$ (a and b); MCS based PDF (100,000 realizations) (c and d).

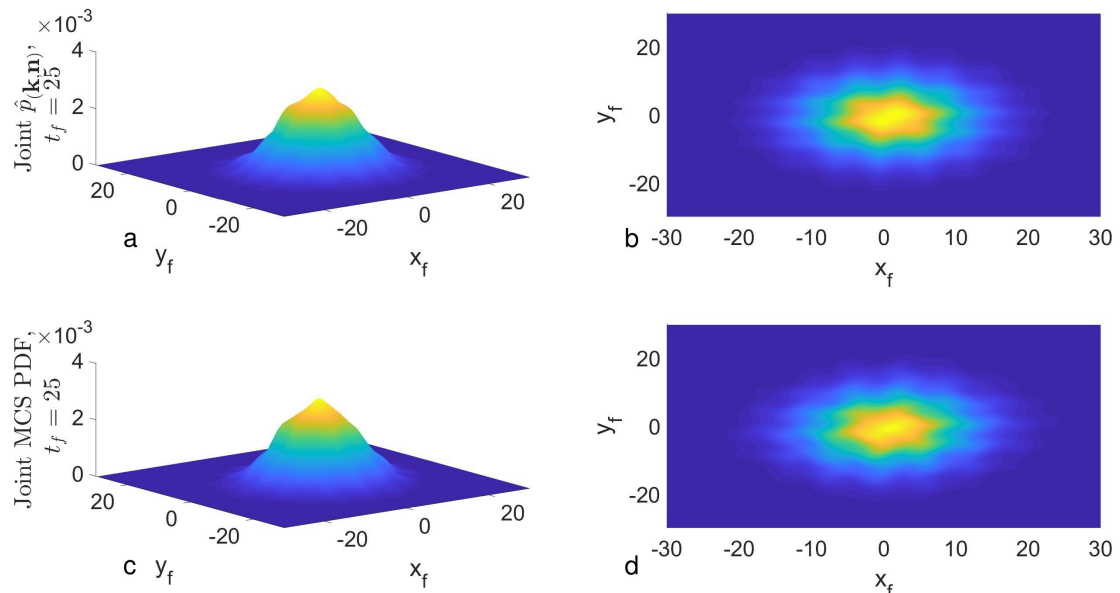


FIGURE 5.4: Joint response PDF at $t_f = 25$ for a coupled nonlinear system of SDEs of the "labyrinth" type: Enhanced approximate PDF $\hat{p}_{(k,n)}$ (a and b); MCS based PDF (100,000 realizations) (c and d).

Chapter 6

Summary and Conclusions

This study has presented a new approach to determine in an approximative manner the solutions of Itô stochastic differential equations in a distributional sense. This technique makes use of the connection between stochastic differential and Fokker-Planck equations as well as the basic elements of the most probable Wiener Path Integral method. The new closed form analytic approach is rather flexible, since substantial improvements have been made when compared to the Wiener Path Integral technique not only in terms of its computational efficiency, but the degree of accuracy as well. This in turn lead to the applicability of the proposed study, in a reliable manner, in various complex stochastic dynamical systems ranging from mechanical, physical, chemical, biological and concluding with economical and ecological systems.

In Chapter 2 the theoretical background and formulation of the the Itô stochastic differential equations has been reviewed with an emphasis on their connection with the Fokker-Planck partial differential equations. The basic technique of the Wiener Path Integral Method has been introduced as well. The main features of the most probable Wiener Path Integral approximate technique were also discussed, together with the critique on its accuracy and efficiency. These topics, together with the concept of multidimensionality, constitute the basis for the following chapters including published material.

In the first paper, presented in Chapter 3, the ideas presented in Meimaris, Kougioumtzoglou, and Pantelous, 2018a have been extended to account for a more flexible approach regarding the trade-off between precision and efficiency. Although, the basic approach is a ready to use approximation in a closed form, its accuracy can be insufficient for certain applications, thus, the enhanced approximation which is developed, increases the accuracy of the basic approximation with the introduction of an optimization problem that needs to be solved. These modifications and improvements, e.g., the introduction of new parameters and their calibration, with respect to Meimaris, Kougioumtzoglou, and Pantelous, 2018a were made, keeping in mind the importance for maintaining a fast code. The implementation has been published in the European Journal of Applied Mathematics, making it the first available paper proposing a closed form approximation based on the Wiener Path Integral method for stochastic analysis applications for a mathematical audience, with specific examples in both mechanical engineering and biochemistry. The set-up of an optimization problem to assist the calibration of parameters in a Wiener Path Integral framework was applied for the first time.

The aforementioned modified Wiener Path Integral approach has been revised in Chapter 4, such that the functions driving the Itô stochastic differential equations are extended to a more general class. Here, only the restriction of time-homogeneity on the drift and diffusion coefficients of the stochastic differential equations is assumed. This requires a more delicate approach in order to escape the time-consuming explicit determination of the most probable path. Indeed, upon untangling this requirement, after cumbersome derivations,

the resulting closed form approximation is then enhanced by the introduction of new parameters to be determined by a new optimization problem, based on the associated Fokker-Planck partial differential equation.

The resulting algorithm is then used in the published paper of Chapter 4 to deal with engineering problems with applications in smart materials. In addition, the applicability of the developed technique is also presented in Quantitative Finance applications, where a model with discontinuity is examined as well as a nonlinear constant elasticity of variance (CEV) model is used to price Bermuda calls in a matter of a tenth of a second. Setting aside the efficiency of this technique, when compared to other techniques the new algorithm has been found to be in good agreement with the data, producing more accurate results than a naive Monte Carlo simulation scheme.

In Chapter 5 a novel Wiener Path Integral based technique has been developed to study the applicability of the previous fundamental results in a setting for systems of stochastic differential equations. While in the one-dimensional model, classic Wiener Path Integral method leads to one equation for determining the most probable paths for the process under consideration, the new models require the solution to a system of differential equations in order to determine the paths, posing an even greater challenge for untangling this highly computationally prohibitive requirement. However, as demonstrated in Chapter 5, understanding even this simple case where the drift coefficient is a nonlinear vector of the stochastic process and the diffusion coefficient is constant, will provide great insight for the proper choice of the Lagrangian that needs to be used in the more general one-dimensional case. As a last addition, this simple multidimensional model has been implemented. The resulting basic and enhanced approximations have been tested and validated in various applications ranging from mechanical and chemical engineering problems to complex nonlinear ecological problems.

Overall, the analytical results of the thesis have introduced a new Wiener Path Integral based technique that is both computationally efficient and can be used with flexibility depending on the application and the accuracy requirement. If accuracy is of greater importance than computational efficiency, then the enhanced approximations, which require a minimal computational cost, are better suited than the basic ones, which require zero computational time. The importance and reliability of this fundamental research is demonstrated by its versatility in numerous applications ranging from the classical engineering disciplines to Quantitative Finance frameworks.

6.1 Future Directions and Projected Impact

Some of the possible future research directions that are based on the fundamental research detailed in this thesis are the following.

First, future work will consider expanding the number of proposed variables to be calibrated by either splitting the space-time intervals of interest or by introducing new functions in the expansion of the exponential. As a consequence, a more precise algorithm will be developed for approximating the desired probability density function associated with the considered stochastic processes. For example, in Section 4.2, by splitting each of the quarterly dates' price intervals (x -axis) into two, two optimal parameters will be sought for, instead of only one optimal value of the parameter k , resulting in an even more accurate approximation of the probability density function and, thus, in an option price converging to the exact solution price.

As discussed in Chapter 5, another direction of research is to expand the applicability of the developed technique to either the most general case of one-dimensional nonlinear Itô stochastic differential equations, or even in the case of coupled nonlinear multidimensional

stochastic differential equations of the form of Eq. (5.2). It is plausible that by using the proper Lagrangian in combination with an inequality, such as the Cauchy-Schwarz which was utilized in this study, the proposed solution methodology could be adapted to provide closed-form approximations to an even greater class of models, without requiring any form of reductions to simpler models of Itô stochastic differential equations. Subsequently, this would broaden the range of multi-disciplinary applications that the developed technique could be useful for, i.e., from systems of non-linear oscillators to an even wider class of predator-prey models and even complex financial applications, such as the Chen model and multi-dimensional versions of Ornstein–Uhlenbeck processes.

Finally, the developed methodology could be further investigated in a framework where in the modelling of the stochastic process jumps are incorporated, or the process is exotically excited (e.g. coloured noise). This kind of modelling will allow the process to have various desired properties, such as memory, and jump processes are useful for modelling complex price movements in Finance. Although, in general, this task seems impossible without the knowledge of the correct Lagrangian, a first approach would be to decompose the complicated stochastic equations into simpler ones that will be filtering out the useless aspects of the vanilla Brownian motion.

Bibliography

- Addison, LM, BS Bhatt, and DR Owen (2016). "A prey-predator model for investing in stocks". In: *International Journal of Pure and Applied Mathematics* 107.2, pp. 487–504.
- Allison, Andrew and Derek Abbott (2000). "Stable processes in econometric time series: Are prices made out of noise?" In: *AIP Conference Proceedings*. Vol. 511. AIP, pp. 221–232.
- Aristotle. *Politics, Book 1*.
- Asada, Toichiro (2012). "Modeling financial instability". In: *European Journal of Economics and Economic Policies: Intervention* 9.2, pp. 215–232.
- Bachelier, Louis (1900). *Théorie de la spéculation*. Gauthier-Villars.
- Bernstein, William J (2008). *A splendid exchange: How trade shaped the world*. Grove Atlantic, New York, USA.
- Blake, Emma and A Bernard Knapp (2005). *The archaeology of Mediterranean prehistory*. Blackwell Publishing Ltd, New Jersey, USA.
- Bolton, Patrick and David S Scharfstein (1990). "A Theory of Predation Based on Agency Problems in Financial Contracting". In: *The American Economic Review* 80.1, pp. 93–106.
- Bonnet, Frederic D.R., Andrew G Allison, and Derek Abbott (2004). "Path integrals in fluctuating markets". In: *Proceedings of SPIE*. Vol. 5471. Noise in Complex Systems and Stochastic Dynamics II, pp. 595–611.
- Bormetti, G et al. (2006). "Pricing exotic options in a path integral approach". In: *Quantitative Finance* 6.1, pp. 55–66.
- Braudel, Fernand (1982). *Civilization and Capitalism, 15th-18th Century: Volume II: The Wheels of Commerce*. William Collins, Sons & Co Ltd, Glasgow, United Kingdom.
- Capriotti, Luca (2006). "The exponent expansion: An effective approximation of transition probabilities of diffusion processes and pricing kernels of financial derivatives". In: *International Journal of Theoretical and Applied Finance* 9.7, pp. 1179–1199.
- Castelli, C. (1877). *The Theory of "Options" in Stocks and Shares*. F.C. Mathieson, London, United Kingdom.
- Chaichian, M and A Demichev (2001). *Path Integrals in Physics: Volume I Stochastic Processes and Quantum Mechanics*. Institute of Physics Publishing, Philadelphia, USA.
- Chen, Linghua, Espen Robstad Jakobsen, and Arvid Naess (2015). *On numerical density approximations of solutions of SDEs with unbounded coefficients*. arXiv:1506.05576.
- Decamps, Marc, Ann De Schepper, and Marc Goovaerts (2006). "A path integral approach to asset-liability management". In: *Physica A* 363, pp. 404–416.
- Dekker, H (1978). "Derivation of the Onsager-Machlup lagrangian for general diffusion processes by means of Fourier series". In: *Physics Letters A* 68A.2, pp. 137–140.
- Di Matteo, Alberto et al. (2014). "Stochastic response determination of nonlinear oscillators with fractional derivatives elements via the Wiener path integral". In: *Probabilistic Engineering Mechanics* 38, pp. 127–135.
- Ed. Frolov, I. (1984). *Dictionary of philosophy*. Progress Publishers, Moscow, U.S.S.R.
- Engels, Frederick (1976). *Dialectics of Nature*. Progress Publishers, Moscow, U.S.S.R.
- Ewing, George McNaught (1969). *Calculus of Variations with Applications*. Dover Publications, New York, USA.
- Eydeland, A (1994). "A fast algorithm for computing integrals in function spaces: Financial applications". In: *Computational Economics* 7, pp. 277–285.

- Fabozzi, Frank J (2002). *The handbook of financial instruments*. John Wiley & Sons, Inc, New Jersey, USA.
- Feynman, Richard Phillips (1948). "Space-Time Approach to Non-Relativistic Quantum Mechanics". In: *Reviews of Modern Physics*, <https://doi.org/10.1103/RevModPhys.20.367> 20.2, p. 367.
- Figlewski, Stephen (1989). "Options arbitrage in imperfect markets". In: *The journal of Finance* 44.5, pp. 1289–1311.
- Graham, Robert (1977). "Path integral formulation of general diffusion processes". In: *Zeitschrift für Physik B Condensed Matter* 26.3, pp. 281–290.
- Grigoriu, Mircea (2002). *Stochastic Calculus: Applications in Science and Engineering*. Springer, New York, USA.
- Hull, John C (2018). *Options, futures, and other derivatives (10th Edition)*. Pearson Education, New York, USA.
- Ingber, Lester (2000). "High-resolution path-integral development of financial options". In: *Physica A* 283, pp. 529–558.
- Kac, M (1966). "Wiener and integration in function spaces". In: *Bulletin of the American Mathematical Society* 72, pp. 52–68.
- Kolmogorov, Andrei Nikolaevich (1950). *Foundations of the Theory of Probability*. Chelsea Publishing Company, New York, USA.
- Kougioumtzoglou, Ioannis A et al. (2015). "An efficient Wiener path integral technique formulation for stochastic response determination of nonlinear MDOF systems". In: *ASME Journal of Applied Mechanics* 82.10, p. 101005.
- Linetsky, Vadim (1998). "The path integral approach to financial modeling and options pricing". In: *Computational Economics* 11, pp. 129–163.
- Louzoun, Yoram and Sorin Solomon (2001). "Volatility driven market in a generalized Lotka–Volterra formalism". In: *Physica A* 302.1, pp. 220–233.
- Malthus, Thomas (1798). *An Essay on the Principle of Population*. St. Paul's Church-Yard, London, England.
- Meimaris, Antonios T., Ioannis A. Kougioumtzoglou, and Athanasios A. Pantelous (2018a). "A closed form approximation and error quantification for the response transition probability density function of a class of stochastic differential equations". In: *Probabilistic Engineering Mechanics*, doi.org/10.1016/j.probengmech.2017.07.005 54, pp. 87–94.
- (2018b). "Approximate analytical solutions for a class of nonlinear stochastic differential equations". In: *European Journal of Applied Mathematics*, doi.org/10.1017/S0956792518000530 30.5, pp. 928–944.
- (2020). "Closed form approximate solutions for a class of coupled nonlinear stochastic differential equations". In: *Applied Mathematics and Computation*, 124669: 1–18.
- Meimaris, Antonios T. et al. (2019). "An approximate technique for determining in closed form the response transition probability density function of diverse nonlinear/hysteretic oscillators". In: *Nonlinear Dynamics*, doi.org/10.1007/s11071-019-05152-w 97.4, pp. 2627–2641.
- Michie, Ranald C (1999). *The London stock exchange: A history*. Oxford University Press, Oxford, United Kingdom.
- Montagna, Guido, Oreste Nicrosini, and Nicola Moreni (2002). "A path integral way to option pricing". In: *Physica A* 310, pp. 450–466.
- Montagna, Guido et al. (2003). "Pricing derivatives by path integral and neural networks". In: *Physica A* 324, pp. 189–195.
- Naess, A and JM Johnsen (1993). "Response statistics of nonlinear, compliant offshore structures by the path integral solution method". In: *Probabilistic Engineering Mechanics* 8.2, pp. 91–106.

- Øksendal, Bernt (1985). "Stochastic differential equations: An Introduction with Applications". In: Springer, New York, USA.
- Oliveira, Agamenon (2014). *A History of the Work Concept: From Physics to Economics*. Springer, New York, USA.
- Otto, Matthias (2000). "Stochastic relaxational dynamics applied to finance: Towards non-equilibrium option pricing theory". In: *The European Physical Journal B* 14, pp. 383–394.
- Piotrowski, Edward W and J Śladkowski (2002). "Quantum market games". In: *Physica A* 312, pp. 208–216.
- Polya, George (1971). *How to Solve it: A New Aspect of Mathematical Method Mathematical Method*. Princeton University Press, Princeton, USA.
- Schilling, René L and Lothar Partzsch (2012). *Brownian motion: An introduction to stochastic processes*. Walter de Gruyter GmbH & Co KG, Berlin, Germany.
- Schulman, LS (1981). *Techniques and applications of path integration*. John Wiley & Sons, Inc, New Jersey, USA.
- Shiryayev, Albert N (1999). *Essentials of stochastic finance: facts, models, theory*. Vol. 3. World scientific, New Jersey, USA.
- Sprott, JC (2004). "Competition with evolution in ecology and finance". In: *Physics Letters A* 325.5-6, pp. 329–333.
- Van Kampen, Nicolaas Godfried (2007). *Stochastic Processes in Physics and Chemistry*. Elsevier, New York, USA.
- Wehner, MF and WG Wolfer (1983). "Numerical evaluation of path-integral solutions to Fokker-Planck equations. II. Restricted stochastic processes". In: *Physical Review A* 28, p. 3003.
- Wiener, Norbert (1921). "The Average of an Analytic Functional and the Brownian Movement". In: *Proceedings of the National Academy of Sciences* 7.10, pp. 294–298.
- Wio, Horacio S (2013). *Path Integrals for Stochastic Processes: An Introduction*. World Scientific, New Jersey, USA.